Alpha-Decomposition for Cause-Informed Common Cause Failure Modeling through Bayesian Inference

February 2013

Xiaoyu Zheng

Graduate School of Engineering

Osaka University

Alpha-Decomposition for Cause-Informed Common Cause Failure Modeling through Bayesian Inference

by

Xiaoyu Zheng

Dissertation submitted to the
Division of Sustainable Energy and Environmental Engineering
Graduate School of Engineering
Osaka University

Advisory Committee:
Professor Akira Yamaguchi, Chair/Advisor
Professor Takao Nakamura, Head of the division
Associate Professor Takashi Takata
Associate Professor Eiji Hoashi

ABSTRACT

Traditional Basic Parameter Models (BPMs) for Common Cause Failure (CCF) modeling has focused on the occurrence frequencies of CCF events. The Alpha-factor model is the most widely adopted parametric model. Joint distributions for lumped parameters in the alpha-factor model are determined by a set of possible causes. Each possible cause has innate CCF-triggering ability and occurrence frequency. Cause-informed CCF modeling aims to provide a quantitative assessment of the risk from the shared causes and coupling factors for a system with redundant components. The purpose of this research is to investigate the numerical relationship between common causes and CCF risk as well as to reduce the uncertainty in the system-specific CCF parameter estimation.

This dissertation presents an approach which is named as the alpha-decomposition method. A Hybrid Bayesian Network is adopted to demonstrate the relationship between component failures and possible causes. The alpha factors in the alpha-factor model are re-notated as global alpha factors and the CCF-triggering abilities of causes are notated as decomposed alpha factors. A regression model is determined and proved by the theory of conditional probability, in which the global alpha factors are represented by explanatory variables (cause occurrence frequencies) and parameters (decomposed alpha factors). A database combining with the CCF data and cause occurrence record is recommended to be built. The features of the alpha-decomposition method and calculation process are illustrated by a numerical example.

This dissertation demonstrates the analysis of modified system involving the construction and degradation of defense barriers against dependent failures. An important element in CCF analysis is the coupling factor. The coupling factor is the condition that multiple components are affected by the same cause. The susceptibility of a certain system to dependent failures will be changed if a defense mechanism is introduced to interrupt the coupling factor. After additional flood barriers are constructed, CCF parameters of the

Auxiliary Feedwater (AFW) Pump system are predicted according to the alpha-decomposition method. Furthermore, the seismic event will initiate the failure of non-safety related water supply systems and the degradation of additional flood barrier. A Markov model is introduced to model the degradation process of flood barriers. It is illustrated by a numerical example that the dynamic CCF risk analysis after the occurrence of seismically-induced internal flood and the failure of flood barriers. The prediction of CCF parameters can be applied in the estimation of basic events in nuclear Probabilistic Risk Assessment (PRA). This research describes an approach which can be used to evaluate the plant- and system- specific CCF parameters based on generic databases.

TABLE OF CONTENTS

This page is intentionally left blank.

LIST OF TABLES

Chapter 5

LIST OF FIGURES

This page is intentionally left blank.

Chapter 1: INTRODUCTION

1.1. Common Cause Failure

1.1.1. Definition of common cause failure

As a conclusion form Probabilistic Risk/Safety Assessment (PRA/PSA) for commercial Nuclear Power Plants (NPPs), the identification and quantification of Common Cause Failure (CCF) are of great importance. When safety analysts perform the plant-level PRA or the system-level reliability analysis, the dependent failures of redundant safety systems will be encountered. The term common cause failure refers to the dependent failures of functionally similar systems, such as backup feedwater pumps or multiple coolant injection systems. In the absence of dependent failures, the availability of safety systems or functions is improved by the introduction of redundancy or diversity, which is regarded as independent failures. Therefore, the effect of CCF is to increase the unavailability of redundant systems compared with cases of independent failures.

The early efforts of CCF analysis can be traced back to 1960s and the formal definition of CCF was preliminarily in one of the first publications in the nuclear industry, WASH-1400 (1975). In WASH-1400, common mode failures are defined as multiple failures that result from a single event or failure. The resulting multiple component failures can likewise encompass a spectrum of possibilities, including, for example, system failure caused by a common external event, multiple component failures caused by a common defective manufacturing process, and a sequence of failures caused by a common human operator. It should be noted that the term "common mode failure" is not precise for communicating the main character of CCF events. The dependent failure resulting from a shared cause or another component state should be distinguished.

Thereafter, several definitions of CCF have been suggested in literature. Mainly all the

definitions of CCF events encompass the dependent failures. The distinction is the definition of time duration during when dependent failures are classified as a group of CCF events. Some definitions are broad and essentially cover the entire set of dependent failures. Some definitions do not explain clearly about the duration of time interval. Other definitions focus on the time duration in the context of a particular application, such as PRA mission.

In NUREG/CR-4780 (A. Mosleh, 1988), common cause events are defined as a subset of dependent events in which two or more component fault states exist at the same time, or in a short time interval, and are a direct result of a shared cause.

In NUREG/CR-5485 (A. Mosleh, 1998), a CCF event consists of component failures that meet four criteria: (1) two or more individual components fail or are degraded, including failures during demand, in-service testing, or deficiencies that would have resulted in a failure if a demand signal had been received; (2) components fail within a selected period of time such that success of the PRA mission would be uncertain; (3) component failures result from a single shared cause and coupling mechanism; and (4) a component failure occurs within the established component boundary.

1.1.2. Main elements of common cause failure analysis

Generally, there are three main elements of CCF events, the failure cause, coupling factor and defense mechanism.

1) *Failure cause*: The cause of a failure event is a condition or a combination of conditions to which a change in the state of a component can be attributed. To identify the failure cause or the causal chain of conditions is important. The collection and classification of CCF data rely on the identification of causes. Several types of causes are applied in CCF analysis. A proximate cause associated with a component failure event is a characterization of the condition that is readily identifiable as having led to the failure. A root cause is the basic reason why components fail. Compared with root

causes, proximate causes are more identifiable but do not necessarily reflect the complete understanding of failure mechanism. Because it is difficult to determine the root causes, current CCF database only codes the proximate cause. In current dissertation, for the consideration of data collection, all causes simply refer to proximate causes.

2) *Coupling factor*: A coupling factor is a characteristic of a group of components that identifies them as susceptible to the same causal mechanisms of failure. After the occurrence of a shared cause, the coupling factor is the conductive meaning of simultaneous dependent failure. Coupling factors include the similarity in design, location, environment, mission and operational, maintenance, and test procedures. Therefore, the coupling factors are usually classified as (1) Quality based; (2) Design based; (3) Maintenance based; (4) Operation based; (5) Environment based.
3) *Defense mechanism*: To protect redundant systems against CCF events, it is necessary to understand and apply defense strategy. In engineering, the defense strategy is noted as defense mechanism. The defense mechanism for CCF systems can be functional barrier, physical barrier, monitoring and awareness, maintenance staffing and scheduling, component identification, diversity and others. As introduced before, there are two important elements related to the CCF occurrence mechanism, so two defense strategies can be applied in engineering: (1) the defense strategy against the failure causes; (2) defense strategy against coupling factors. Based on the seismic fragility analysis, to enhance the seismic capacity of safety-related components can defend against the earthquake. To construct flood barriers between compartments can preclude the propagation of flood, and the coupling factor is interrupted.

1.1.3. Parametric modeling for common cause failure

The mathematical treatment of CCF in PRA and reliability studies is well established in the literature and in practice. References have been published to introduce the basic principles and guidance for CCF analysis. The basic quantitative screening and parameterization of CCF event are simply introduced as follows.

Based on the qualitative analysis of redundant system, the system boundary can be identified. The group of components in the qualitative process is named as the Common Cause Component Group (CCCG). Generally, the functionally-identical components of a redundant system are assigned to a CCCG. To consider the CCF risk of a CCCG, the complete quantitative process is inevitable to be determined. The objective of quantitative screening is to decide reasonable parameters to represent the potential failure risk in a redundant system. The risk of independent dependent failure can be decided based on the parametric model, and then the failure probability of the redundant system can be calculated. The relationship between components failure and system failure can be displayed with fault trees. Let us consider a CCCG composed of three redundant components A, B, and C. There are three basic events in the fault tree, (1) A Fails; (2) B Fails; (3) C Fails. There two possible failure scenarios for each component, independent failure or CCF. If only independent failure and global CCF are considered, the basic events can be shown as Figure 1.1.

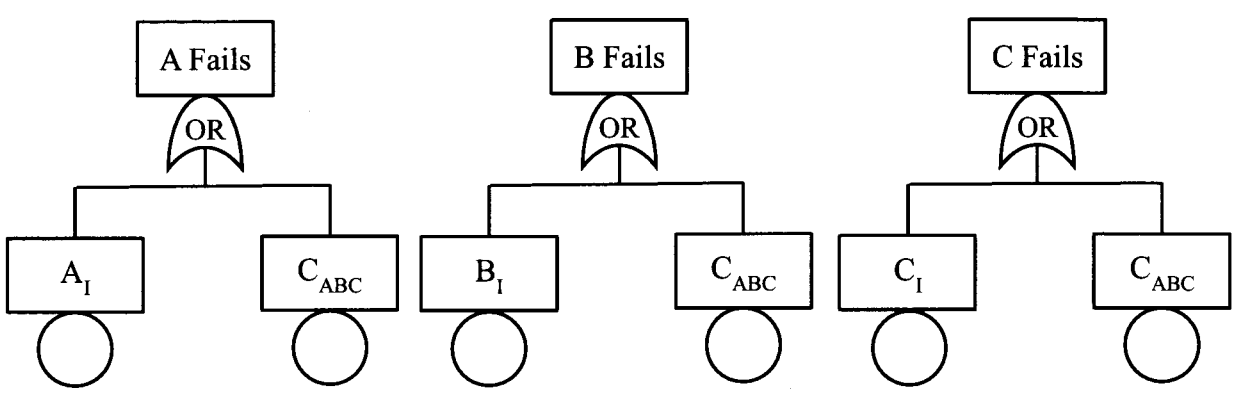

Figure 1.1 Fault trees for basic events

The simplest model of CCF basic events can be represented with a single parameter model. Take the basic event of the component A as an example,

$$P(A_I) = (1-\beta) \bullet P(A)$$
$$P(C_{ABC}) = \beta \bullet P(A) \qquad \text{Equation 1.1}$$

Here, $P(A)$ is the total failure probability of the component A; $P(A_I)$ is the independent failure probability of the component A; $P(C_{ABC})$ is the CCF probability of components A, B and C; β is the single parameter which represents the ratio of common cause failure.

The single parameter model provides a simple way to model the CCF risk. This representative example shows the basic quantitative process of CCF modeling. More detailed review of previous CCF modeling can be obtained in Chapter 2.

1.2. Bayesian Inference in Probabilistic Risk Assessment

1.2.1. Hierarchical model in probabilistic risk assessment

The term "inference" is defined as the process of obtaining a conclusion based on the information available, e.g. operational data and expert experience, etc. The Bayesian inference means the using of Bayes' theorem in which information is used to obtain the most reasonable posterior distribution of a parameter. Probabilistic Risk Assessment (PRA) is a mature technology that can provide a quantitative assessment of the risk from accidents in nuclear power plants. In the process of PRA, it involves the development of models via tool such as Fault Trees and Event Trees, etc. According to the occurrence of initiating events, the response of safety-related systems can be delineated by PRA models. Therefore, the estimation of risk can be obtained by propagating the uncertainty distributions of key parameters through these models. The calculation of final integrated parameters is of great

importance, e.g. Core Damage Frequency (CDF), Large Early Release Frequency (LERF), etc. The PRA models are hierarchical and complex, so the integrated parameters are intractable by traditional probabilistic methods.

1.2.2. Bayesian inference with conjugate prior distribution

In nuclear PRA, the values of observations x are initially uncertainty and described through a probability distribution with probability density function $f(x|\theta)$. Here, the mathematical treatment is unified without differentiation between discrete and continuous quantities. The quantity θ is the index of the family of interested parameters. With the consideration of important parameters, the observations can be predicted with reasonable uncertainties. Therefore, the probability density function of θ is of great interests. It is likely PRA analysts has some knowledge about the density function of $\pi_0(\theta)$, even though the knowledge may not be precise. Hence, it is useful to incorporate the knowledge $\pi_0(\theta)$ with the observations x. Usually, is called prior distribution. Observational $f(x|\theta)$ is called likelihood function. The likelihood function provides the chances of each θ leading to observed value of x. The posterior distribution $\pi_1(\theta|x)$ of θ can be obtained via Bayes' theorem

$$\pi_1(\theta|x)=\frac{f(x|\theta)\pi_0(\theta)}{\int f(x|\theta)\pi_0(\theta)d\theta} \qquad \text{Equation 1.2}$$

Because the denominator is simply a constant, the Bayes' theorem can be written in a more compact chain form

$$\pi_1(\theta|x)\propto f(x|\theta)\pi_0(\theta) \qquad \text{Equation 1.3}$$

The target posterior distribution is not analytically tractable. In the past, intractability was avoided via the use of conjugate prior distributions. If the posterior distribution $\pi_1(\theta|x)$ are in the same family as the prior distribution $\pi_0(\theta)$, the prior and posterior are then called conjugated distributions, and the prior is called a conjugate prior for the likelihood. For example, the gamma distribution is conjugate to itself, and for the binomial distribution, the conjugate prior is a beta distribution. Different distributions can have the same conjugate prior e.g. Poisson and Exponential distributions are conjugate to gamma distributions.

Prior distributions can be classified as either informative or noninformative. Informative priors contain previous known information about the value of parameters. Noninformative priors do not contain substantive information about the value of parameters. Noninformative priors (such as Jeffreys noninformative prior) are widely used in nuclear PRA, which allow the observation to speak for themselves. There is a compromise distribution between an informative prior and the noninformative prior, which is called constrained noninformative prior. For Poisson distribution, the constrained noninformative prior is a gamma distribution with certain shape parameters.

Example 1.1 Poisson inference with conjugate prior

The Poisson distribution is widely used to model the Sampling Test in Quality Assurance. The numbers of flows and failures in one test scheme are denoted by g^{Fl} and g^{Fa}, respectively. Hence, the probability density distribution can be written as

$$g^k \sim Poisson(\lambda^k), k \in \{Fl, Fa\} \qquad \text{Equation 1.4}$$

Here, λ^{Fl} is the expected number of flaws; λ^{Fa} is the expected number of failures.

If there is no available information, the low-informative prior (e.g. $gamma(0.01,0.01)$) can be used. During two testings, it is assumed that the record of flaws

and failures is $g^{Fl}=(3,4)$ and $g^{Fa}=(2,1)$, so the posterior distribution $\pi_1\left(\lambda^k|g^k\right)$ of parameters can be written as

$$\lambda^{Fl}|\boldsymbol{g} \sim gamma(7.01,2.01)$$
$$\lambda^{Fa}|\boldsymbol{g} \sim gamma(3.01,2.01) \qquad \text{Equation 1.5}$$

The posterior distributions are shown in Figure 1.2. The mean value of flaws and failures can be calculated as

$$E\left(\lambda^{Fl}|\boldsymbol{g}\right)=3.488,\ E\left(\lambda^{Fa}|\boldsymbol{g}\right)=1.498.$$

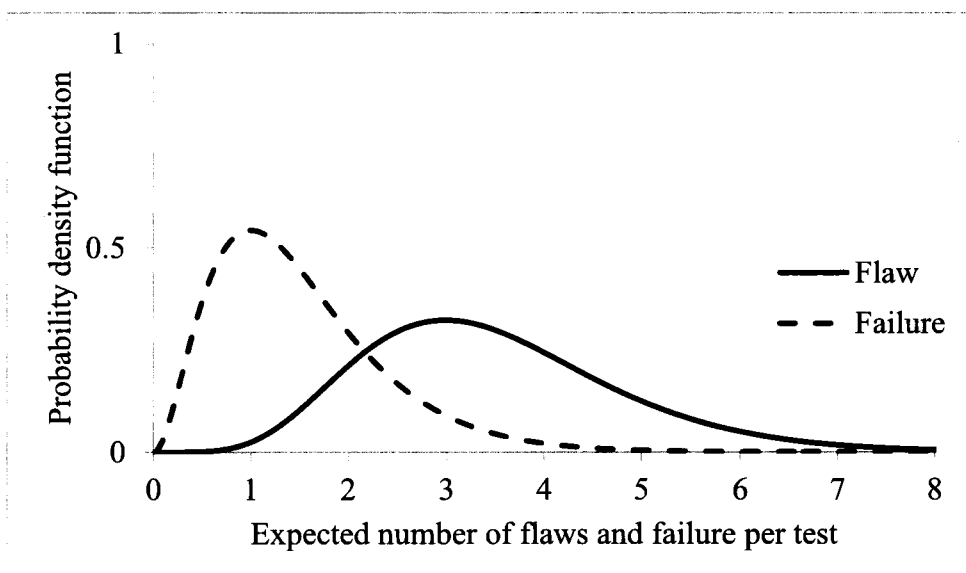

Figure 1.2 Posterior distributions for conjugate example

However, not every aleatory model will have an associated conjugate prior. In the practical PRA analysis, analysts may sometimes choose to use a nonconjugate prior even when a conjugate prior exists. Under these scenarios, the integration will become intractable and Monte Carlo integration will be necessary.

1.2.3. Bayesian inference with Markov Chain Monte Carlo

For many years, Bayesian theory was unable to be established as a well-accepted quantitative approach for data analysis. The main reason is the intractable integration involved in the calculation of the posterior distribution. Asymptotic methods had provided solutions to specific problems, such as conjugate distributions, but no generalization was available. Since the beginning of 21^{st} century, the application of Bayesian statistics in science and engineering has been becoming fashionable. The advent of Markov Chain Monte Carlo (MCMC) sampling opened highways for statistical research. With the MCMC sampling, the Bayesian inference works for simple and well-supported cases, but more importantly, it works efficiently on complex and multi-dimensional problems.

With the development of MCMC algorithms, computational software appeared. During the late 1990s, Bayesian inference Using Gibbs Sampling (BUGS) emerged in the foreground. BUGS is a free software that fits complicated hierarchical models in a relatively easy manner. Thereafter, the Window version of BUGS (WinBUGS) has earned great popularity in various fields. Now, more recent advances leads the software to an open-source version (OpenBUGS). The intractable integrations can now be solved with these software packages.

Example 1.2 Poisson inference with nonconjugate prior

Take the Poisson distribution in Sampling Test as an example again. If a lognormal distribution is assumed by PRA analysts as the prior for the lambda in the Poisson distribution, the computation can be fulfilled with OpenBUGS. During two identical testing interval, the observed data of flaws and failures is $g.Fl = (3,4)$, and $g.Fa = (2,1)$, respectively. The nonconjugate prior distributions for parameters (lambda in Poisson distributions) are assumed as lognormal distribution (with a median of 1×10^{-8} / *testing episode* and a range factor of

100). Hence, the posterior distributions for parameters can be obtained. The OpenBUGS script is shown in Table 1.1. The summary of posterior distributions for parameters is shown in Table 1.2. The expected value of flaws and failures during one testing interval can be calculated. The observed data and previous knowledge of testing results are credited. The density curves of posterior probabilities are shown in Figure 1.3. Curves show different attributes compared with the example of conjugate priors. It is important to find a minimally informative prior distribution in Bayesian inference.

Table 1.1 OpenBUGS script for Poisson inference with nonconjugate prior

```
model {
for (i in 1:2) {
g.Fl[i] ~ dpois(lambda.Fl)                    # Poisson distribution for flaws
g.Fa[i] ~ dpois(lambda.Fa)                      and failures
}
lambda.Fl ~ dlnorm(mu.Fl, tau.Fl)             # Lognormal prior distribution for
lambda.Fa ~ dlnorm(mu.Fa, tau.Fa)               lambda.Fl and lambda.Fa
mu.Fl <- log(prior.median.Fl)                 # Calculate prior mu.Fl and
mu.Fa <- log(prior.median.Fa)                   mu.Fa from lognormal mean
tau.Fl <- pow(log(RF.Fl)/1.645, -2)           # Calculate prior tau.Fl and tau.Fa
tau.Fa <- pow(log(RF.Fa)/1.645, -2)             from lognormal range factor
}
data
list(g.Fl = c(3,4), g.Fa = c(2,1), prior.median.Fl = 1.E-8,
prior.median.Fa = 1.E-8, RF.Fl = 100, RF.Fa = 100)
```

Table 1.2 Summary of posterior distribution for the nonconjugate example

Parameter	Mean	Median	95% Interval
Lambda (Flaw)	2.285	2.122	(0.715, 4.799)
Lambda (Failure)	0.407	0.275	(0.015, 1.527)

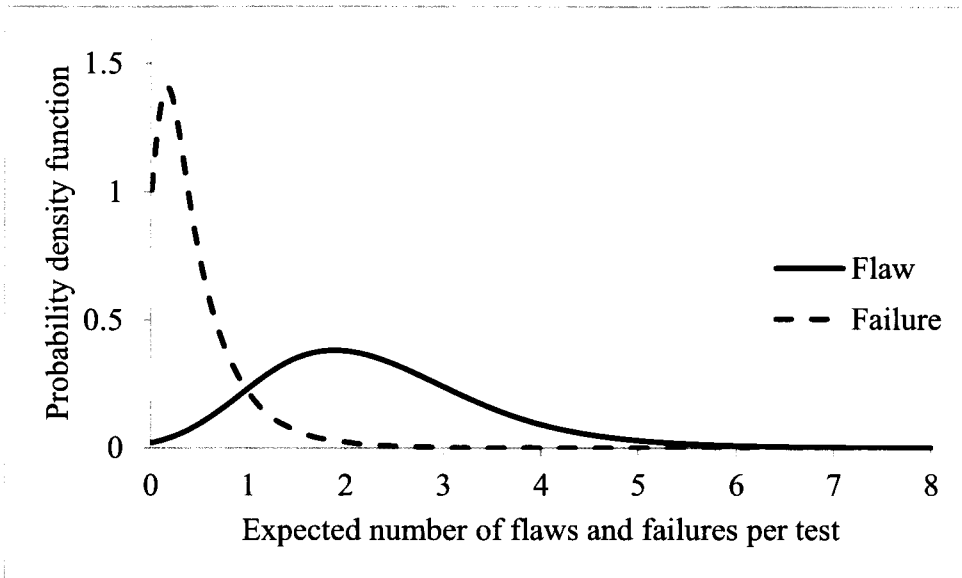

Figure 1.3 Posterior distributions for the nonconjugate example

1.3. Research Motivation

In recent decades, great achievements have been obtained in the context of CCF modeling. Basic parameter models for CCF analysis have been well established in the literature and in practice. The lumped basic parameters reflect the CCF risk of targeted redundant systems. The estimation of basic parameters is based on the generic operation data. From the perspective of Bayesian inference, the posterior distributions for basic parameters are updated according to the evidence of failure event data. Basic parameters are integrated result of failure information and cause occurrence information. There are unknown uncertainties in the probability or density distribution of parameters, which can result from

1) Scarce common cause failure data and imprecise CCF data.

2) The generic operation database which is used to estimate the plant-specific and system-specific CCF parameters.
3) Omission of valuable information, e.g. causal inference.
4) Dynamic operation conditions which are not reflected in the CCF parameters but important in time-dependent reliability analysis.
5) Innate known uncertainty in the prediction of some common causes, which rarely happen but are of significant risk.

Therefore, it is important to estimate CCF parameters from the viewpoint of uncertainty analysis. The uncertainty sources in parameter estimation should be determined. Previous parametric model cannot evaluate the uncertainty sources in basic parameters. It is interesting to develop a method for further analysis of CCF.

The quantitative analysis procedure of plant-specific and system-specific CCF event should be determined. In response to the lessons learned from the Fukushima-Daiichi nuclear power station accident, the safety margins evaluation and safety enforcement of the NPPs are necessary immediately. The defense strategies against the CCF are of great importance, especially that against CCFs which are caused by external events. It is necessary to consider the change of safety-related parameters in the procedure of PRA when modifications are applied. However, the generic data based basic parameter models of CCF cannot take into account the specific system-design. For instance, flood barriers are recommended to be built in Turbine Building at the PWR NPP. The operation environment of Auxiliary Feedwater (AFW) pumps is modified. The CCF parameters should be able to reflect certain improvement and modification. Moreover, the happen of an earthquake will exacerbate the operation environment of AFW pump. The conditional risk of internal flood and flood barrier failure will propagate. The CCF parameter estimation should be able to reflect the dynamic or event-based scenario. Therefore, it is necessary to develop a method to update CCF parameters based on possible modification of redundant system.

Chapter 2: LITERATURE REVIEW

In recent decades, numerous parametric models have been proposed, and some have been widely used in the nuclear PRA analysis. Parameters in models represent the CCF risk of targeted redundant systems. In this chapter, the main characteristics of these useful models are reviewed. Two major categories of parametric models are Nonshock Model and Shock Model.

The nonshock model estimate CCF event probabilities without considering the failure process. The Beta Factor Model, Multiple Greek Letter (MGL) Model and Alpha Model are representative models of the nonshock category, which are also called Basic Parameter Models (BPMs). The parameters of BPMs can be estimated based on a source of data, e.g. generic operation database.

The shock model takes into account of failure mechanism. Causes are divided as independent causes and common causes, so the shock model treated the causal analysis in a rather simple way. The CCF event in shock model is considered as the shock-caused consequence, and the conditional probability given the occurrence of shocks.

2.1. Beta Factor Model

The beta factor model is a single parameter model. The factor (β) represents the ratio of CCF probability in total failure probability. The beta factor model is the simplest BMP. It is assumed that whenever a common cause event occurs, all components in a CCCG fail simultaneously. Hence, as shown in Figure 2.1, the total failure probability (Q_t) of one component is separated as the independent part (Q_I) and the CCF part (Q_{CCF}).

$$Q_I = (1-\beta)Q_t$$

$$Q_{CCF} = \beta Q_t \qquad \text{Equation 2.1}$$

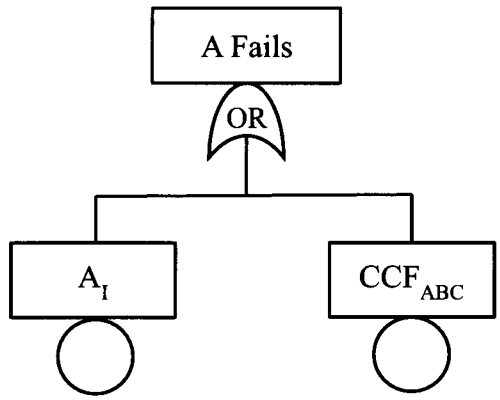

Figure 2.1 Fault tree of component A failure

Using the beta factor model can simply model the CCF risk of a redundant system. Let consider a 2-out-of-3 system as an example. It means that there are three redundant components in the targeted system. If two of two components fail, the system will fail. The fault tree of the system failure is shown in Figure 2.2. Therefore, there is no CCF event involving two component with the beta factor model.

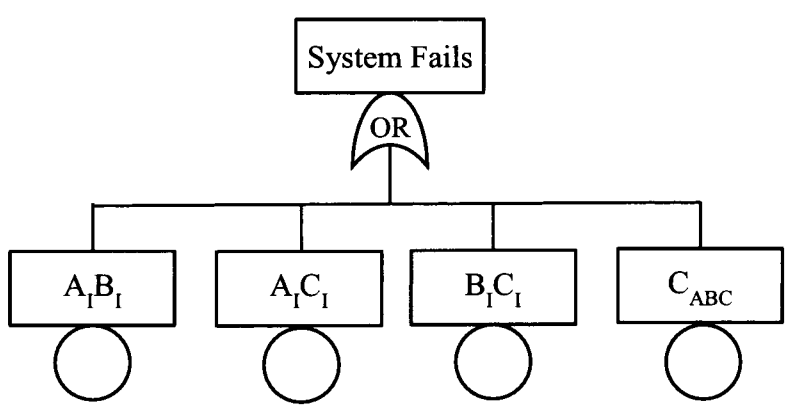

Figure 2.2 Fault tree of 2-out-of-3 system with the beta factor model

The mathematical form of beta factor can be obtained by

$$\beta = \frac{Q_{CCF}}{Q_I + Q_{CCF}} = \frac{Q_{CCF}}{Q_t} \qquad \text{Equation 2.2}$$

Therefore, the estimation of the beta factor can be conducted by Bayesian inference. The proper prior distribution and likelihood function should be well defined. According to the observed CCF data, the posterior distribution of the beta factor can be calculated.

Example 2.1 Bayesian inference for Beta Factor estimation

The binomial can be used as the aleatory model for failure states of components in the beta factor model. When a failure is observed, the failure is either an independent failure or global dependent failure. A conjugate prior of binomial distribution is the beta distribution. Two parameters (a_{prior} and b_{prior}) are required to specify the prior beta distribution. The posterior distribution is also a beta distribution with parameters (a_{post} and b_{post}). If n failures are observed and x failures are CCFs, so $n-x$ failures are independent failures. The parameters of posterior beta distribution can be written by

$$a_{post} = a_{prior} + x \qquad \text{Equation 2.3}$$

$$b_{post} = b_{prior} + n - x \qquad \text{Equation 2.4}$$

Therefore, the mean values of prior and posterior beta factors are given by

$$\beta_{prior} = \frac{a_{prior}}{a_{prior} + b_{prior}} \qquad \text{Equation 2.5}$$

$$\beta_{post} = \frac{a_{post}}{a_{post} + b_{post}} = \frac{a_{prior} + x}{a_{prior} + b_{prior} + n} \qquad \text{Equation 2.6}$$

The noninformative beta prior is the beta distribution with all parameters equaling 0. The calculation of the posterior beta factor can be conducted with BETAINV() function in a spreadsheet or by OpenBUGS. The script of OpenBUGS for the beta factor estimation is

shown in Table 2.1. An informative beta distribution is assumed as the prior distribution. Prior parameters and observed data are assumed as $a_{prior} = 2, b_{prior} = 18; x = 19, n = 115$. The probability density functions of prior and posterior distributions for beta factor are shown in Figure 2.3. The posterior distribution of beta factor is the integrated result of the informative prior distribution and the observed data. The estimate based on more observed information is of less uncertainty. The posterior beta factor is attributed with the mean value of 0.156 and the 95% credible interval of (0.099, 0.221).

Table 2.1 OpenBUGS script for the beta factor estimation

```
model {
x ~ dbin(beta, n)                          # Binomial aleatory model
beta ~ dbeta(a.prior, b.prior)             # Conjugate beta prior for beta factor
beta.0 ~ dbeta(a.prior, b.prior)           # Prior distribution for comparison
}
data
list(a.prior = 2, b.prior = 18, x = 19, n = 115)   # Observed failure data and prior parameters
```

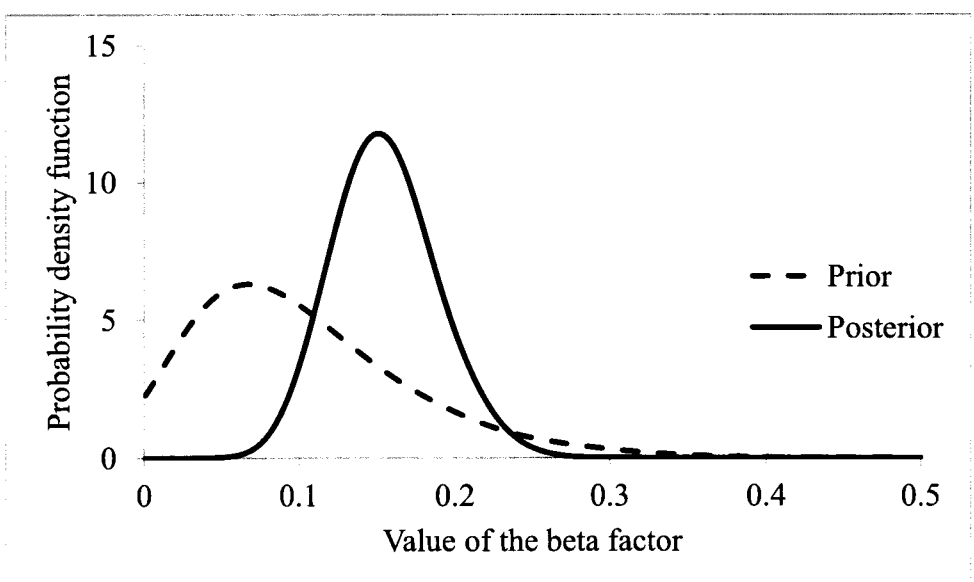

Figure 2.3 Prior and posterior distributions for the beta factor model

For a redundant system of multiple components, the beta factor model generally generates conservative. Because of the limitation of single parameter model, multi-parameter model are recommended to be used.

2.2. Multiple Greek Letter Model

The MGL model is the most general extension of the beta factor model. Except for the beta factor, more parameters are introduced to account for higher order redundancies. In other words, not only the independent failure and global dependent failure, but also the partial dependent failure can be expressed by the MGL model.

The total failure probability of one component is denoted as Q_t. The total failure probability includes all types of failure for one component, such as independent, partial and total dependent failures. Take the 2-out-of-3 system as an example, the total failure probability can be written as

$$Q_t = Q_1 + 2Q_2 + Q_3 \qquad \text{Equation 2.7}$$

Here, $Q_k \ (k = 1,2,3)$ is the failure including k components.

Therefore, the MGL parameters can be given by the failure probabilities of single component. For the 2-out-of-3 components, two parameters (β *and* γ) are used to represent the risk of CCF event. The parameter (β) is the conditional probability that the cause of a component failure will be shared by one or two additional components, given that a specific component has failed. The parameter (β) is the conditional probability that the cause of a component failure that is share by one or more components will be shared by two or some additional components, given that two specific components have failed.

$$\beta = \frac{2Q_2 + Q_3}{Q_1 + 2Q_2 + Q_3}$$

$$\gamma = \frac{Q_3}{2Q_2 + Q_3} \qquad \text{Equation 2.8}$$

Estimates for the MGL parameters are relatively difficult to obtain, but the calculation process can be simplified via another BPM (the alpha factor model). The calculation example of the MGL model by Bayesian inference will be introduced in next section. The conversion formulae between the MGL model and the alpha factor model are given in related references.

2.3. Alpha Factor Model

The alpha factor model is most widely used BPM in nuclear PRA. The calculation process is much easier than the MGL model. The alpha factor model is a multi-parameter model. Parameters in the alpha factor model are event-based, which can be obtained from generic operation database. The estimation of alpha factors are affected by the specific testing scheme applied in actual analysis. The alpha factor model is the basis of this dissertation. The fault tree on component level of 2-out-of-3 system is shown in Figure 2.4. Three identical components, A, B, and C, are assumed in the redundant system.

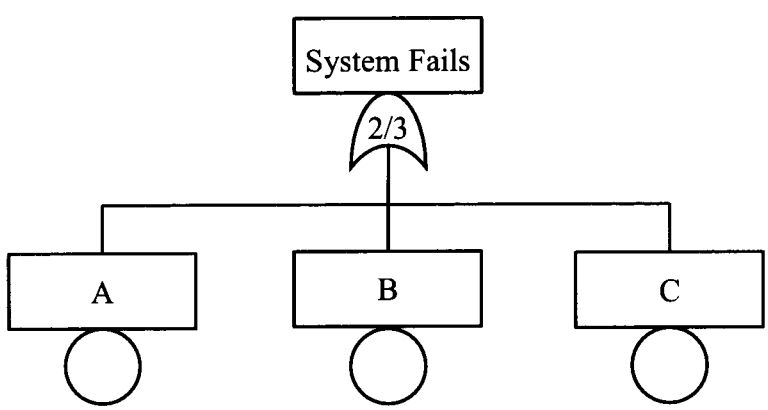

Figure 2.4 Fault tree on component level

From Figure 2.3, the basic events of this redundant system can be written as

$$\{A,B\};\{A,C\};\{B,C\};\{A,B,C\}$$

Here, the first three events compose of the minimal cutsets of the redundant system. Generally, the theory of minimal cutset is used in reliability analysis, but the separation of minimal cutsets will neglect the global common cause failure of three redundant components.

The fault tree on component level can be expanded to learn the failure mechanism of one component. The expansion of the fault tree for component A is displayed in Figure 2.5. There are three failure types of component A including independent failure, partial CCF and global CCF. Therefore, the basic events of system failure can be given by the failure types of components.

$$\{A_I,B_I\};\{A_I,C_I\};\{B_I,C_I\};\ \{C_{AB}\};\{C_{AC}\};\{C_{BC}\};\ \{C_{ABC}\};$$

Here, X_I is the failure of component X from independent causes; C_{XY} is the failure of components X and Y from common causes; C_{ABC} is the failure of components A, B, and C from common causes.

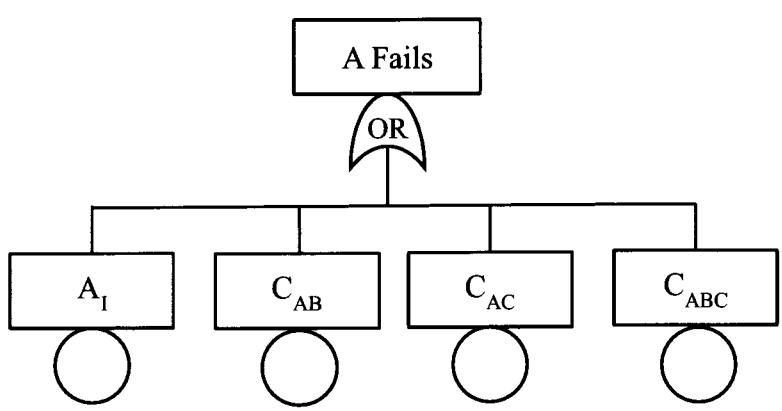

Figure 2.5 Fault tree of component A failure

Using the rare event approximation, the system failure probability of the 2-out-of-3 system is given by

$$P(S)=P(A_I)P(B_I)+P(A_I)P(C_I)+P(B_I)P(C_I)+P(C_{AB})+P(C_{AC})+P(C_{BC})+P(C_{ABC})$$

Equation 2.9

The total failure probability of component A is denoted as Q_t. It is the same to the MGL model that the total failure probability (Q_t) can be expressed by

$$Q_t = Q_1 + 2Q_2 + Q_3 \qquad \text{Equation 2.10}$$

Therefore, the definition of alpha factors can be obtained based on certain testing schemes. Different testing schemes affect the collection of CCF data and the estimates of CCF parameters are different. Usually, there two testing schemes: staggered testing scheme and non-staggered testing scheme. In the case of staggered testing scheme, only one component is tested in a test episode. If the result is a failure, the rest of components will be tested. In the case of non-staggered testing scheme, all components in the CCCG are tested in a test episode. Regarding the way systems in the databases are tested, it is necessary to select different parameter models reasonably.

For a staggered testing scheme, the alpha factors of the 2-out-of-3 system are written as

$$\alpha_1 = \frac{Q_1}{Q_t}$$

$$\alpha_2 = \frac{2Q_2}{Q_t} \qquad \text{Equation 2.11}$$

$$\alpha_3 = \frac{Q_3}{Q_t}$$

For a non-staggered testing scheme, the alpha factors of the 2-out-of-3 system are written as

$$\alpha_1 = \frac{Q_1}{Q_t} \times \alpha_t$$

$$\alpha_2 = \frac{Q_2}{Q_t} \times \frac{\alpha_t}{2} \qquad \text{Equation 2.12}$$

$$\alpha_3 = \frac{Q_3}{Q_t} \times \frac{\alpha_t}{3}$$

Here, $\alpha_t = \alpha_1 + 2\alpha_2 + 3\alpha_3$.

In this dissertation, the staggered testing scheme is selected to introduce current research. The alpha factors represent the CCF risk involving respective number of components. The estimation of alpha factors can be conducted by the Bayesian inference.

When the alpha factor model is applied, there are multiple possible outcomes and the CCF probabilities are constant alpha factors. The aleatory model for CCF events is generally assumed as multinomial distribution. For the system with three redundant components, the vector $\boldsymbol{X} = (x_1, x_2, x_3)$ follows a multinomial distribution with parameters $\boldsymbol{\alpha} = (\alpha_1, \alpha_2, \alpha_3)$. The $x_j \ (j = 1,2,3)$ is the CCF event including j components and the respective $\alpha_j \ (j = 1,2,3)$ represents the probability of the CCF event including j components. Because the sum of all alpha factors equals 1 (as shown in Equation 2.13), the vector of alpha factors can be well established as Dirichlet distribution. The conjugate prior of multinomial distribution is the Dirichlet distribution. A noninformative prior for the multinomial distirubion is the Dririchlet with $\theta_k = 1 (k = 1,2,3)$.

$$\sum_{j=1}^{3}\alpha_j = 1 \qquad \text{Equation 2.13}$$

Example 2.2 Bayesian inference for the alpha factor model and MGL model

The redundant have a CCCG of three components. According the observed data, it has suffered 50 failures. 40 of these are independent failures, 7 are partial dependent failures, and 3 are global dependent failures. So the vector of CCF events is $\boldsymbol{X} = (40,7,3)$, which follows multinomial distribution. Alpha factors are inferred based on this operation data. The informative prior of Dirichlet distribution is assumed.

$$\boldsymbol{X} \sim Multinomial(\alpha_1, \alpha_2, \alpha_3) \qquad \text{Equation 2.14}$$

$$Prior\ \boldsymbol{\alpha} \sim Dirichlet(1,1,1) \qquad \text{Equation 2.15}$$

The parameters in the MGL model are given according to the conversion formulae from alpha factors to MGL parameters. The OpenBUGS script for estimation CCF parameters is shown in Table 2.2.

$$\beta = \alpha_2 + \alpha_3$$

$$\gamma = \frac{\alpha_3}{\alpha_2 + \alpha_3} \qquad \text{Equation 2.16}$$

The summary of posterior distributions for CCF parameters is shown in Table 2.3. The probability density functions are shown in Figures 2.6 and 2.7. Alpha and MGL factors reflect the CCF risk including certain number of components. According to the curves in Figure 2.6, prior alpha factors are of great uncertainty. The posterior distributions integrate the observed data information and prior judgment, so these are of less uncertainty. The estimation of CCF

parameters provides more accurate PRA results.

Table 2.2 OpenBUGS script for the estimation of the alpha and MGL factors

```
model {
x[1:3] ~ dmulti(alpha[1:3], X)          # Aleatory model with multibinomial
                                          likelihood function
X <- sum(x[1:3])                        # Total of failure events
alpha[1:3] ~ ddirich(theta[])           # The noninformative prior for alpha
alpha.0[1:3] ~ ddirich(theta[])         # Prior for comparison
beta <- alpha[2] + alpha[3]             # Conversion from the alpha factor model
gamma <- alpha[3]/(alpha[2] + alpha[3])   to the MGL model
beta.0 <- alpha.0[2] + alpha.0[3]       # Prior for comparison
gamma.0 <- alpha.0[3]/(alpha.0[2] + alpha.0[3])
}
data
list(x=c(40,7,3), theta=c(1,1,1))
```

Table 2.3 Summary of posterior distribution for alpha and MGL factors

Parameter	**Mean**	**Median**	**95% Interval**
Alpha-1	0.774	0.778	(0.652, 0.872)
Alpha-2	0.151	0.147	(0.070, 0.256)
Alpha-3	0.075	0.069	(0.021, 0.161)
Beta	0.226	0.223	(0.128, 0.348)
Gamma	0.331	0.319	(0.109, 0.613)

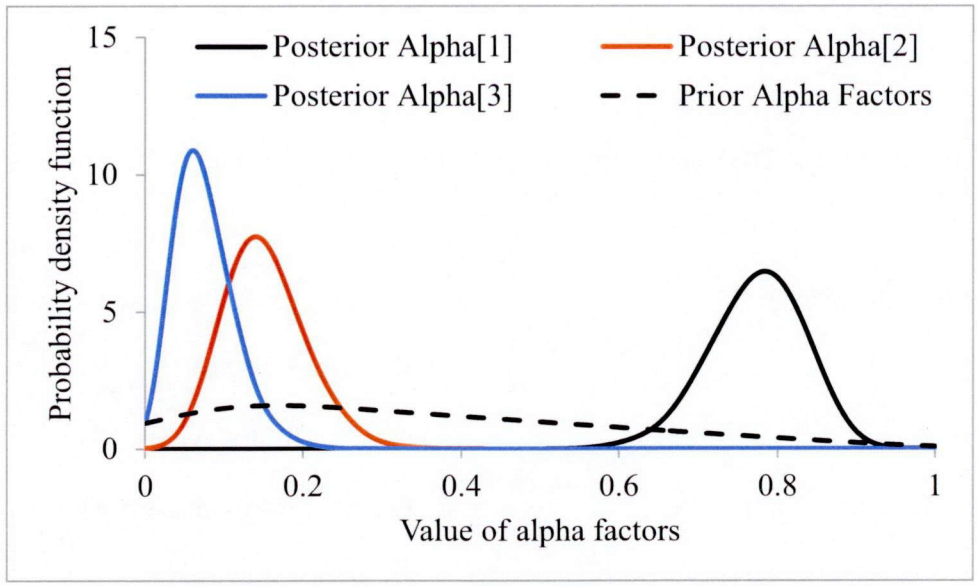

Figure 2.6 Prior and posterior distributions for alpha factors

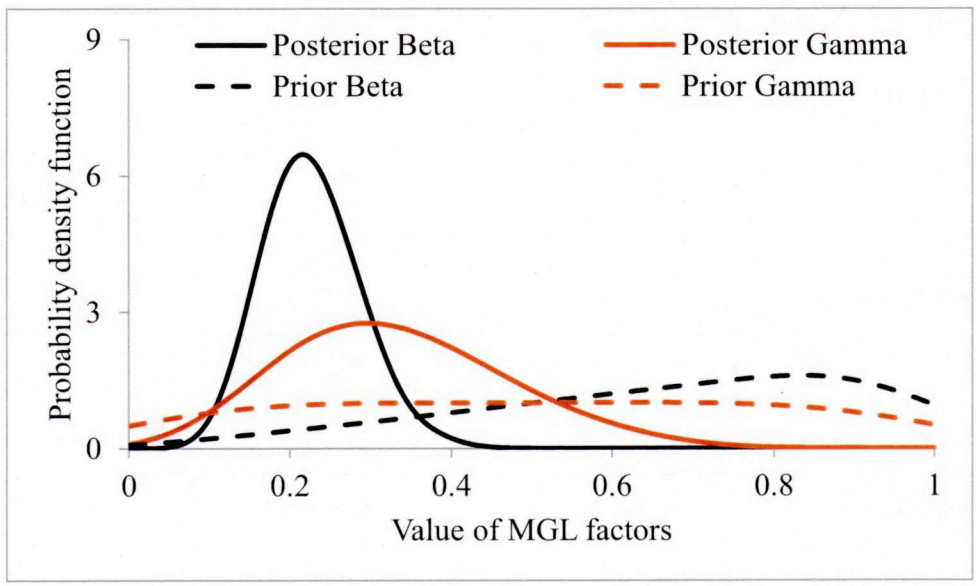

Figure 2.7 Prior and posterior distributions for MGL factors

2.4. Binomial Failure Rate Model

The Binomial Failure Rate (BFR) model is a shock model. The same to previous introduced nonshock models, the BFR model includes two types of failures. One is independent failures and the other is dependent failures caused by shocks. Shocks are

classified as lethal shock and nonlethal shock. The probability of independent failure is assumed as a constant. The lethal shock leads to a global CCF event. The nonlethal shock leads to a failure of one component following a binomial distribution. Therefore, the occurrence frequency of shocks and the conditional probability given a shock are important elements in the BFR model. The assumptions of constant independent failure probability and conditional CCF risk restrict the application of the BFR model. Both of aleatory models are assumed as binomial distribution.

The failure probability of CCF event involving j components for a system with n redundant components is given as

$$Q_j^{(n)} = \begin{cases} Q_I + \mu\rho(1-\rho)^{n-1} & j=1 \\ \mu\rho^j(1-\rho)^{n-j} & 2 \le j \le n-1 \\ \mu\rho^n + \omega & j=n \end{cases} \qquad \text{Equation 2.17}$$

Here, Q_I is the independent failure probability of each component; μ is the occurrence frequency of nonlethal shocks; ρ is the conditional probability of each component given a nonlethal shock; ω is the occurrence frequency of lethal shocks. It can be seen from Equation 2.17 that all the CCF risk significance from nonlethal shocks are treated as same. The dual separation of shocks is too rough to estimate a system of high redundancy. In other words, the failure probability will be underestimated for highly redundant system. The estimation process of conditional failure probability is similar to that of the beta factor model.

2.5. Event Assessment and Dana Kelly Causal Inference Framework

Event assessment is an application of PRA in which observed equipment failures and outages are mapped on to the risk model to obtain a numerical estimation of the event's risk significance. In an event assessment, the failure probability is considered given the event or

conditions that exist, for instance, a redundant component fails or goes to out of service. The availability of the redundant system is changed after the occurrence of these events. The CCF probability is accounted given on certain scenarios to avoid underestimating important safety-related parameters. The main mathematical theory used in event assessment of CCF is conditional probability.

Dana Kelly et al. proposed a preliminary framework for CCF analysis, which uses a Bayesian network to model underlying causes of failure, and which has the potential to overcome the limitations of the basic parameters models with respect to event assessment. The risk significance of degraded conditions can be evaluated by the causal inference framework.

Consider a CCCG consisting of two redundant Emergency Diesel Generators (EDGs). During a surveillance test, EDG A fails to run. There is a root cause of the failure of EDG A. The risk evaluation of this scenario requires an estimate of the failure probability of EDG B given the failure of EDG A and the investigated root cause. This framework can provide an analysis of CCF from the perspective of Bayesian network based causality and conditional probability.

Chapter 3: THE ALPHA-DECOMPOSITION METHOD

3.1. The Concept of Decomposition in Parameter Estimation

During the last decades, the nuclear industry has recognized the PRA has evolved to the point where it can be used in a variety of applications including as a tool in the regulatory decision-making process. One requirement for PRA analysis used to develop risk-specific application is to determine the important parameter distributions. For instance, in the severe accident analysis, an accident sequence's possibility of damaging reactor fuel, Core Damage Frequency (CDF), Large Early Release Frequency (LERF) or latent cancer fatality are used as surrogates for risk. These risk surrogated are most distinct representatives of accident risk or consequence. Tremendous effort and knowledge should be relied on to learn these risk surrogates. Efforts include determination of both plant-specific and generic estimates for initiating event frequencies, important safety-related system failure rates and unavailability, and component and equipment failure or non-recovery probabilities.

Because the important risk surrogates (CDF, LERF) are affected by the parameters, the relationship between risk surrogates and parameters should be determined by PRA methods. Event Trees (ET) and Fault Trees (FTs) are used to do the inference. It is called the decomposition of final states on system and component level in this dissertation, which means that the accident risk is an integrated reflection of multiple independent or partially dependent elements. Figure 3.1 shows the PRA analysis of Pressurized Thermal Shock (PTS), which is a severe transient in a PWR NPP. The risk of PTS and Core Damage (CD) are affected by the states of secondary feedwater systems. In order to quantitatively estimate the risk surrogates, the failure probabilities of feedwater systems should be well established. The ET in Figure 3.1 shows the relationship between interested end states and parameters on system level (failure probabilities of feedwater systems). The status of secondary pressure influences the pressure and temperature in the Reactor Coolant System (RCS), since the RCS and the secondary side

of the PWR are thermally-hydraulically coupled in most scenarios. Moreover, the status of secondary feedwater systems influences the pressure and temperature in the RCS. To calculate the failure probability of each system, the FT tool is used. For instance, the availability of Auxiliary Feedwater systems is affected by the status of three AFW pumps. This is called the decomposition on component level. Based on the failure probabilities of components, the unavailability of the targeted system can be obtained. Therefore, the complicated estimates of PTS and CD can be expressed by parameters on system- and component-level via the tools of ET/FT.

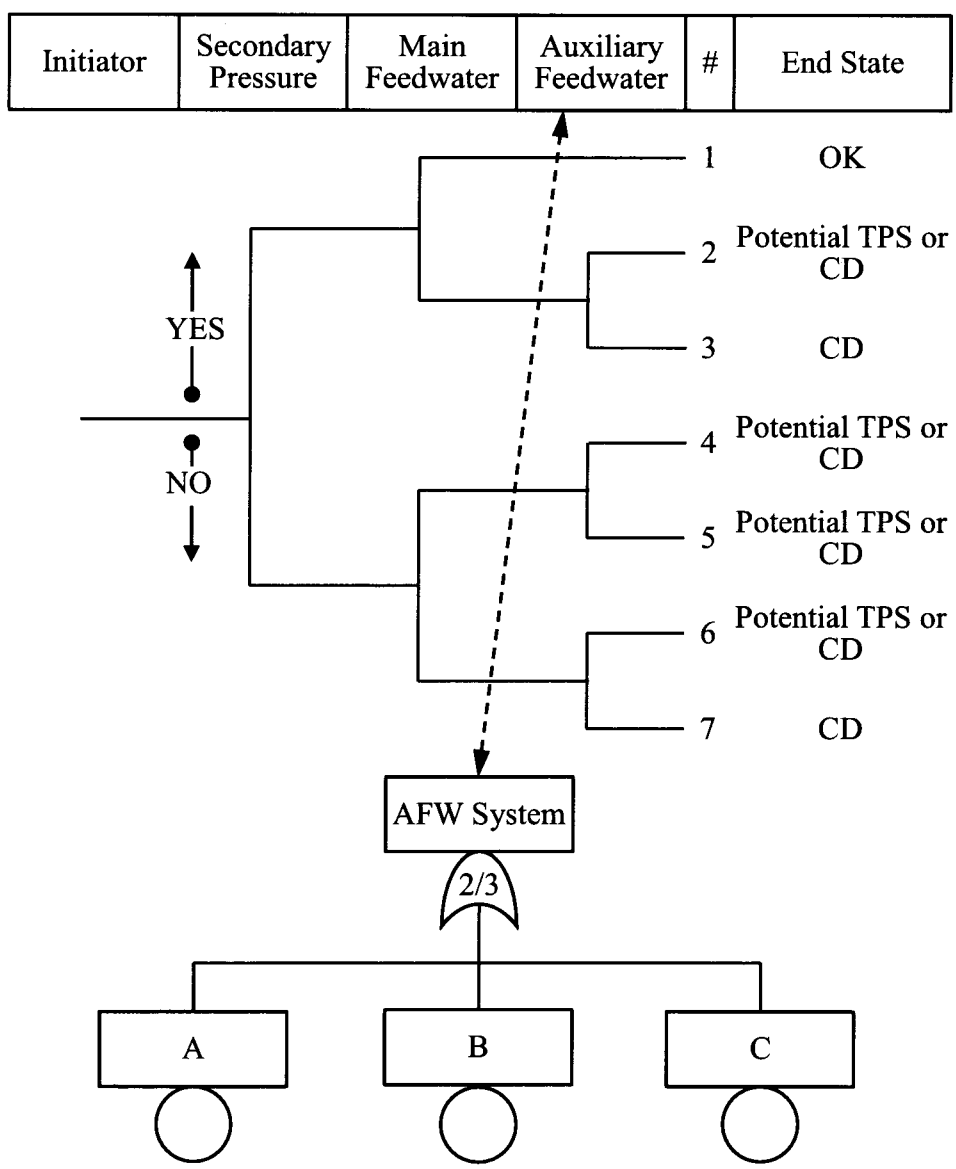

Figure 3.1 Simplified event tree for PTS PRA analysis

This characteristic of risk surrogates is denoted as decomposability on system level. The ET can be used to exploit this representation of integrated risk surrogates. Assumed the end state is affect by three systems, hence, based on the theory of structure inference and conditional probability, the end states can be expressed as

$$P(CD)=\sum_{i=1}^{3}P(CD|Sys_i=Failure)P(Sys_i=Failure) \qquad \text{Equation 3.1}$$

Here, the failure probabilities are important explanatory variables to influence the estimate of end states. The condition probabilities of end states given system failures are important parameters that determine the relationship between the end state and each system.

The failure probability of each safety-related system can be repressed by sub-parameters. This characteristic of system failure probabilities is called decomposability on component level. Integrated failure probability of can be decomposed by the tool of FT. Based on the theory of structure inference and conditional probability, the failure probability can be expressed as

$$P(Sys_i)=\sum_{A,B,C}P(Sys_i|IF)P(IF)+\sum_{A,B,C}P(Sys_i|CCF)P(CCF) \qquad \text{Equation 3.2}$$

Here, IF is the independent failure and CCF is the common cause failure. The probabilities of independent failure and CCF are explanatory variables of system failure probability, which can be calculated by CCF modeling (beta-factor or alpha-factor, etc.). The conditional probability of system given each failure mechanism is the parameters that determine the relationship between the system failure and component failure.

Based on the concept of decomposition, at first we proposed the framework of parameter estimation on cause level, which is under the system level and component. The causal inference and decomposition can be used to estimate CCF parameters. Table 3.1 shows

the conceptual framework of decomposition.

Table 3.1 The framework of decomposition

	Tools	**Important parameters**
Accident risk & System level	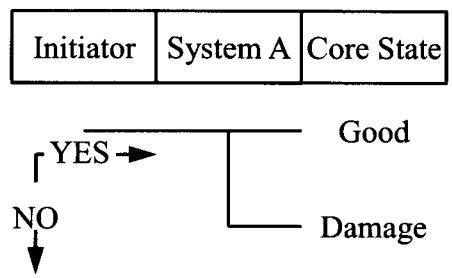	$P(Init)$ $P(Sys.A)$ $P(CD\|Init)$ $P(CD\|Sys.A)$
System level & Component level	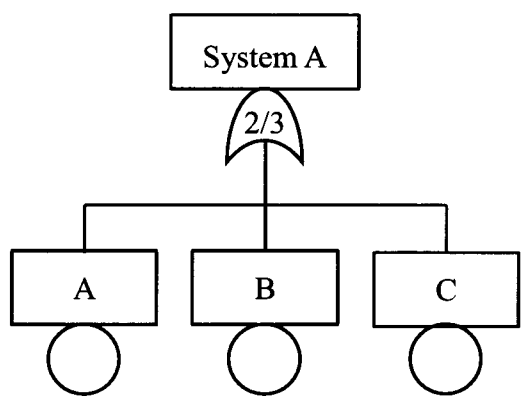	$P(Compt.A)$ $P(Compt.B)$ $P(Compt.C)$ $\alpha_1, \alpha_2, \alpha_3$
Component level & Cause level	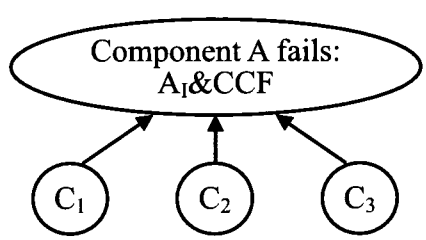	$P(A_I\|C_1), P(CCF\|C_1), P(C_1)$ $P(A_I\|C_2), P(CCF\|C_2), P(C_2)$ $P(A_I\|C_3), P(CCF\|C_3), P(C_3)$

From Table 3.1, it can be seen that by the process of decomposition, the important parameters are distinguished. The next step is to determine how the important parameters on

cause level influence the CCF parameters. This dissertation focuses on the inference on the cause level so that the CCF parameters can be learned.

3.2. Risk Analysis of Common Causes

In the context of the present discussion, the cause of a failure event is a condition or combination of conditions to which a change in the state of a component can be attributed. Usually, the failure mechanism of a CCF event is complicated and a causal chain will be inferred, so the causes have been classified as proximate causes and root causes. A proximate cause associated with a component failure event is a characterization of the condition that is readily identifiable as having to the failure. A root cause is the basic reason why the component fails. For instance, a component failed because of flood. However, to recognize the risk of common cause failure, it is necessary to identify what triggered the flood. The failure frequency of pipe break or a seismic shock should be quantified. In this dissertation, to describe a failure in terms of a single cause is a simplification of failure mechanism. We focus on the mathematical illustration of the alpha-decomposition method. So the causes in the process of alpha decomposition are referred to the most identifiable proximate causes.

Therefore, causes should be classified for further analysis. The classification of causes is referred to the standards and guidance published by U.S. NRC for collecting, classifying and coding CCF events. Figure 3.2 shows the classification of causes. It is subdivided as seven categories.

1) Design/Construction/Manufacture Inadequacy.

   It encompasses actions and decisions taken during design, manufactures, or installation of components both before and after the plant is operational.

2) Operations/Human Error (Plant Stuff Error).

   It represents causes related to errors of omission and commission on the part of plant staff. An example is a failure to follow the standard procedure.

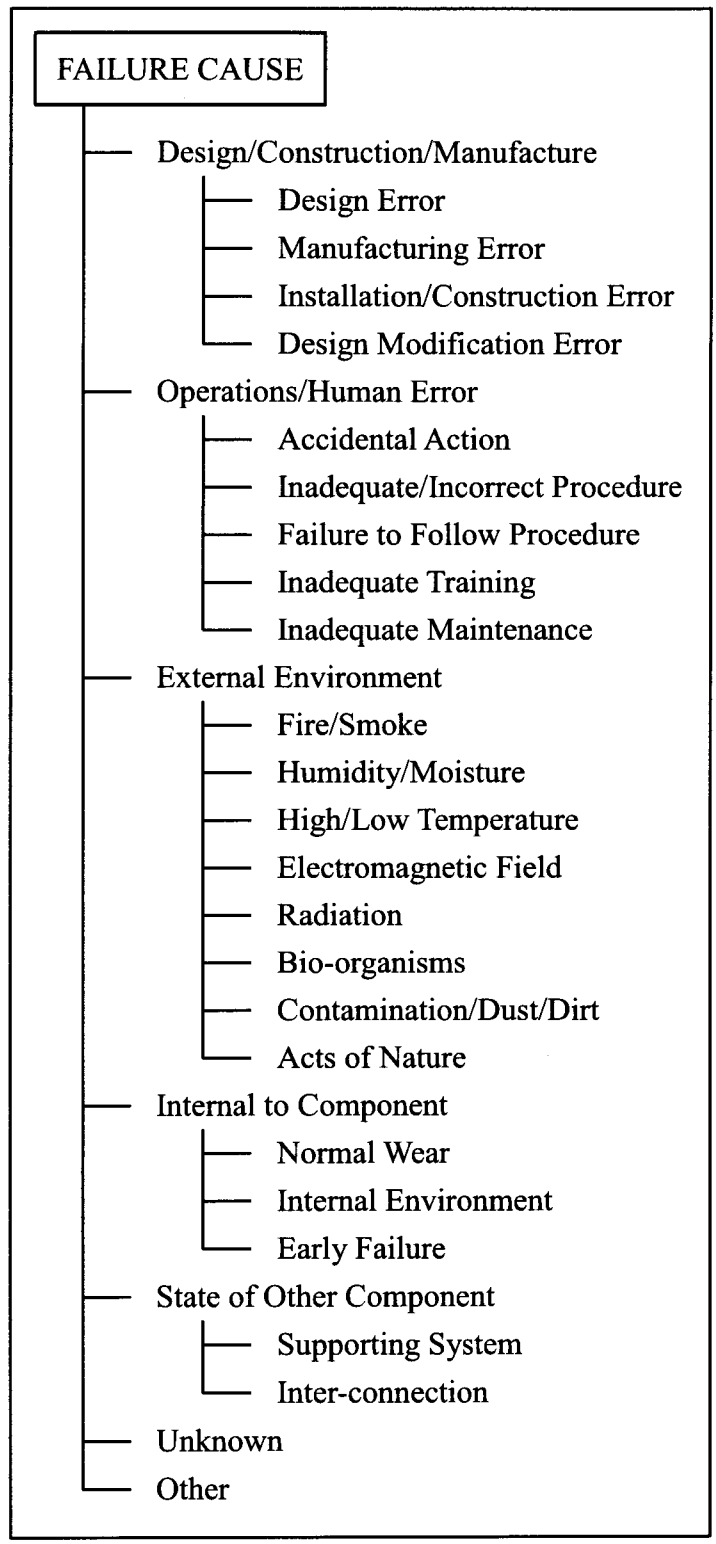

Figure 3.2 Potential causes classification

3) External Environment.

It represents causes related to a harsh external environment that is not within component design specifications. For example, the earthquake and tsunami are the external events that occurred in Fukushima Daiichi nuclear station. External events are always hard to predict.

4) Internal to Component.

It results from phenomena such as wear or other intrinsic failure mechanism. These are malfunctions internal to the component.

5) State of other component.

The component is functionally unavailable because of failure of a supporting component or system. For example, an air supply line to a valve breaks or a fuse in a control circuit blows. It is important in the nuclear PRA analysis.

6) Unknown.

Sometimes the cause of failure state cannot be identified.

7) Others.

Used when the cause cannot be attributed to any of the previous causes categories. This category is most frequently used for causes of setpoint drift.

There are two aspects should be considered for the CCF risk analysis of causes. One is the occurrence frequencies of potential causes. The other is the CCF triggering ability of each cause. Table 3.2 contains the occurrence information of CCF events in the engine sub-system of the EDG system, which is a record of EDG CCF database made by U.S. NRC. There are totally 21 CCF events are collected in the database. The Design/Construction/Installation/Manufacture Inadequacy cause group has 10 events (48 percent) of which one is Complete and non are Almost Complete. The Internal to Component cause group has 8 CCF events (38 percent) of which two are Complete and two are Almost Complete. The Operational/Human Error cause group contains three CCF events (14 percent) of which none are Complete and Almost Complete. There no CCF event results from other

cause groups. It can be judged from Table 3.2 that each cause group has difference occurrence frequencies and results in different amounts of CCF events. Therefore, these two elements influence the CCF risk of each cause group for the targeted system.

Table 3.2 CCF events in engine sub-system of EDG system

Cause Group	Complete	Almost Complete	Partial	Total	Percent
Design/Construction/Installation/ Manufacture Inadequacy	1	0	9	10	47.6%
Internal to Component	2	2	4	8	38.1%
Operational/Human	0	0	3	3	14.3%
External Environment	0	0	0	0	0.0%
Other	0	0	0	0	0.0%
Total	3	2	16	21	100.0%

For the simplest consideration, it is assumed that there are three potential common causes. As shown in Table 3.3, three causes have innate occurrence frequencies and CCF triggering abilities. Similar to the actual common causes database, there are three potential causes denoted as Cause 1, Cause 2 and Cause 3. The Cause 1 is labeled as a black diamond (♦) which is of high occurrence frequency and relatively low CCF triggering ability. The risk of Cause 1 can be read from Figure 3.3, so the CCF risk is medium. The Cause 2 is labeled as a black triangle (▲) which is of relatively low occurrence frequency and high CCF triggering ability, so the risk of Cause 2 is high based on Figure 3.3. The Cause 3 is labeled as a black circle (●) which is of extremely low occurrence frequency and extremely high CCF triggering ability, so the CCF risk is high based on Figure 3.3. Table 3.3 and Figure 3.3 demonstrate the conceptual evaluation of common causes. Two important elements are found and explained. The basic function can be given as

$$\alpha_j = \sum_i f(C_i, Tr_i) \qquad \text{Equation 3.3}$$

Here, α_j is the alpha factor involving j components fail for common causes, C_i is the Cause i; Tr_i is the triggering ability of Cause i. This conceptual equation roughly shows the alpha factors are the integrated reflection of potential common causes' CCF risk. The next step is to find and prove the relationship among these two elements and CCF parameters (alpha factors).

Table 3.3 Assumed causes for CCF risk comparison

Cause Group	**Occurrence Frequency**	**CCF Triggering Ability**	**Label**
Cause 1	High	Relatively Low	♦
Cause 2	Relatively Low	High	▲
Cause 3	Extremely Low	Extremely High	●

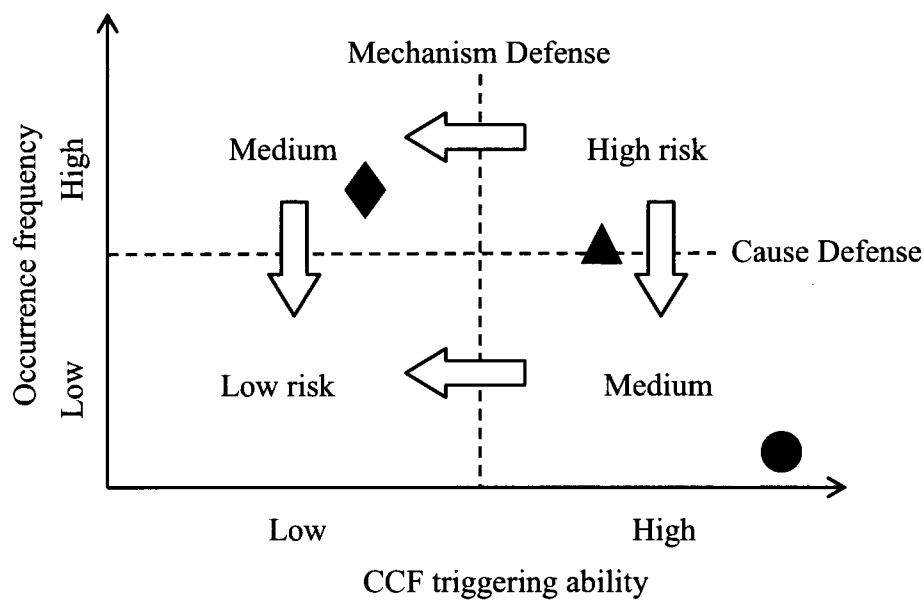

Figure 3.3 CCF risk map of potential causes

3.3. Proposed the Alpha Decomposition Method via Hybrid Bayesian Network

Based on the previous discussion, the lumped alpha factors are the integrated reflection of cause and failure information, so these are decomposable. This section focuses on the derivation of the mathematical function. For distinction, the alpha factors in the alpha factor model is denoted as global alpha factors (α_j) and the CCF triggering abilities of causes are denoted as decomposed alpha factors ($\alpha_j^{C_i}$). This section aims to determine the specific form of Equation 3.3.

Definition 1 Alpha Decomposition

Since the global alphas are lumped parameters which are the integrated reflection of failure and cause information in the common cause failure system. The global alpha factors are decomposed according to a function of two types of elements. These explanatory variables include occurrence frequencies and CCF triggering abilities (denoted as decomposed alpha factors).

The process of decomposition can be well explained via the tool of Hybrid Bayesian Network (HBN). The hybrid network includes the Fault Tree (FT) and Bayesian Network. The FT is used to represent the relationship between component failures and system failure. The Bayesian Network is used to represent the process of causal inference. By the combination of two tools, the analysis of CCF event on system level, component level and cause level can be established, and the relationship of parameters can be discussed. Figure 3.4 shows the HBN of a redundant system with three components (A, B, and C) and three potential common causes (C_1, C_2, and C_3). As discussed in the context, different causes are of different abilities to result in CCF events and of difference occurrence frequencies. According to the process of classification, the causes in this model are assumed as independent.

Therefore, the failure probability of components can be given by conditional

probability.

$$P(A)=\sum_{i=1}^{3}P(A|C_i)P(C_i)$$
$$P(B)=\sum_{i=1}^{3}P(B|C_i)P(C_i) \qquad \text{Equation 3.4}$$
$$P(C)=\sum_{i=1}^{3}P(C|C_i)P(C_i)$$

It shows that if the occurrence frequencies and hazard of independent causes can be determined, the failure probability of the targeted components and system can be decided.

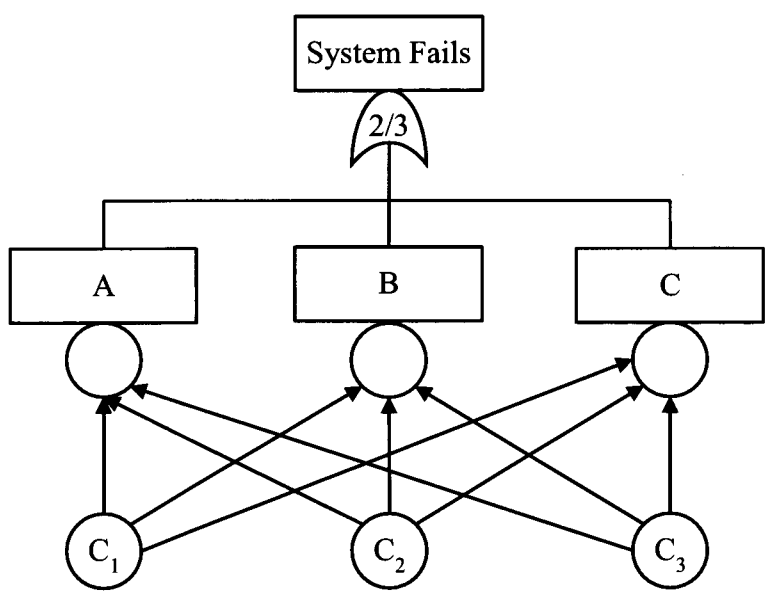

Figure 3.4 Hybrid Bayesian Network of causal inference for system

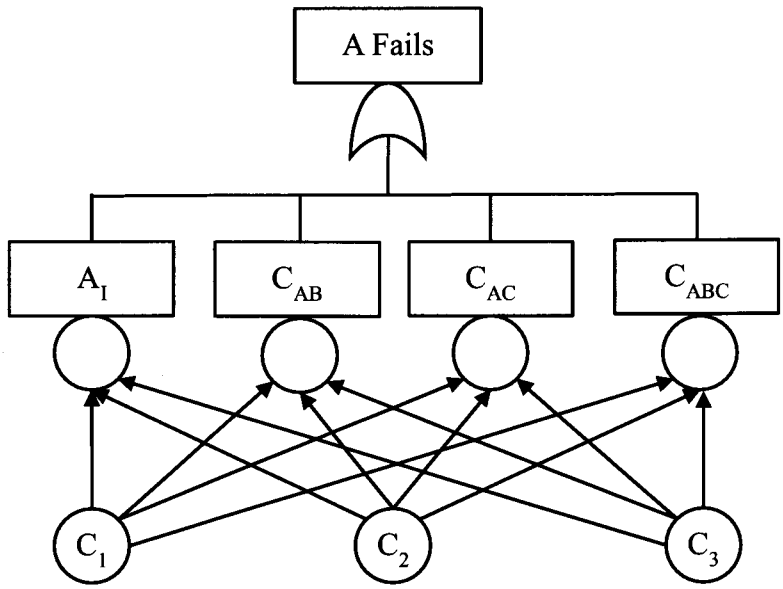

Figure 3.5 Hybrid Bayesian Network of causal inference for Component A

Figure 3.5 shows the HBN for the modeling of Component A. The independent failure, partial CCF and complete CCF can be explained by the theory of conditional probability. It is easier for the deduction of CCF parameters to focus on one component.

$$
\begin{aligned}
P(A_I) &= \sum_{i=1}^{3} P(A_I|C_i)P(C_i) \\
P(C_{AB}) &= \sum_{i=1}^{3} P(C_{AB}|C_i)P(C_i) \\
P(C_{AC}) &= \sum_{i=1}^{3} P(C_{AC}|C_i)P(C_i) \\
P(C_{ABC}) &= \sum_{i=1}^{3} P(C_{ABC}|C_i)P(C_i)
\end{aligned}
$$

Equation 3.5

Here, A_I is the independent failure of Component A; C_{AB} and C_{AC} are the partial CCF events involving Component A and one other component; C_{ABC} is the complete CCF event involving all three components. It is given the relationship that the Cause 1 results in the failure of Component A by the law of total probability.

$$P(A|C_1)=P(A_I|C_1)+P(C_{AB}|C_1)+P(C_{AC}|C_1)+P(C_{ABC}|C_1) \qquad \text{Equation 3.6}$$

Therefore, the CCF risk of Cause1 is decomposed as three parts. These are $P(A_I|C_1)$, $P(C_{AB}|C_1)+P(C_{AC}|C_1)$, and $P(C_{ABC}|C_1)$, which have physical meaning. The $P(A_I|C_1)$ represents the hazard of Cause 1 which triggers independent failure of Component A; the $P(C_{AB}|C_1)+P(C_{AC}|C_1)$ represents the hazard of Cause 1 which triggering partial CCF event involving Component A; the $P(C_{ABC}|C_1)$ represents the complete CCF event involving Component A. Divide the Equation 3.6 by $P(A|C_1)$

$$1=\frac{P(A_I|C_1)+P(C_{AB}|C_1)+P(C_{AC}|C_1)+P(C_{ABC}|C_1)}{P(A|C_1)} \qquad \text{Equation 3.7}$$

According the Equation 3.6 and Equation 3.7, the definition of decomposed alpha factors can be given

$$\begin{aligned}
\alpha_1^{C_1} &= \frac{P(A_I|C_1)}{P(A|C_1)} \\
\alpha_2^{C_1} &= \frac{P(C_{AB}|C_1)}{P(A|C_1)}+\frac{P(C_{AC}|C_1)}{P(A|C_1)} \\
\alpha_3^{C_1} &= \frac{P(C_{ABC}|C_1)}{P(A|C_1)}
\end{aligned} \qquad \text{Equation 3.8}$$

Here, similarly to the definition of global alpha factors, all decomposed alpha factors have practical meaning. The $\alpha_1^{C_1}$ is the ratio of independent failure in total failure probability given the occurrence of Cause 1. If a cause of high quantity of $\alpha_1^{C_1}$, this cause is more possible to result in an independent failure. The $\alpha_2^{C_1}$ is the ratio of partial CCF in total failure probability given Cause 1. If a cause of high quantity of $\alpha_2^{C_1}$, this cause is more possible to result in a partial CCF event. The $\alpha_3^{C_1}$ is the ratio of complete CCF in total failure probability

given Cause 1. If a cause of high quantity of $\alpha_3^{C_1}$, this cause is more possible to result in a complete CCF event.

The sum of decomposed alpha factors of Cause 1 is 1. The constraint of Sum-to-One makes it reasonable that the prior distribution of a set of decompose alpha factors can be assumed as Dirichlet distribution.

$$\alpha_1^{C_1} + \alpha_2^{C_1} + \alpha_3^{C_1} = 1 \qquad \text{Equation 3.9}$$

Similarly, the relationship that the Cause 2 and Cause 3 result in the failure Component A can be given by

$$\begin{aligned} P(A|C_2) &= P(A_I|C_2) + P(C_{AB}|C_2) + P(C_{AC}|C_2) + P(C_{ABC}|C_2) \\ P(A|C_3) &= P(A_I|C_3) + P(C_{AB}|C_3) + P(C_{AC}|C_3) + P(C_{ABC}|C_3) \end{aligned} \qquad \text{Equation 3.10}$$

The decomposed alpha factors of Cause 2 can be written as

$$\begin{aligned} \alpha_1^{C_2} &= \frac{P(A_I|C_2)}{P(A|C_2)} \\ \alpha_2^{C_2} &= \frac{P(C_{AB}|C_2)}{P(A|C_2)} + \frac{P(C_{AC}|C_2)}{P(A|C_2)} \\ \alpha_3^{C_2} &= \frac{P(C_{ABC}|C_2)}{P(A|C_2)} \end{aligned} \qquad \text{Equation 3.11}$$

The Sum-to-One constraint for decomposed alpha factors of Cause 2 can be given by

$$\alpha_1^{C_2} + \alpha_2^{C_2} + \alpha_3^{C_2} = 1 \qquad \text{Equation 3.12}$$

The decomposed alpha factors of Cause 3 can be written as

$$\alpha_1^{C_3} = \frac{P(A_I|C_3)}{P(A|C_3)}$$
$$\alpha_2^{C_3} = \frac{P(C_{AB}|C_3)}{P(A|C_3)} + \frac{P(C_{AC}|C_3)}{P(A|C_3)} \qquad \text{Equation 3.13}$$
$$\alpha_3^{C_3} = \frac{P(C_{ABC}|C_3)}{P(A|C_3)}$$

The Sum-to-One constraint for decomposed alpha factors of Cause 3 can be given by

$$\alpha_1^{C_3} + \alpha_2^{C_3} + \alpha_3^{C_3} = 1 \qquad \text{Equation 3.14}$$

Moreover, according to the Equation 3.5, the independent failure probability of Component A can be represented by the total failure probability law.

$$P(A_I) = P(A_I|C_1)P(C_1) + P(A_I|C_2)P(C_2) + P(A_I|C_3)P(C_3) \qquad \text{Equation 3.15}$$

Based on Equation 3.8, Equation 3.15 can be replaced by decomposed alpha factors and conditional probability of Component A.

$$P(A_I) = \alpha_1^{C_1} P(A|C_1)P(C_1) + \alpha_1^{C_2} P(A|C_2)P(C_2) + \alpha_1^{C_3} P(A|C_3)P(C_3)$$

Equation 3.16

If the Equation 3.16 is divided by $P(A)$, the global alpha factors and decomposed alpha factors can be connected.

$$\frac{P(A_I)}{P(A)} = \alpha_1^{C_1} \frac{P(A|C_1)P(C_1)}{P(A)} + \alpha_1^{C_2} \frac{P(A|C_2)P(C_2)}{P(A)} + \alpha_1^{C_3} \frac{P(A|C_3)P(C_3)}{P(A)}$$

Equation 3.17

According to the definition of alpha factors (Equation 2.11), the left side of Equation 3.17 can be given by

$$\alpha_1 = \frac{P(A_I)}{P(A)}$$ Equation 3.18

The element on the right side of Equation 3.17 is the ratios of failure that are caused by Cause i. It can be written as

$$\begin{aligned} r_1 &= \frac{P(A|C_1)P(C_1)}{P(A)} \\ r_2 &= \frac{P(A|C_2)P(C_2)}{P(A)} \\ r_3 &= \frac{P(A|C_3)P(C_3)}{P(A)} \end{aligned}$$ Equation 3.19

Here, r_1 is the occurrence frequency of Cause 1 among the failure events of Component A; r_2 is the occurrence frequency of Cause 2 among the failure events of Component A; r_3 is the occurrence frequency of Cause 3 among the failure events of Component A.

The sum of occurrence frequencies of causes also equals 1.

$$r_1 + r_2 + r_3 = 1$$ Equation 3.20

Thus, Equation 3.17 can be written as a very simple regression function.

$$\alpha_1 = \alpha_1^{C_1} r_1 + \alpha_1^{C_2} r_2 + \alpha_1^{C_3} r_3 \qquad \text{Equation 3.21}$$

Similarly, the partial and complete CCF events can be written as

$$P(C_{AB} \& C_{AC}) = P(C_{AB} \& C_{AC} | C_1) P(C_1) + P(C_{AB} \& C_{AC} | C_2) P(C_2) + P(C_{AB} \& C_{AC} | C_3) P(C_3)$$
$$P(C_{ABC}) = P(C_{ABC} | C_1) P(C_1) + P(C_{ABC} | C_2) P(C_2) + P(C_{ABC} | C_3) P(C_3)$$

Equation 3.22

Then the regression functions of global alpha factors (α_2 and α_3) can be given by

$$\alpha_2 = \alpha_2^{C_1} r_1 + \alpha_2^{C_2} r_2 + \alpha_2^{C_3} r_3$$
$$\alpha_3 = \alpha_3^{C_1} r_1 + \alpha_3^{C_2} r_2 + \alpha_3^{C_3} r_3 \qquad \text{Equation 3.23}$$

As a conclusion, for system with *n* components and *m* potential common causes, the general decomposition form of alpha factors can be given by

$$\alpha_j = \sum_{i=1}^{m} \alpha_j^{C_i} r_i \qquad \text{Equation 3.24}$$

Here, α_j represents the CCF risk involving *j* components; $\alpha_j^{C_i}$ represents the CCF risk of Cause *i* involving *j* components; r_i represents the occurrence frequency of Cause *i*.

3.4. Summary

Each common cause is of different ability to result in independent or dependent failures. Causes are classified according to innate failure mechanism and other characteristics. The lumped alpha factors are recognized as decomposable based on causal inference. In Section 3.3, the alpha-decomposition method is proposed to quantitatively evaluate CCF parameters. The global alpha factors are decomposed according to a function of two types of elements. These explanatory variables include occurrence frequencies and CCF triggering abilities (denoted as decomposed alpha factors). The regression model of the alpha decomposition method is established and proved by the theory of conditional probability as well as hybrid Bayesian Network.

Chapter 4: BUILDING OF DATABASE AND BAYESIAN INFERENCE PROCEDURES

This chapter illustrates the procedure of Bayesian inference for the alpha decomposition method as well as the building of corresponding databases. An example of parameter estimation is discussed with hypothetical databases. Posterior distributions for CCF parameters are obtained. The uncertainty in the estimation CCF parameters is discussed.

4.1. Building of recommended database

Usually, there are two types of data sources can be used to produce the various parameter estimates in PRA. These are plant-generic data sources and plant-specific data sources. Because of the rarity of CCF event on a plant- or system-specific basis, the plant-specific PRA has to rely heavily on the industry experience to develop a statistically significant data bases. The alpha decomposition method is a quantitative assessment to interpret generic CCF data and to translate them for plant-specific (or system-specific, or design-specific) applications.

The database including the CCF events information and cause information for target system should be collected. The classification of possible causes is shown in Figure 3.2. Hence, records of two causes should be independent in the database, and the occurrence frequency can be given by

$$P(Cause\ 1 \cap Cause\ 2) = P(Cause\ 1) \bullet P(Cause\ 2) \qquad \text{Equation 4.1}$$

$$r_i = \frac{Cause\ i's\ occcurrence}{Total} \qquad \text{Equation 4.2}$$

Based on the whether the CCF data is rare, two types of databases are recommended to be built. One is the recommended database and the other is the so-called alternative database. There is only rough information of cause occurrence in the generic database. The system assumed in this chapter is a redundant system with three components and there are three potential causes.

4.1.1. Recommended database

The generic database means the collection of cause information and CCF event are not specifically related. There is no detailed record of the cause's hazard, but only the occurrence frequency is collected. This generic database is used when the cause information is rare. The correlation between decomposed alpha factors with global alpha factors is a latent property which can be predicted by the process of Bayesian inference. The recommended database has advantage that different data sources can be combined. If there is no system-specific data collected, the cause occurrence data from other industry or from plant-generic database can be used.

Table 4.1 is the hypothetical database proposed to collect the data of cause occurrence. It can be obtained from the Table 4.1 that the occurrence information of each cause. Based on Equation 4.2, the occurrence frequency can be calculated. Cause data of 16 systems are collected. The System #1 has 127 CCF events occurred of which 25.20% is the result of Cause 1, 22.05% is Cause 2 and 52.76% is Cause 3. The Cause 3 happens most frequently in System #1. System 2 has totally 106 CCF events of which 16.04% is the result of Cause 1, 73.58% is Cause 2 and 10.38% is Cause 3. The Cause 2 happens most frequently in System 2.

As the analysis of CCF risk of causes, the causes have different occurrence frequencies and different CCF hazard. All the hazard of a cause to a system is affected by the property of the system as well. The CCF events of each system can be obtained from Table.4.2.

Table 4.1 Hypothetical CCF database including cause information

System	Common Causes			Total	Occurrence frequency		
	Cause 1	Cause 2	Cause 3		Cause 1	Cause 2	Cause 3
# 1	32	28	67	127	25.20%	22.05%	52.76%
# 2	17	78	11	106	16.04%	73.58%	10.38%
# 3	18	19	50	87	20.69%	21.84%	57.47%
# 4	29	6	31	66	43.94%	9.09%	46.97%
# 5	7	33	10	50	14.00%	66.00%	20.00%
# 6	15	9	17	41	36.59%	21.95%	41.46%
# 7	12	15	7	34	35.29%	44.12%	20.59%
# 8	2	22	7	31	6.45%	70.97%	22.58%
# 9	7	4	11	22	31.82%	18.18%	50.00%
# 10	10	8	3	21	47.62%	38.10%	14.29%
# 11	3	6	10	19	15.79%	31.58%	52.63%
# 12	7	3	6	16	43.75%	18.75%	37.50%
# 13	3	5	7	15	20.00%	33.33%	46.67%
# 14	5	3	7	15	33.33%	20.00%	46.67%
# 15	4	5	2	11	36.36%	45.45%	18.18%
# 16	1	6	2	9	11.11%	66.67%	22.22%

Table 4.2 is the database proposed to collect the data of CCF events. Three types of CCF events are recorded that is single failure, partial common cause failure and complete common cause failure. For instance, System has a total number of 127 CCF events of which 113 are single failure, 11 are partial CCF events and 3 complete CCF events. It is recommended to build a database including not only CCF events but single failures. The data of single failure is important to evaluate the alpha factor involving single component failure.

Table 4.2 Hypothetical CCF database including failure information

System	Single & Common Cause Failure			Total
	Single (1/3)	Partial (2/3)	Complete (3/3)	
# 1	113	11	3	127
# 2	98	7	1	106
# 3	73	9	5	87
# 4	53	5	8	66
# 5	45	4	1	50
# 6	33	3	5	41
# 7	32	2	0	34
# 8	29	2	0	31
# 9	20	2	0	22
# 10	20	1	0	21
# 11	16	2	1	19
# 12	14	1	1	16
# 13	13	1	1	15
# 14	12	1	2	15
# 15	9	1	1	11
# 16	7	1	1	9

4.1.2. Alternative database

To use the plant-specific and detailed data in the PRA procedures will reflect the actual plant risk performance. If there is enough CCF data can be collected in the PRA procedure, the more detailed database is recommended to be used. The database is named as alternative database in this dissertation. In this database, all failure types and causes are well defined which can provide more reliable estimates.

Table 4.3 Hypothetical specific CCF database for System #1

Cause Group	Single & Common Cause Failure			Total	Percent
	Single (1/3)	Partial (2/3)	Complete (3/3)		
Cause 1	24	6	2	32	25.20%
Cause 2	24	3	1	28	22.05%
Cause 3	65	2	0	67	52.76%
Total	113	11	3	127	100.0%

Because in the actual plant-specific PRA analysis, there are rare CCF events available for one certain system, this database is called alternative database.

Table 4.3 shows the specific CCF database for System #1 including the cause and failure events. Only the CCF events happened in the boundary of System #1 is collected. The cause of each failure is well recorded. There are three types of failures: single failure, partial common cause failure and complete common cause failure. The occurrence of three potential causes is collected including the occurrence frequencies and the hazard of cause. There are totally 32 failures triggered by Cause 1 of which 24 are single failures, 6 are partial CCF and 2 are complete CCF. Cause 1 has different possibility to result in different failure types, in which single failures most frequently happen. The Cause 1 triggered 2 complete CCF events, Cause 2 triggered 1 complete CCF event, and Cause 3 triggered 0 complete CCF event. It can be seen that three causes are of different CCF hazard. There are totally 127 failure events occurred of which 25.20% is the result of Cause 1, 22.05% is the result of Cause 2, and 52.76% is the result of Cause 3. Causes have innate occurrence frequency which is an important point to analyze the caused-informed CCF modeling. It should be noticed that the data of single failure should be record since it directly affect the estimate of the alpha factor involving one single component.

The calculation procedures of Bayesian inference on basis of two databases are slightly different. It will be discussed separately by examples in the rest of this chapter.

4.2. Hierarchical Bayesian Modeling

This section introduces the evaluation process of the alpha decomposition method. This process includes the prediction of unknown parameters (decomposed alpha factors) and the update of important variables (global alpha factors). The hierarchical Bayes method embodies a complete Bayesian approach to the problem of estimating the unknown probability distributions based on the available data, information or knowledge. The hierarchical Bayesian approach expresses the initial uncertainty (that is, the uncertainty before the data are considered) about the unknown hyperparameters using another prior, a so-called hyperprior distribution.

Therefore, the definition of hierarchical Bayesian model can be well explained. At first, in the full Bayesian model all the unknown parameters (including prior distribution, hyperprior distributions and hyperparameters) are assigned probability distributions that express the analyst's initial uncertainty about these parameters. Secondly, the observed data are used to solve the model and the required posterior distributions for the interested parameters can be obtained. As introduced in the previous sections, the solution can be done using the MCMC algorithm.

4.2.1. Standard hierarchical model

Bayesian models have an inherently hierarchical structure. Figure 4.1 shows the typical procedure of Bayesian inference which is used in Examples 1.1 and 1.2. Squared nodes refer to constant parameters, and oval nodes refer to stochastic components of the model. The solid arrows indicate stochastic dependence between parameters and variables. The posterior distributions of parameters theta can be obtained based on the observations and prior distributions, so the mathematical form of Figure 4.1 is the same as Equation 1.3, which can be written as

$$\pi_1(\boldsymbol{\theta}|\boldsymbol{x}) \propto f(\boldsymbol{x}|\boldsymbol{\theta})\pi_0(\boldsymbol{\theta},\boldsymbol{a}) \propto f(\boldsymbol{x}|\boldsymbol{\theta})\pi_0(\boldsymbol{\theta}|\boldsymbol{a}) \qquad \text{Equation 4.3}$$

Here, $\pi_1(\boldsymbol{\theta}|\boldsymbol{x})$ is the posterior distribution of parameter theta; $\pi_0(\boldsymbol{\theta},\boldsymbol{a})$ is the prior distribution of theta which is represented by the set of constant parameters $\boldsymbol{a}$; $f(\boldsymbol{x}|\boldsymbol{\theta})$ is the likelihood function.

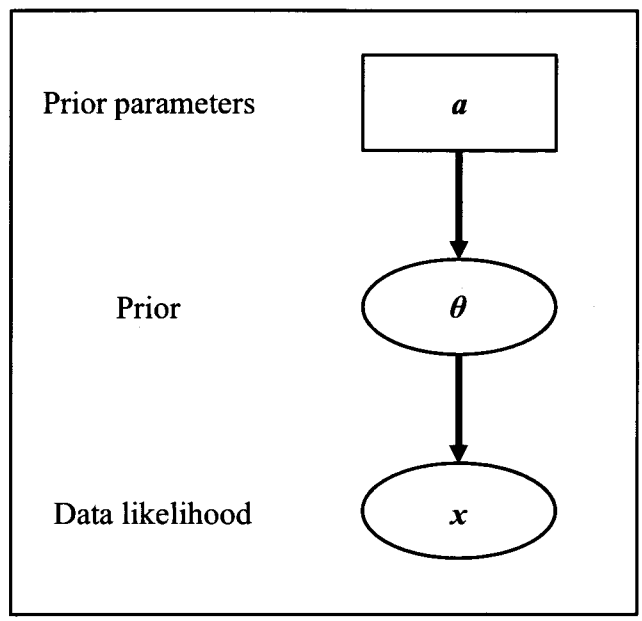

Figure 4.1 Graphical representation of standard one-stage Bayesian model

The one-stage Bayesian model has a simple structure. The one stage refers to that only one prior is assumed. Parameters of the prior distribution are constant. Based on the observation, the parameters of the posterior distribution will be changed, so the process is also called Bayesian Update.

To capture the complicated structure of some estimates, the prior is frequently structured using a series of conditional distributions. Hence, a more complicated hierarchical Bayesian model is defined when a prior distribution is also assigned on the prior parameters $\boldsymbol{a}$ associated with the likelihood parameters $\boldsymbol{\theta}$. The graphical structure is shown in Figure 3.2. A two-stage hierarchical Bayesian model is depicted. In this two-stage model, one so-called

hyperprior distribution is assigned on the previous node ***a***. This hyperprior has constant parameters which are named as hyperparameters, so the hyperprior is no longer constant. The hyperprior will be updated with the prior when observed data is obtained.

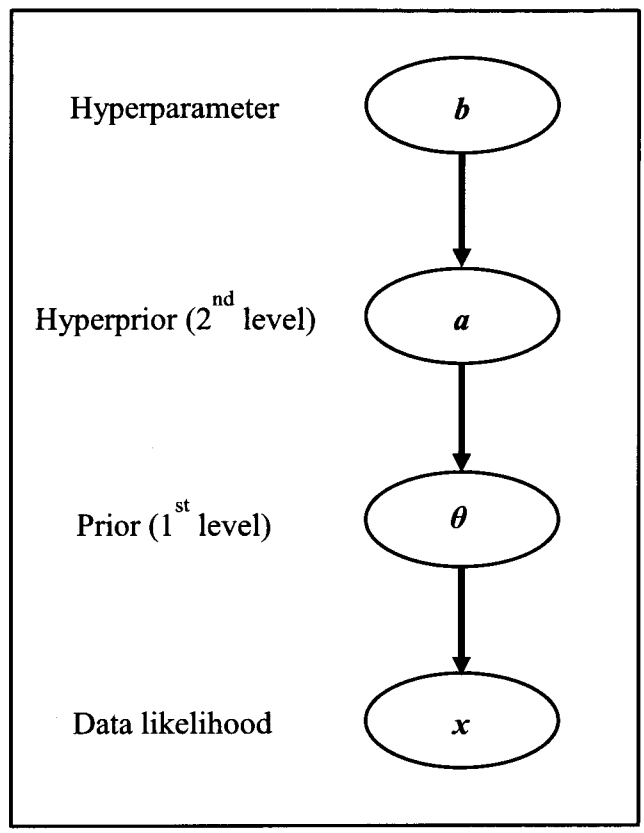

Figure 4.2 Graphical representation of standard two-stage Bayesian model

Similar to the Equation 4.3, the mathematical form of two-stage hierarchical Bayesian model can be given by

$$\pi_1(\boldsymbol{\theta}|\boldsymbol{x}) \propto f(\boldsymbol{x}|\boldsymbol{\theta})\pi_0(\boldsymbol{\theta},\boldsymbol{a})\pi_{hp}(\boldsymbol{a},\boldsymbol{b}) \propto f(\boldsymbol{x}|\boldsymbol{\theta})\pi_0(\boldsymbol{\theta}|\boldsymbol{a})\pi_{hp}(\boldsymbol{a}|\boldsymbol{b}) \quad \text{Equation 4.4}$$

Here, $\pi_{hp}(\boldsymbol{a}|\boldsymbol{b})$ is the hyperprior distribution of the node ***a***. Hence, two levels of prior distributions can be defined. $\pi_0(\boldsymbol{\theta}|\boldsymbol{a})$ is the first level and $\pi_{hp}(\boldsymbol{a}|\boldsymbol{b})$ is the second level. Prior distributions of the upper levels of a hierarchical prior are called hyperpriors and the

corresponding parameters are called hyperparameters. In Figure 3.7, $\pi_0(\theta|a)$ is the hyperprior and the set of b are the hyperparameters the hyperprior.

As a conclusion, hierarchical models describe efficiently complex datasets incorporating correlation or including other properties in PRA models. The relationship between parameters can be well reflected in the hierarchical Bayesian models. These models imply a random calculation of conditional probabilities by MCMC model. Either conjugate distributions or nonconjugate distributions can be calculated in an easy way.

In the some PRA analysis, the double-counting of operation data should be avoided in the two-stage hierarchical Bayesian model. There are only one type of data is used in the early PRA. For instance, the generic data is used to estimate the hyperparameters and to obtain the estimate of $f(\theta|a,b)$. Then one specific data is used to estimate posterior distributions combining with the obtained prior $f(\theta|a,b)$. Because the specific data is one part of the generic database, the data are double counted.

However, the two-stage hierarchical Bayesian model is useful when there are new correlation and data sources.

1) When new correlation or properties can be included in the upper level of two-stage model, the two-stage model should be applied to reach more reliable results.
2) When there are reliable corresponding data (other data source) can be used as hyperparameters, the two-stage Bayesian model should be efficient to combine different data sources.

The correlation between global alpha factors and decomposed alpha factors are discovered and the cause information can be integrated in the estimation of CCF parameters. Therefore, the alpha decomposition method is considered to use the two-stage hierarchical Bayesian model.

4.2.2. Hierarchical model of the alpha decomposition method

The estimation of global alpha factors based and only based on observed failure data is a one-stage hierarchical Bayesian model. The script of modeling using OpenBUGS is shown in Example 2.2. The estimation of global alpha factors and decomposed alpha factors based on failure and cause information is a two-stage hierarchical Bayesian model. We illustrate the graphical modeling of the alpha factor model in this section, and then introduce the Bayesian inference procedure of the alpha decomposition method.

The one-stage modeling for the alpha factor model is shown in Figure 4.3. As introduced previously, the squared nodes refer to the constant prior parameters. The oval nodes refer to stochastic components of the model. The solid arrows refer to stochastic dependence and the hollow arrows are logical dependence by arithmetic functions. As introduced in Example 2.2, the estimates of MGL parameters can be obtained by the conversion function between the alpha factor model and the MGL model, so there is a logical dependence between two nodes.

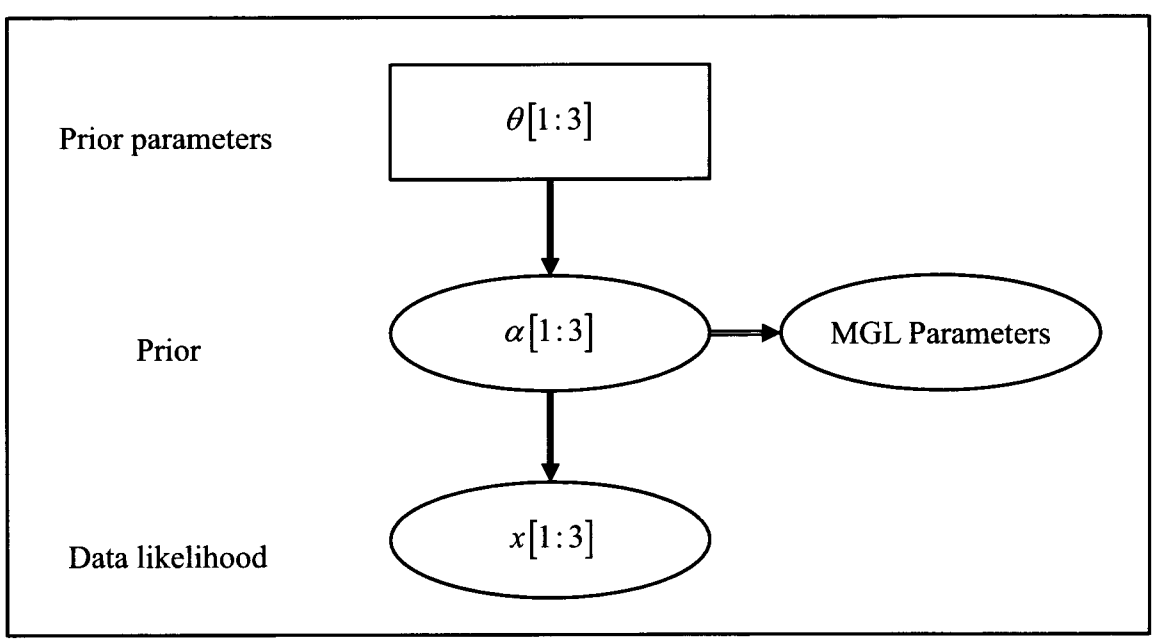

Figure 4.3 Graphical representation of previous Bayesian modeling for the alpha factor model

In Figure 4.3, the node ($x[1:3]$) refers to the observed data of CCF events. Usually, the likelihood function of the node ($x[1:3]$) is assumed as a multinomial distribution. The node ($\alpha[1:3]$) refers to the alpha factors. The alpha factors are assumed as a Dirichlet distribution, which is conjugate to the multinomial distribution. The node ($\theta[1:3]$) is the set of constant prior parameters. If the equation $\theta[k]=1$ $(k=1,2,3)$ is assumed, it is a noninformative prior distribution. The node (MGL Parameters) refers to CCF parameters of the MGL model which can be obtained via the Equation 2.16. The MGL model does not have a well-defined likelihood function, so it is hard to do direct Bayesian inference. This conversion is the easiest way to estimate MGL parameters.

The posterior distribution of global alpha factors in the one-stage model can be deduced based on the theory of conditional probability.

Discrete form:

$$P(\boldsymbol{\alpha}|\boldsymbol{x})=\frac{P(\boldsymbol{\alpha},\boldsymbol{x})}{P(\boldsymbol{x})}=\frac{P(\boldsymbol{x}|\boldsymbol{\alpha})P(\boldsymbol{\alpha})}{P(\boldsymbol{x})} \qquad \text{Equation 4.5}$$

Continuous Form:

$$\pi_1(\boldsymbol{\alpha}|\boldsymbol{x})=\frac{f(\boldsymbol{x}|\boldsymbol{\alpha})\pi_0(\boldsymbol{\alpha})}{\int(\boldsymbol{x}|\boldsymbol{\alpha})\pi_0(\boldsymbol{\alpha})d\boldsymbol{\alpha}} \qquad \text{Equation 4.6}$$

$$\pi_1(\boldsymbol{\alpha}|\boldsymbol{x})\propto f(\boldsymbol{x}|\boldsymbol{\alpha})\pi_0(\boldsymbol{\alpha})$$

Here, $\pi_1(\boldsymbol{\alpha}|\boldsymbol{x})$ is the posterior distribution for global alpha factors given observed CCF data; $f(\boldsymbol{x}|\boldsymbol{\alpha})$ is the likelihood function of observed CCF data given prior distributions; $\pi_0(\boldsymbol{\alpha})$ are the prior distributions for global alpha factors.

The two-stage hierarchical Bayesian modeling for the alpha decomposition method is shown in Figure 4.4. The prior parameters in the one-stage model are no longer constant. The node ($\theta[1:3]$) is an oval rather than a rectangle. The node ($\alpha^{C[1:3]}[1:3]$) is the set of decomposed alpha factors of three potential causes. The node (μ, σ) represents the prior parameters of the hyper prior node which is constant. Since the decomposed alpha factor of one cause can be summed to one, the hyperprior can be assumed as Dirichlet distribution. The noninformative hyperprior is a Dirichlet distribution with all parameters equaling 1. The node ($r[1:3]$) refers to the occurrence frequencies of causes.

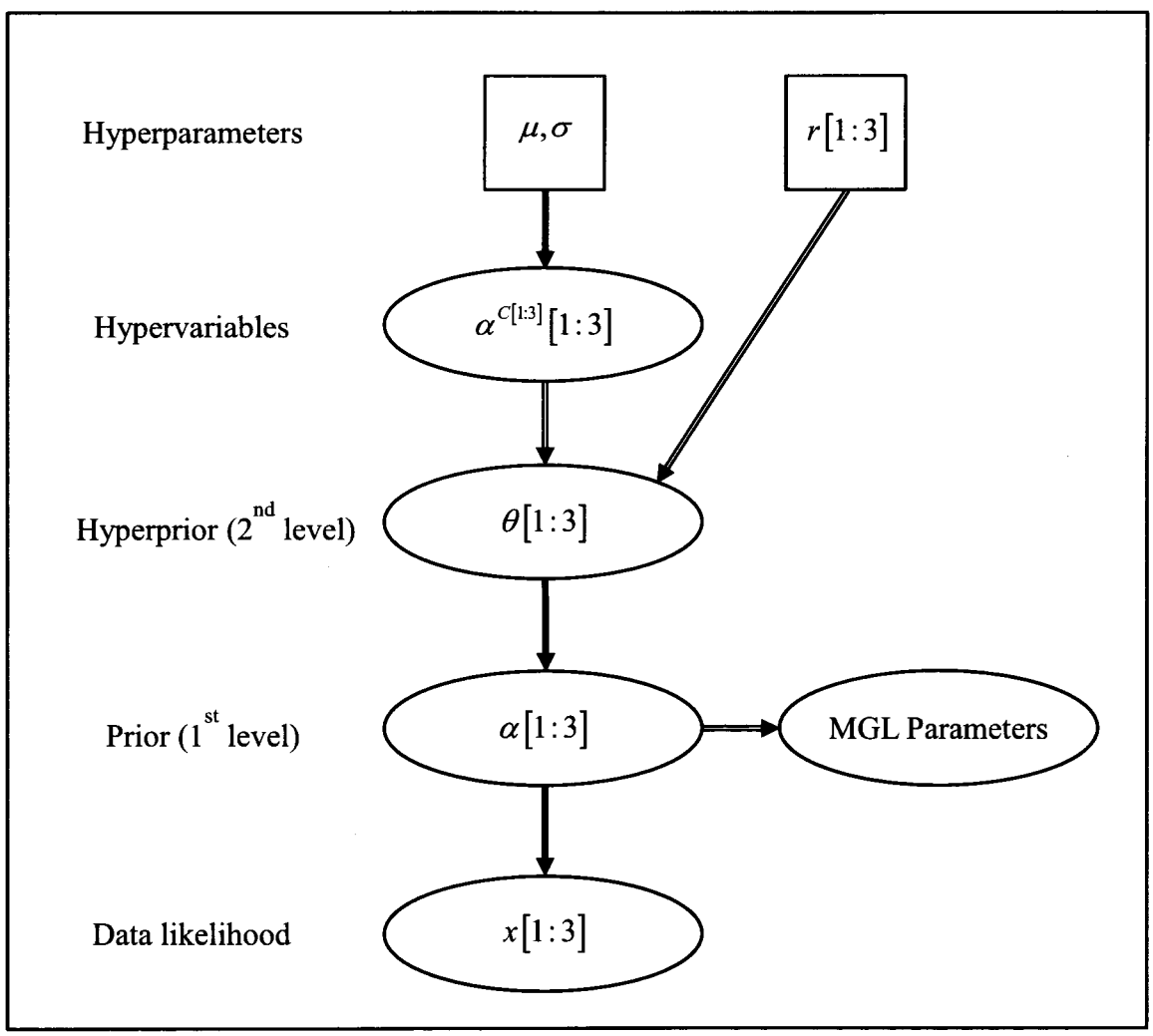

Figure 4.4 Graphical representation of current Bayesian modeling for the alpha decomposition

Generally, if the joint prior in a Bayesian model is decomposed to a series of conditional probability, the Bayesian model can be written in a hierarchical structure with more stages. The hyperprior can be represented by decomposed alpha factors and causes' occurrence frequencies. This correlation combines the cause information into the Bayesian inference for CCF parameters. The CCF risk of potential causes can be quantified and the estimates of global alpha factors are more reliable.

The procedure of Bayesian inference for the alpha decomposition method is illustrated in this section. The necessary database and detailed calculation are discussed via a example in the next chapter.

Similarly to Equations 4.5 and 4.6, the posterior distribution of decomposed alpha factors in the two-stage model can be deduced based on the theory of conditional probability.

Discrete form:

$$P\left(\boldsymbol{\alpha}^{C}\middle|\boldsymbol{x},\boldsymbol{r},\boldsymbol{\alpha}\right)=\frac{P\left(\boldsymbol{\alpha}^{C},\boldsymbol{x},\boldsymbol{r},\boldsymbol{\alpha}\right)}{P\left(\boldsymbol{x},\boldsymbol{r},\boldsymbol{\alpha}\right)}=\frac{P\left(\boldsymbol{x},\boldsymbol{r},\boldsymbol{\alpha}\middle|\boldsymbol{\alpha}^{C}\right)P\left(\boldsymbol{\alpha}^{C}\right)}{P\left(\boldsymbol{x},\boldsymbol{r},\boldsymbol{\alpha}\right)} \qquad \text{Equation 4.7}$$

Continuous form:

$$\pi_2\left(\boldsymbol{\alpha}^{C}\middle|\boldsymbol{x},\boldsymbol{\alpha},\theta,\boldsymbol{r}\right)=\frac{f_x\left(\boldsymbol{x}\middle|\boldsymbol{\alpha}\right)f_\alpha\left(\boldsymbol{\alpha}\middle|\theta\right)f_\theta\left(\theta\middle|\boldsymbol{\alpha}^{C},\boldsymbol{r}\right)\pi_0\left(\boldsymbol{\alpha}^{C}\right)}{\int f_x\left(\boldsymbol{x}\middle|\boldsymbol{\alpha}\right)f_\alpha\left(\boldsymbol{\alpha}\middle|\theta\right)f_\theta\left(\theta\middle|\boldsymbol{\alpha}^{C},\boldsymbol{r}\right)\pi_0\left(\boldsymbol{\alpha}^{C}\right)d\boldsymbol{\alpha}^{C}} \qquad \text{Equation 4.8}$$

$$\pi_2\left(\boldsymbol{\alpha}^{C}\middle|\boldsymbol{x},\boldsymbol{\alpha},\theta,\boldsymbol{r}\right)\propto f_x\left(\boldsymbol{x}\middle|\boldsymbol{\alpha}\right)f_\alpha\left(\boldsymbol{\alpha}\middle|\theta\right)f_\theta\left(\theta\middle|\boldsymbol{\alpha}^{C},\boldsymbol{r}\right)\pi_0\left(\boldsymbol{\alpha}^{C}\right)$$

The posterior distribution of global alpha factors in the two-stage model can be obtained similarly.

4.3. Examples for the alpha decomposition method

The targeted system is a redundant system with three component and three potential causes. The hierarchical Bayesian model for the procedure of the alpha decomposition method is shown in Figure 4.4.

The likelihood function of CCF events is assumed as a multinomial distribution.

$$x[1:3] \sim dmulti(\alpha[1:3], X) \qquad \text{Equation 4.9}$$

The prior distribution is assumed as a Dirichlet distribution.

$$\alpha[1:3] \sim ddirich(\theta[1:3]) \qquad \text{Equation 4.10}$$

The hyperprior can be expressed by decomposed alpha factors and occurrence frequencies.

$$\theta[j] = \left(\sum_{i=1}^{3} \alpha_j^{C_i} \bullet r_i \right) \bullet X \qquad \text{Equation 4.11}$$

The decomposed alpha factors of Cause i are assumed as a noninformative prior that is the Dirichlet distribution with all parameters ($\delta^{C_i}[1:3]$) equaling to 1.

$$\alpha^{C_i}[1:3] \sim ddirich(\delta^{C_i}[1:3]) \qquad \text{Equation 4.12}$$

Based on Equations 4.7 and 4.8, the posterior distributions for global alpha factors and decomposed alpha factors can be calculated. Two examples are provided to illustrate the application of the alpha decomposition method in the estimation of CCF parameters. The

Example 4.1 is based on the recommended database without detailed system-specific data. The Example 4.2 is based on the specific database with detailed system-specific data.

Example 4.1 Bayesian inference based on the recommended database (*Section 4.1.1*)

The recommended database introduced in 4.1.1 is used in this example. There is failure data of 16 systems considered. Occurrence data of three potential causes are collected. The procedure of parameter estimation is introduced in Figure 4.5. The parameter *group.size* equals 3, and the parameter *case.number* equals 16. Two plates represent two repeated loops. Oval nodes are stochastic components and squared nodes are constant components. Lined arrows are stochastic dependence and hollow arrows are logical dependence.

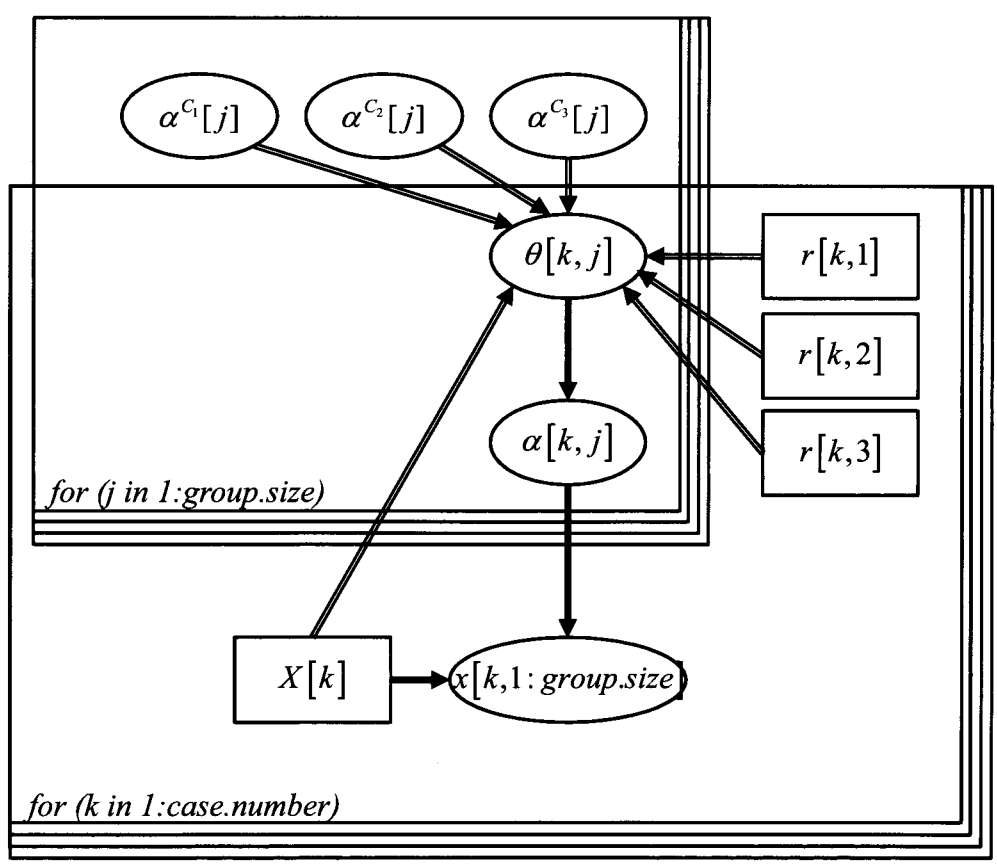

Figure 4.5 The alpha decomposition process for targeted systems with recommended database

Table 4.4 OpenBUGS script for Example 4.1 based on recommended database

```
model{
for(k in 1:case.number){                    # Model's likelihood
x[k, 1:group.size] ~ dmulti(alpha[k,        # Stochastic model with multinomial
1:group.size], X[k])                          likelihood function
X[k] <- sum(x[k, 1:group.size])             # X is the total number of "group failure
                                              events"
alpha[k, 1:group.size] ~ ddirich(theta[k, ]) # Transition variable
for (j in 1:group.size){
theta[k, j] <- (alpha.c[1, j]*r[k, 1] + alpha.c[2,  # Predicted function for the alpha
j]*r[k, 2] + alpha.c[3, j]*r[k, 3])*X[k]          decomposition
}
}
for (i in 1:cause.number){
alpha.c[i, 1:3] ~ ddirich (delta[i, ])
delta[i, 1] <- 1                            # A noninformative prior distributions for
delta[i, 2] <- 1                              decomposed alpha factors with each
delta[i, 3] <- 1                              parameter in dirichlet distributions
}                                             equaling 1
}

DATA
list(x=structure(.Data=c(...),.Dim=c(16,3)),
r=structure(.Data=c(...), .Dim=c(16,3)),    # Observed data and parameters
group.size=3, case.number=16,
cause.number=3)
```

The OpenBUGS script for the alpha decomposition process based on recommended database is provided in Table 4.4. The result of Bayesian inference can be obtained based on the alpha-decomposition method and recommended database. Table 4.5 shows the summary of posterior distributions for decomposed alpha factors. Figures (4.6 - 4.8) show the probability density curves of posterior decomposed alpha factors. It can be concluded that causes are of different CCF risk significance, which can be given by the ranking of decomposed alpha factors. The Cause 2 is of the largest quantity of decomposed Alpha 1, and of the smallest quantity of decomposed Alpha 2 and 3. Cause 2 is the cause of least CCF risk among three possible causes. Cause 1 tends to result in complete CCF events more frequently than Cause 3, but Cause 3 tends to result in partial CCF events more frequently.

$$\alpha_1^{C_1} < \alpha_1^{C_3} < \alpha_1^{C_2}$$
$$\alpha_2^{C_2} < \alpha_2^{C_1} < \alpha_2^{C_3}$$
$$\alpha_3^{C_2} < \alpha_3^{C_3} < \alpha_3^{C_1}$$

Table 4.5 Summary of posterior distribution for decomposed alpha factors

Parameter		Mean	Median	95% Interval
Cause 1	$\alpha_1^{C_1}$	0.8170	0.8233	(0.6208, 0.9647)
	$\alpha_2^{C_1}$	0.1009	0.0872	(0.0043, 0.2681)
	$\alpha_3^{C_1}$	0.0821	0.0750	(0.0040, 0.2006)
Cause 2	$\alpha_1^{C_2}$	0.9086	0.9118	(0.8194, 0.9765)
	$\alpha_2^{C_2}$	0.0738	0.0706	(0.0109, 0.1554)
	$\alpha_3^{C_2}$	0.0175	0.0137	(0.0005, 0.0552)
Cause 3	$\alpha_1^{C_3}$	0.8206	0.8244	(0.6815, 0.9375)
	$\alpha_2^{C_3}$	0.1073	0.1053	(0.0138, 0.2151)
	$\alpha_3^{C_3}$	0.0721	0.0703	(0.0061, 0.1533)

The specific posterior probability density curves are provided in Figures 4.6 – 4.8. Figure 4.6 shows the result of decomposed Alpha-1 which represents the ability of respective cause triggering an independent failure. In the figure, Alpha[C1,1] refers to the decomposed alpha factor ($\alpha_1^{C_1}$) of Cause 1 involving the failure of one component. All other terms refer to respective decomposed alpha factors. Figure 4.7 shows the result of decomposed Alpha-2 which represents the ability of respective cause triggering a partial CCF event. Figure 4.8 shows the results of decomposed Alpha-3 which represent the ability of respective cause triggering a complete CCF event.

The positions of curves suggest the risk significances of causes and ranges suggest the uncertainty in the estimates. One important topic in PRA is to evaluate the source of uncertainty in the estimates. The alpha decomposition method can provide a way to determine the source of uncertainty in the CCF parameter estimation. For instance, Figure 4.8 shows the posterior distributions for decomposed alpha factors of complete CCF. The estimate of $\alpha_3^{C_2}$ (Alpha[C2,3]) is of the least uncertainty among three causes. It means the uncertainty in the estimate of Alpha 3 is mainly from Cause 1 and Cause 3.

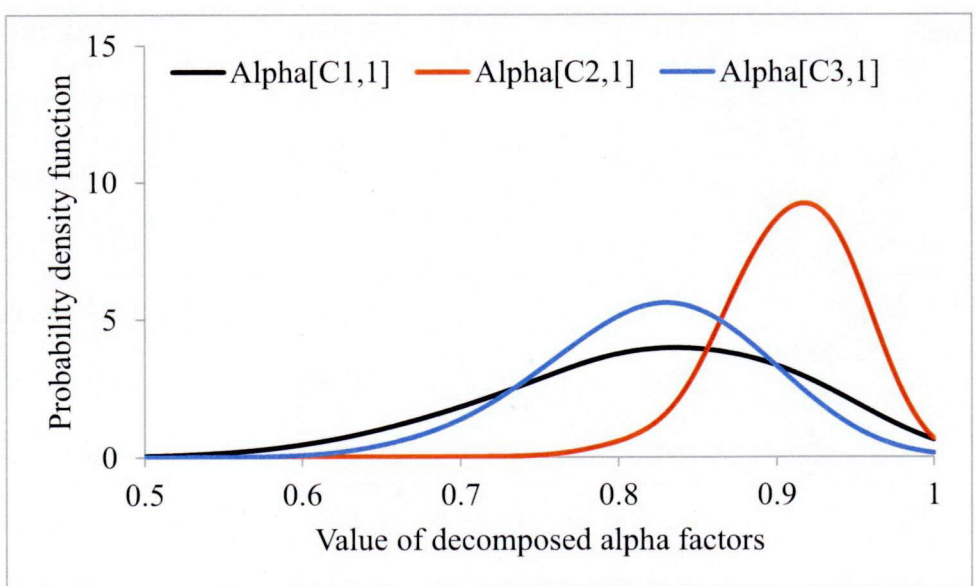

Figure 4.6 Posterior distributions for decomposed alpha-1

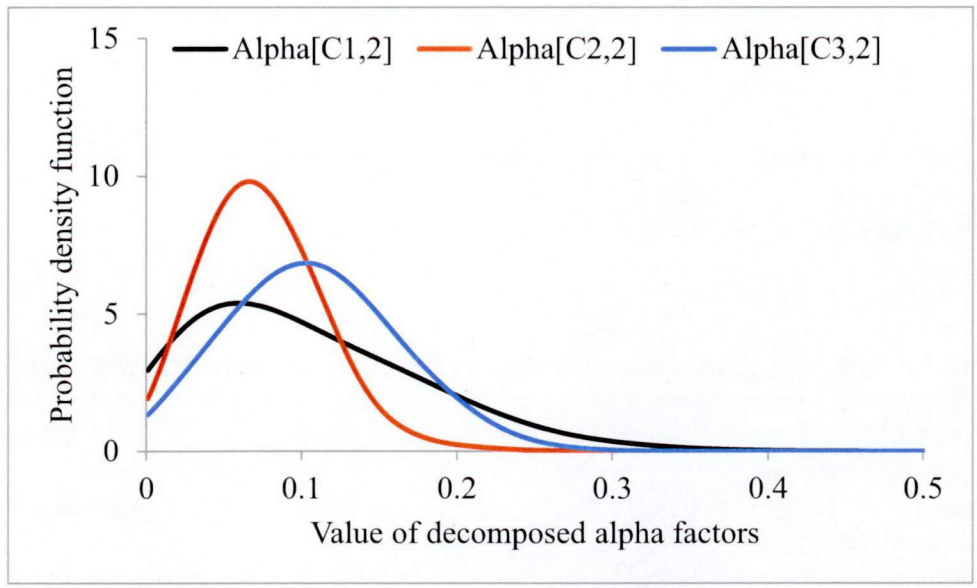

Figure 4.7 Posterior distributions for decomposed alpha-2

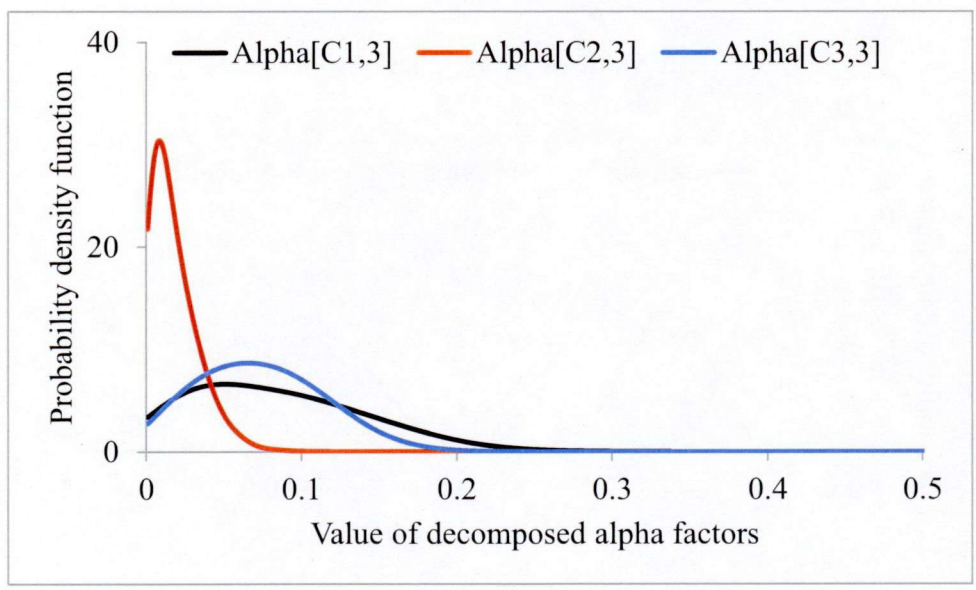

Figure 4.8 Posterior distributions for decomposed alpha-3

Table 4.6 shows the summary of posterior distributions for global alpha factors of System #1. Figure 4.9 shows the probability density curves of posterior global alpha factors of System #1. This estimation of global alpha factors via the alpha decomposition method can combine the system-specific and system-generic data together to provide more reliable results. At first, the CCF risk significance of the same cause has correlation between different causes

which can be utilized. The previous Bayesian inference based on failure data cannot utilize cause information reasonably, and it is difficult to combine generic and specific database together. The comparison of previous method and the Bayesian inference with cause information is provided in Section 4.4.

Table 4.6 Summary of posterior distribution for global alpha factors (System #1)

Parameter	Mean	Median	95% Interval
Alpha-1	0.8648	0.8661	(0.8142, 0.9097)
Alpha-2	0.0921	0.0911	(0.0560, 0.1351)
Alpha-3	0.0431	0.0416	(0.0190, 0.0761)

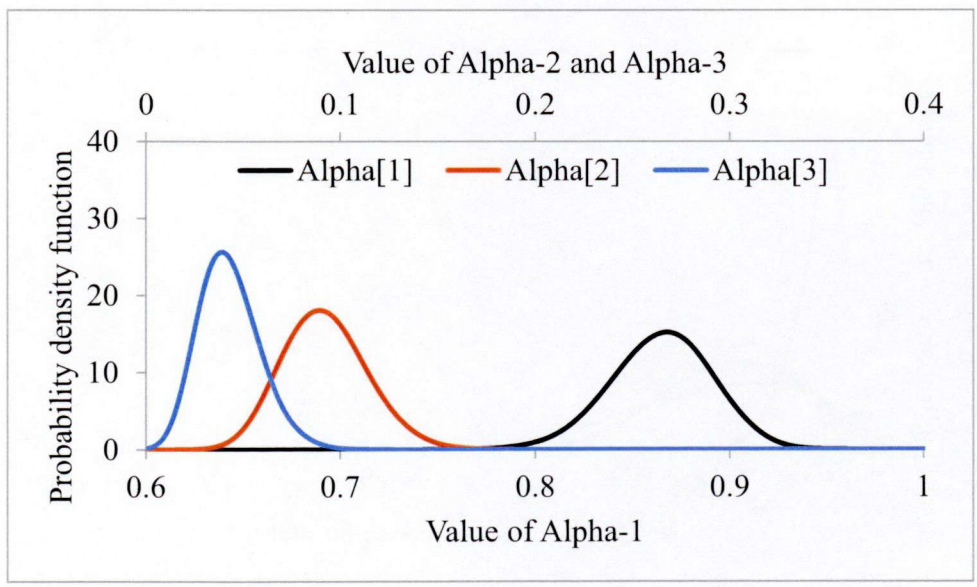

Figure 4.9 Posterior distributions for global alpha factors (System #1)

Example 4.2 Validation of the alpha decomposition method based on the alternative database (*Section 4.1.2*)

This example is provided to validate the alpha decomposition method when a system-specific database is proposed with sufficient CCF information. The database is

introduced in Table 4.3 with the occurrence information of causes as well as failure for one targeted system.

Figure 4.10 depicts the procedure of validation for System #1. The meaning of nodes is same to Figure 4.5. There are two type of global alpha factors one is predicted by the alpha decomposition process, and the other is the result by the failure information. Based on the specific CCF database, the risk of each cause can be directly established, so the prediction of global alpha factors can be obtained. The prediction is more reliable than the two-stage hierarchical Bayesian structure which is reduced to one stage in this example. This database has advantages and disadvantages. The advantage is that the calculation procedure will be simplified and the estimation of cause risk will be more reliable. The disadvantages are that there is always not enough data for one specific system and it is hard to combine generic CCF data and causal information of other systems as some properties of causes are shared by different systems.

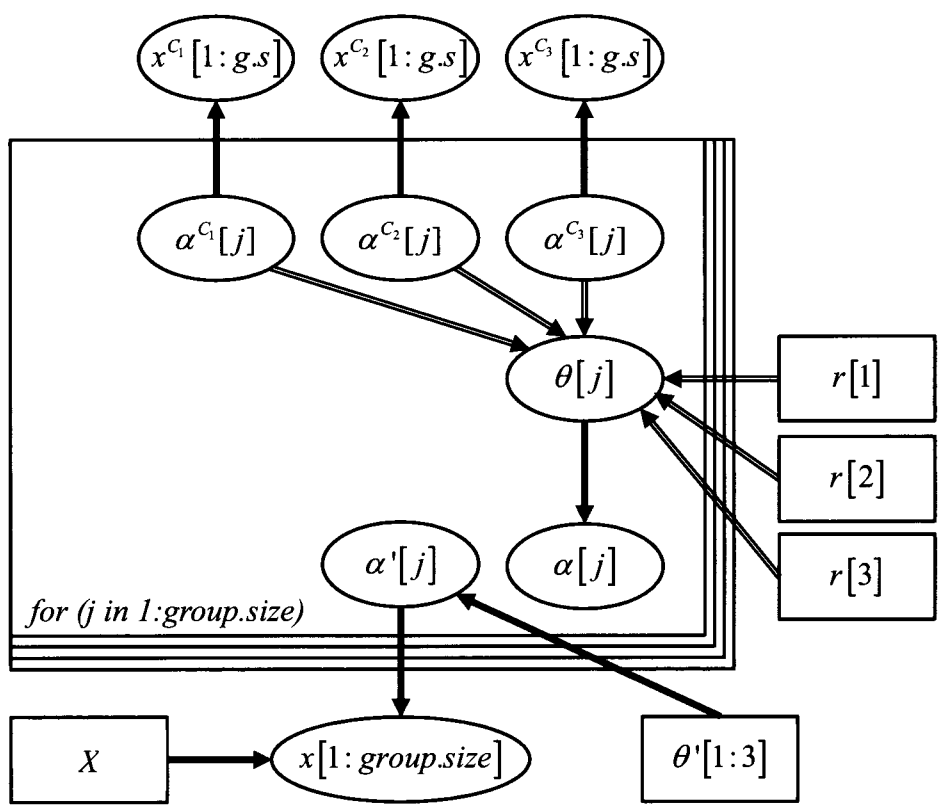

Figure 4.10 The alpha decomposition process for System #1 with specific database

Table 4.7 OpenBUGS script for Example 4.2 based on alternative database

```
model{
x[1:group.size] ~ dmulti(alpha.dash[1:group.size], X)   # Stochastic model with multinomial likelihood function (validation model)
X <- sum(x[1:group.size])
alpha.dash[1:group.size] ~ ddirich(theta.dash[ ])       # Prior for global alpha factors
alpha[1:group.size] ~ ddirich(theta[ ])                 # Prediction of global alpha factors (alpha decomposition model)
for (j in 1:group.size){
x[j] <-x.c[1, j] + x.c[2, j] + x.c[3, j]                # Event number of each failure
theta[j] <- (alpha.c[1,j]*r[1] + alpha.c[2,j]*r[2] +    # Predicted function for the parameters
alpha.c[3,j]*r[3])*X
theta.dash[j] <- 1                                      # A noninformative prior for validation model
}
for (i in 1:cause.number){
x.c[i,1:group.size] ~ dmulti (alpha.c[i, ],X.c[i])      # Likelihood for causality inference
alpha.c[i,1:group.size] ~ ddirich(delta[i,])            # Prior for decomposed alpha factors
delta[i,1] <- 1                                         # A noninformative prior for decomposed alpha factors
delta[i,2] <- 1
delta[i,3] <- 1
X.c[i] <- sum(x.c[i,1:group.size])                      # Number of each cause group
}
}
DATA                                                    # Observed data and parameters
list(x.c=structure( .Data=c(24,6,2,24,3,1,65,2,0), .Di
m=c(3,3)), r=c(0.2520,0.2205,0.5276), group.size=3,
cause.number=3)
```

There are two parts of calculation in the Figure 4.10.

1) The prediction of global alpha factors is obtained based on the estimates of decomposed alpha factors as well as the data of causes' occurrence frequencies. The estimation of decomposed alpha factors are based on the system-specific database via a one-stage hierarchical Bayesian model.
2) The estimation of global alpha factors is obtained based on the CCF events, and no causal information is used in this part.

If two groups of results are roughly same with acceptable uncertainty, it is proved that the alpha decomposition method can suitably utilize the causal information in the estimation of CCF parameters. It can be foreseen that the first prediction will of more uncertainty as no failure information is directly use to estimate the alpha factors and the innate uncertainty of Dirichlet will propagate to the predicted results. The uncertainty brought by the Dirichlet distribution is acceptable.

Table 4.7 shows the OpenBUGS script for the process of validation. The summary of results is shown in Table 4.8. Two groups of estimates are obtained. One is the estimation of global alpha factors totally based on the causal risk significance (decomposed alpha factors) and causes' occurrence frequencies. The other estimation of global alpha factors is totally based on the failure data, which use to decide the reliability of the alpha decomposition method. The respective predicted alpha factors are mainly same, and there are different uncertainties in the distribution. These uncertainties might be from the innate uncertainty of the Dirichlet distribution. Because there are multiple combinations given same quantity of CCF events, this specific is only one case of them. The estimation will be different from the results only according to failure data. The Figure 4.11 also shows this conclusion. The positions of respective curves are almost same. The range of curves shows the acceptable uncertainties.

It is concluded that all the global alpha factors are decomposable. The decomposability of alpha factors can be proved by the theory of Hybrid Bayesian Network or

by the numerical computation based on system-specific database. This decomposability shows that the lumped alpha factors are the integrated reflection of the risk of common causes to the redundant systems. The alternative database applied in this example is a very important form of CCF database. If enough plant- or system-specific data can be obtained, it is recommended to do the one-stage Bayesian inference to analyze the risk of common causes directly. The shared properties of common cause to different systems can be deduced via more complicated hierarchical Bayesian models.

Table 4.8 Validation of the alpha decomposition method

	Parameter	**Mean**	**Median**	**95% Interval**
Estimates with causal risk only	Alpha-1	0.8552	0.8578	(0.7646, 0.9286)
	Alpha-2	0.1013	0.0980	(0.0403, 0.1803)
	Alpha-3	0.0435	0.0395	(0.0073, 0.1032)
Estimates with failure data only	Alpha_dash-1	0.8772	0.8794	(0.8162, 0.9283)
	Alpha_dash-2	0.0921	0.0898	(0.0487, 0.1481)
	Alpha_dash-3	0.0307	0.0284	(0.0084, 0.0666)

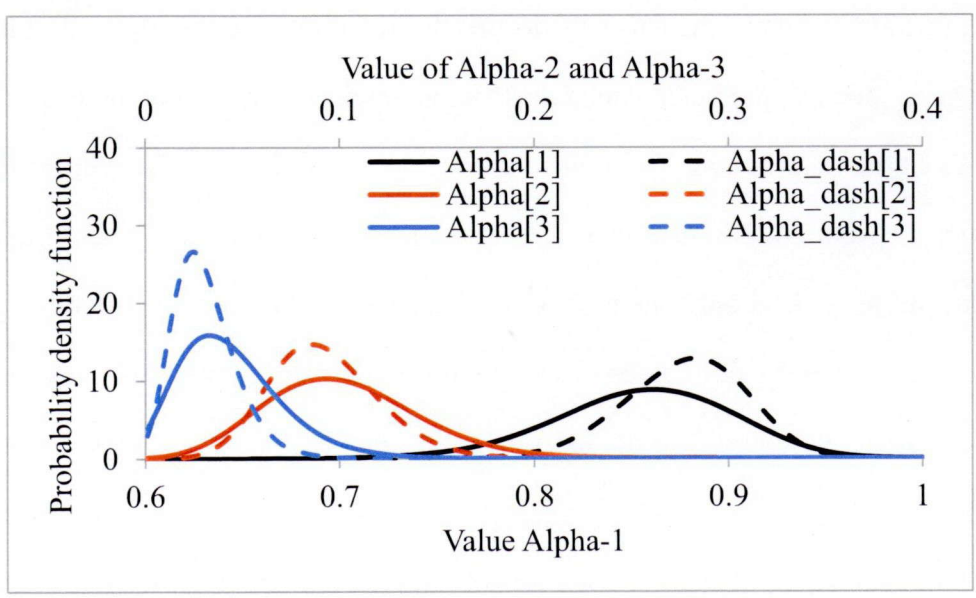

Figure 4.11 Comparison of estimates based on causal risk and failure data

Considering the rarity of CCF information and cause information, the first recommended database (Section 4.1.1) is used in this dissertation. The generic databases include the causal information and failure information. The share properties of common causes to different redundant systems can be used to estimate the CCF parameters. The application of these latently share properties can reduce the uncertainty in the estimates which will be discussed in next section.

4.4. Uncertainty Analysis

The uncertainty in the estimates of CCF parameters is analyzed in this section. Two methods are compared. One is the alpha decomposition method based on the recommended database of cause and failure information (Table 4.1 and Table 4.2), and the other is the traditional alpha factor model with failure data (Table 4.2).

The Figure 4.12 shows the uncertainty comparison for the results of System #1. Solid curves are the estimates based on the alpha decomposition method and dashed curves are the estimates based on the alpha factor model. The ranges of solid curves are narrower than the dashed curves. The tendency is also demonstrated in the Table 4.9 where the 95% internal of estimates (the alpha decomposition method) is narrower than that of estimates (the alpha factor model). The alpha factor model only uses the failure data of System #1, while the alpha decomposition process combines the shared properties of common causes. It can provide a more reliable prediction of CCF risk especially when the CCF data is rare and the generic database must be used. For instance, to estimate a newly modified system, there is no operation data and the recorded generic CCF data cannot reflect the modified characteristics of the new system. Therefore, the specific inference of causal mechanism and coupling factor can provide reliable evidences. The alpha decomposition method as well as recommended databases is recommended to be applied in the PRA analysis to estimate the failure probabilities of initiating events.

Table 4.9 Comparison of uncertainty between the alpha decomposition method and the alpha factor model for System #1

	Parameter	Mean	Median	95% Interval
The alpha decomposition method	Alpha-1	0.8648	0.8661	(0.8142, 0.9097)
	Alpha-2	0.0921	0.0911	(0.0560, 0.1351)
	Alpha-3	0.0431	0.0416	(0.0190, 0.0761)
The alpha factor model	Alpha_dash-1	0.8772	0.8794	(0.8162, 0.9283)
	Alpha_dash-2	0.0921	0.0898	(0.0487, 0.1481)
	Alpha_dash-3	0.0307	0.0284	(0.0084, 0.0666)

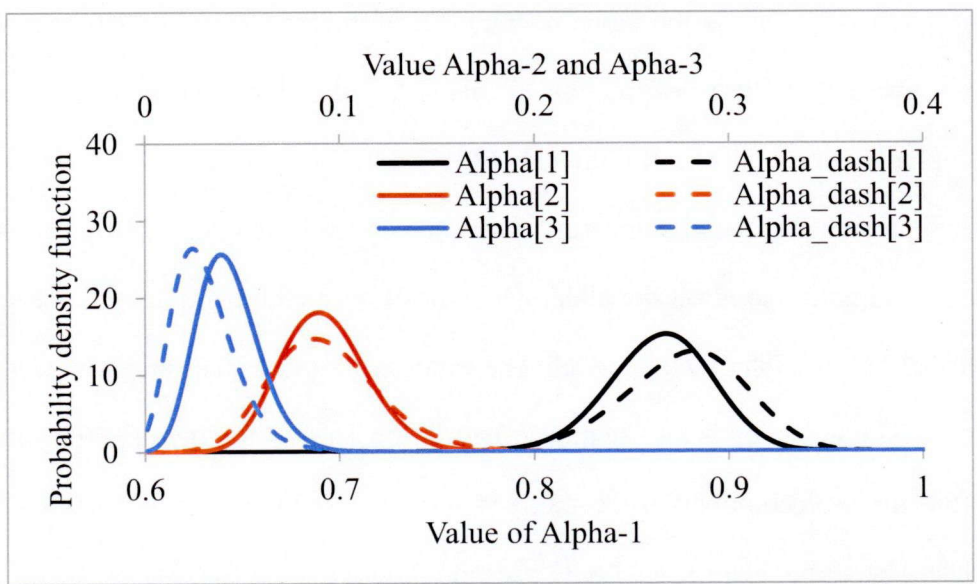

Figure 4.12 Comparison of uncertainty between the alpha decomposition method and previous alpha factor model for System #1

Figure 4.13 show the uncertainty analysis for all 16 redundant systems in the recommended databases. The solid lines are the estimates based on the alpha decomposition method and the dashed lines are the estimates based on the alpha factor model. Three aspects of uncertainty analysis are discussed.

1) Compared with results of the alpha factor model, the uncertainties in the posterior

distributions of the alpha decomposition method are reduced. It is concluded that the current method can combine valuable information from cause level to reduce the uncertainties in the PRA parameter estimation.

2) In the recommended databases, systems are listed according to the number of CCF events for largest to smallest. Usually, the scarcity of CCF data is a major source of uncertainty. In Figure 4.13, all lines have the same trend that uncertainties increase with the decreasing of CCF data.

3) Since it is a stochastic modeling of CCF events, there are innate uncertainties in the estimates. The uncertainties in the parameter estimation can be reduced but cannot be diminished.

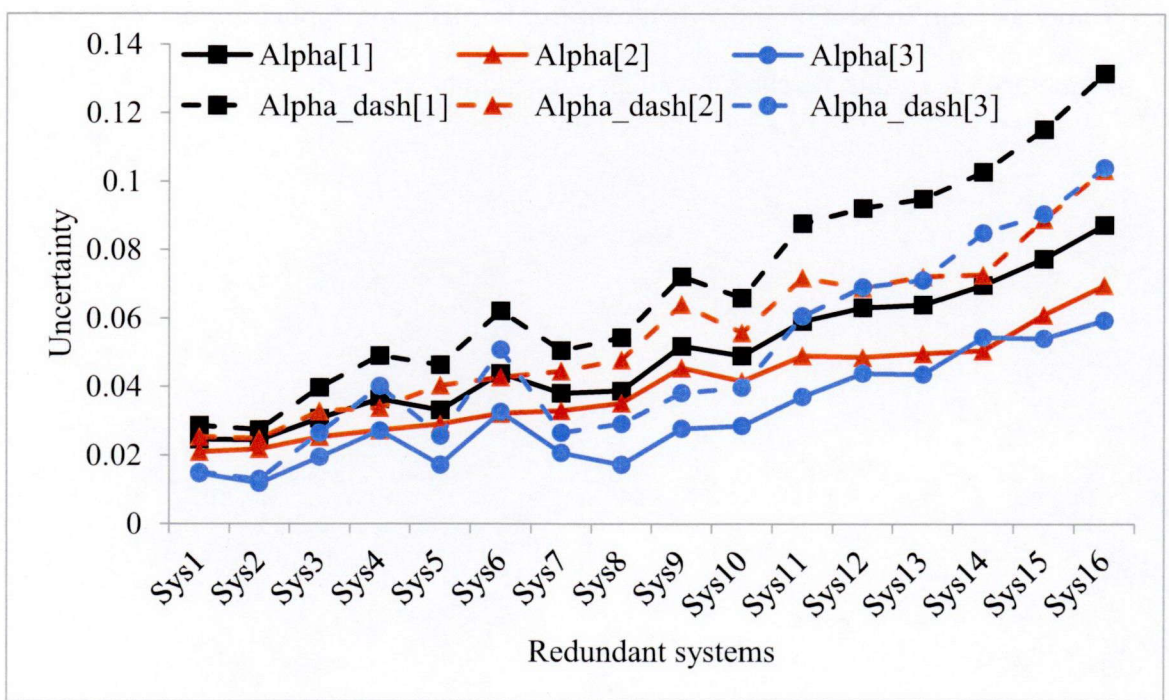

Figure 4.13 Comparison of uncertainty between the alpha decomposition method and previous alpha factor model for all redundant systems

4.5. Summary and Results

In Section 4.1, two types of databases are recommended to be built for the estimation of CCF parameters including global alpha factors and decomposed alpha factors. Based on the recommended databases, the numerical approach by hierarchical Bayesian modeling has been schematically discussed in Section 4.2. In Section 4.3, numerical examples are demonstrated to show the computation process of the alpha decomposition method. Posterior distributions of CCF parameters have been obtained. Decomposed alpha factors can represent the CCF risk of causes. Results for different databases are compared and discussed. Moreover, by the hypothetical system-specific database, the alpha decomposition can be numerically validated. The sources of uncertainty in the estimates of alpha factors can be evaluated by decomposed alpha factors as well. In Section 4.4, when causal information is applied to the estimation of CCF parameters, the results are shown with less uncertainty.

Chapter 5: PROBABILISTIC MODELING OF FLOODING RISK FOR AUXILIARY FEEDWATER SYSTEM PROTECTED BY FLOOD BARRIERS

This chapter discusses the application of the alpha decomposition method to modified Auxiliary Feedwater (AFW) system when no historical operation data can be used. There is safety-related equipment (American Nuclear Society Safety Class I) in PWR safeguards alley compartments which is affected by the failure of non-Class I systems in the turbine building. It includes AFW pumps, emergency diesel generators and safe shutdown panel, etc. Previous inspection found that there was inadequate design control to ensure Class I equipment protect against internal flood. The internal flood results from the failures of Non-safety water system piping and equipment. For instance, water sources include circulating water system, fire water pipes, feedwater pipes and reactor makeup storage tanks, etc. The random or seismically-induced ruptures of these non-Class I systems will results in severe flooding or excessive steam release. Flood water will flow into the area where systems of Safety Class I located. Especially, the AFW pumps' function will be impaired which is an initiating event of the loss of secondary feedwater. The AFW pump system is a redundant system with three redundant pumps. The flood is an important common cause for the AFW pump system.

Additional flood barriers are introduced to be built to defend against the potential internal flood. The CCF risk of AFW pump system will be changed after the construction of flood barriers. Usually, the available CCF parameter database is a generic database without consideration of the modified design of one redundant system. Because the internal flood risk depends on the state of flood barriers and it affects the global alpha factors, the dynamic CCF analysis of the AFW pump system can be quantitatively estimated based on hypothetical databases and Bayesian approaches. Two major topics are discussed in this chapter, one is the change of CCF risk after the construction of flood barriers, and the other is the change of CCF risk when the flood barriers degrade because of an earthquake and a flood.

5.1. Additional Flood Barriers in Turbine Building

Potential failures of non-Class I water system piping and equipment are investigated. Systems with sufficient inventory and flow rates to failure AFW pumps in the safeguard alley are determined to be: (1) Circulating water, (2) Service water, (3) Fire waters, (4) Feedwater, (5) Condensate; (6) Condensate and reactor makeup water storage tanks. The initiating events of internal flood include nine types of random failures, tornado-induced failure, turbine-missile induced failure, and seismic-induced failure. This dissertation analyzes the risk of seismic-induced internal flood and flood barriers failure as an example.

Figure 5.1 shows the conceptual layout in the turbine building. For the simplest consideration, three AFW pumps (A, B and C) are assumed as identical pumps which actually are two motor-driven AFW pumps and one turbine-driven AFW pump. Potential water sources are represented by the blue rectangle. After the occurrence of an external event or a random failure, the flood will flow through entrance gates and then impair the safety-related components.

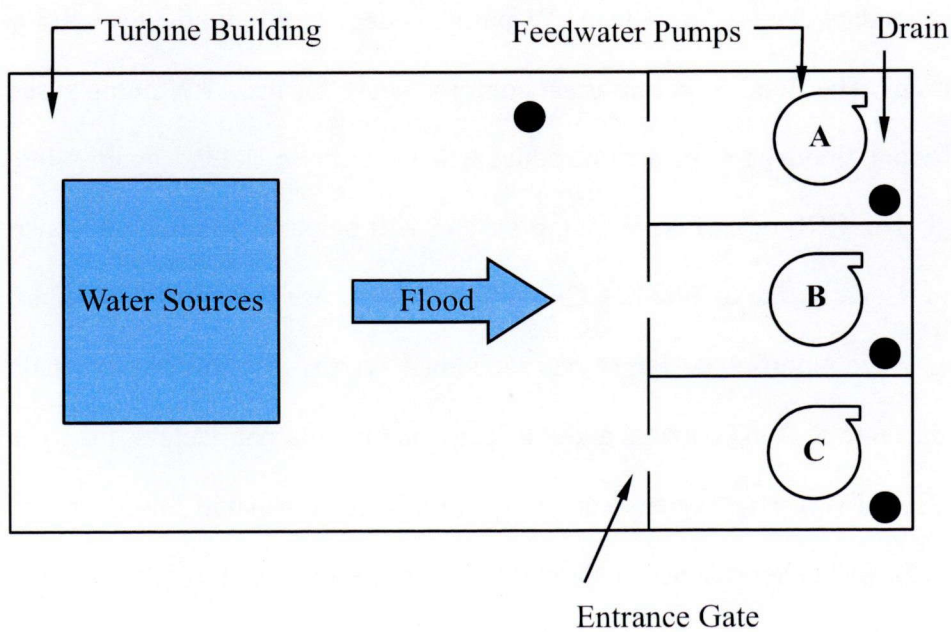

Figure 5.1 Turbine building without flood barriers

To protect the AFW pump system from the risk of internal flood, additional barriers are recommended to be constructed at the entrance gates. Figure 5.2 shows the location of additional barriers. The green circles refer to the flood barriers. The flood barriers physically separate the flood sources and other redundant components. Therefore, if a random failure happens at one flood barrier, only the respective pump is affected by the internal flood. Such sort of physical separation is an effective means to interrupt the coupling factor of the flood.

Let us compare Figure 5.1 and Figure 5.2, it is obvious that the CCF risk of the redundant AFW system is different. Moreover, if flood barriers fail for as a result of shared causes, the CCF risk of the degraded AFW pump system will change. In the following sections, the quantitative analysis of CCF risk based on the alpha factor method will be discussed.

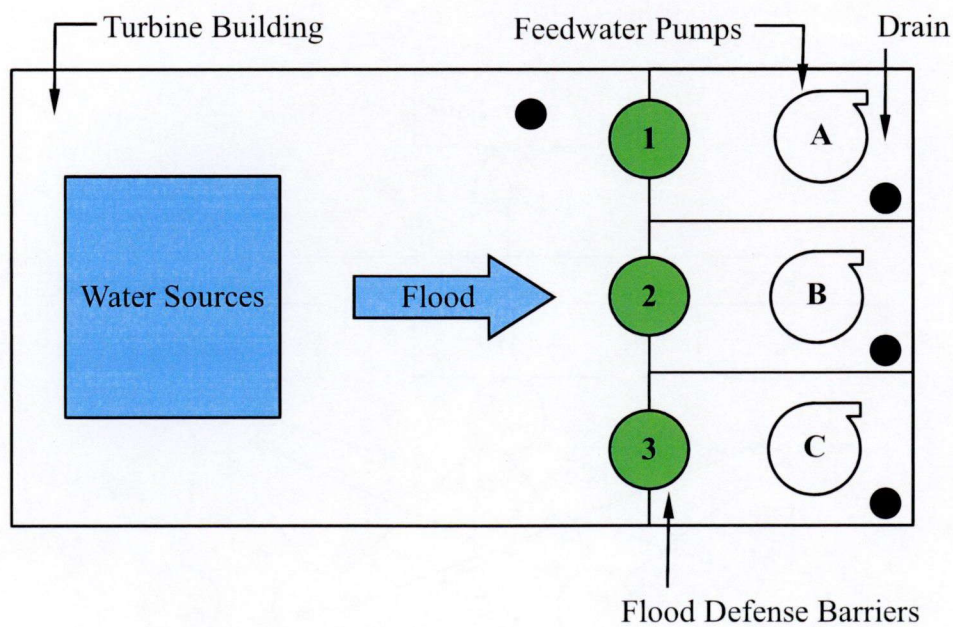

Figure 5.2 Additional flood barriers recommended to be built in the turbine building

5.2. Probabilistic CCF Modeling for AFW Pump System after the Construction of Flood Barriers

5.2.1. Causal inference for modified AFW pump system via HBN

The Hybrid Bayesian Network (HBN) for modified AFW pump system is shown in Figure 5.3. Three redundant pumps (A, B, and C) are assumed in the system. There three possible causes and Cause 1 is assumed as the internal flood that is of interest. When the flood barriers are constructed in the turbine building, the flood flow paths are blocked and three redundant pumps are physically separated. Two dashed lines mean the physical separation of redundant pumps. When there is no serious external disaster happens, only random failures happen in flood barriers. Hence, all three redundant are well separated.

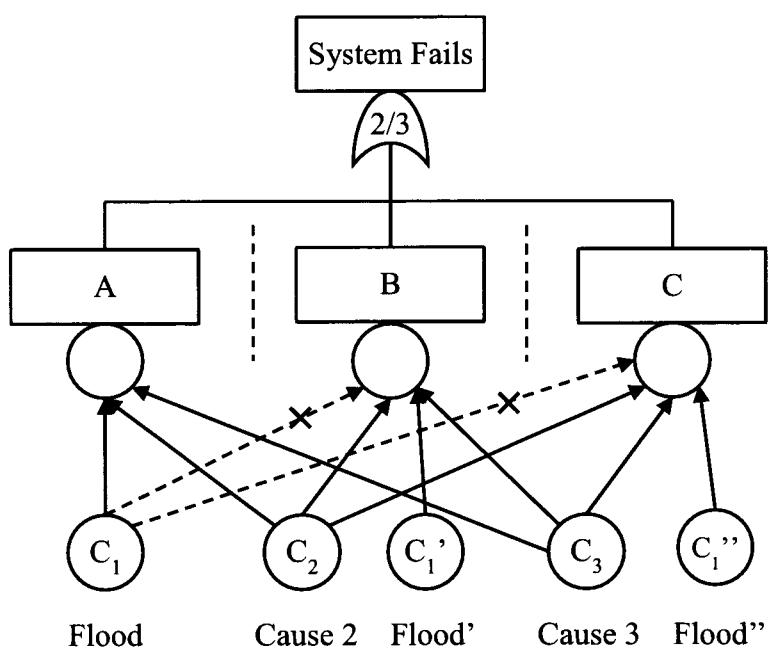

Figure 5.3 Causal inference for the system with flood barrier

In Figure 5.3, the flood is an independent cause when three flood barriers are functionally available. Causes (C_1', C_2' and C_3') are independent flood. The C_1 induced

failures of Pump B and C are diminished. Since there is no defense mechanism introduced to protect the system against Cause 2 and Cause 3, these two causes are still common causes.

Figure 5.4 shows the HBN modeling for the Pump A. The same to the previous introduced models, there are three types of failures involving Pump A: (1) Independent failure (A_I), (2) Partial common cause failure (C_{AB} and C_{AC}), (3) Complete common cause failure (C_{ABC}). Based on the system analysis, the flood with random barrier failure only generates independent failure of Pump A.

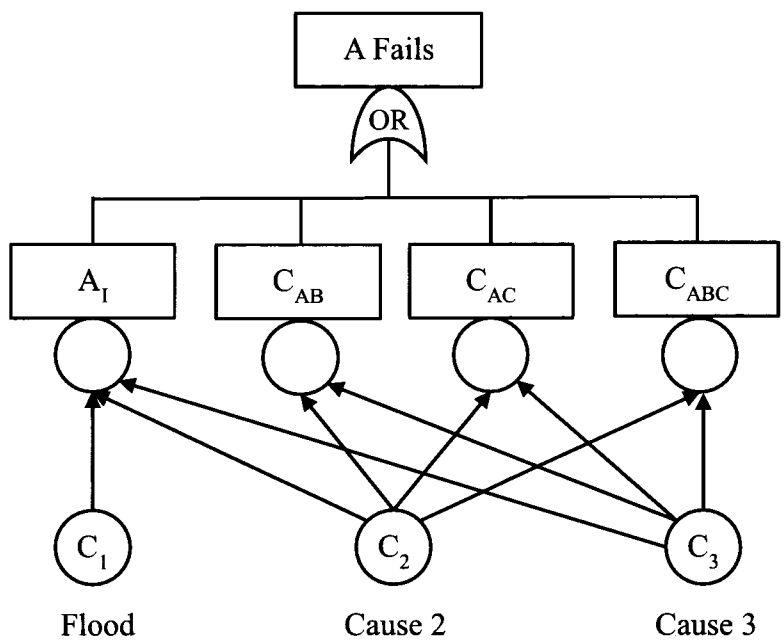

Figure 5.4 Causal inference for Pump A after the construction of flood barrier

5.2.2. Flood induced CCF risk analysis via the alpha decomposition method

The updated decomposed alpha factor for the modified AFW pump system is analyzed in this chapter. As shown in the Figure 5.4, with the construction of flood barriers, the CCF risk induced by the flood changes. The CCF risk induced by Cause 2 and Cause 3 does not change. The change of CCF risk can be expressed by the update of decomposed alpha factors for the Cause 1 (Flood). This process can be written by conditional probability.

$$P\left(C_{AB} \cup C_{AC} \cup C_{ABC} \middle| Flood\right) \rightarrow P\left(A_I^* \middle| Flood\right) \qquad \text{Equation 5.1}$$

The Equation 5.1 demonstrates the degradation of CCF events to independent failures. From the perspective of conditional probability, it shows that the flood coupling with failure of flood barrier #1 (Figure 5.2) only results in independent failures. The flood barrier #2 and #3 are still available. The success law of redundant system is assumed as 2-out-of-3, so the AFW pump system is still available.

It is proved previously that the decomposed alpha factors represent the CCF triggering abilities of causes. Thus, the updated decomposed alpha factors of the flood can be given by

$$\begin{aligned} updated\ \alpha_1^{C_1*} &= 1 \\ updated\ \alpha_2^{C_1*} &= 0 \\ updated\ \alpha_3^{C_1*} &= 0 \end{aligned} \qquad \text{Equation 5.2}$$

Here, $\alpha_1^{C_1*}$ refers to the updated ability of the internal flood to cause an independent failure; $\alpha_2^{C_1*}$ refers to the constrained ability of the internal flood to cause a partial CCF involving two pumps; $\alpha_3^{C_1*}$ refers to the constrained ability of the internal flood to cause a complete CCF involving all three pumps. Equation 5.2 numerically demonstrates that the flood only generate independent failure.

5.2.3. Bayesian inference with the alpha decomposition method

According to the alpha decomposition method introduced in the last chapter, the estimation of CCF parameters of modified safety-related systems can be obtained by the Bayesian inference. The estimates of CCF parameters can be applied to the calculation of failure probability of basic events as well as systems, which are important in the PRA procedures. The uncertainty in the estimation on component-level and system-level will be

propagated along with fault trees and event trees. The overestimation and underestimation of safety-related parameters should be considered. The uncertainty in the CCF parameters partially results from the rough utilization of CCF database without the consideration of the difference in the targeted system. As introduced previously, for the AFW systems with and without flood barriers, the CCF risk of flood is different. Bayesian inference is a useful method to solve the problem even if limited CCF databases are available.

Example 5.1 CCF parameters estimation of the modified AFW system

A numerical example is provided to illustrate the calculation process of Bayesian inference with the alpha decomposition method for the modified AFW system. There are three redundant pumps in the targeted AFW system. The multinomial distributions serve as the aleatory model for CCF events. The prior distributions for global alpha factors are assumed as Dirichlet distributions. Moreover, the noninformative prior for decomposed alpha factors of one cause is assumed as Dirichlet distribution with all parameters $\delta^{C_i}[1:3]=[1,1,1]$. All of the equations for the prior and posterior distributions are shown in Chapter 4, as Equation 4.9 ~ Equation 4.12. Therefore, the CCF risk of internal flood can be expressed by the decomposed alpha factors. Based on the causal inference in Section 5.2.1, the new decomposed alpha factors of internal flood can be confirmed via Equation 5.2. Hence, the updated global alpha factors should show the change of modification based on the new decomposed alpha factors.

Figure 5.5 shows the graphical model of parameter estimation for modified system by the alpha decomposition process. There are mainly two routes: one is the estimation of decomposed alpha factors by two-stage hierarchical Bayesian inference; the other is the prediction of updated global alpha factors by the updated decomposed alpha factors as well as other unchanged decomposed alpha factors.

At first, it is shown that global alpha factors ($\alpha[k,j]$) and decomposed alpha factors ($\alpha^{C_i}[j]$) are obtained based on the failure data ($x[k,1:group.size]$) and causes' occurrence frequency ($r[k,1:3]$). Here, there are totally 16 candidate systems are considered, so $case.number = 16$. There are three redundant components in the targeted system, so $group.size = 3$.

Secondly, after the construction of flood barriers, the CCF risk generated by the flood is changed. The updated decomposed alpha factors of the internal flood ($\alpha^{C_1}[1:3]^*$) and updated occurrence frequencies ($r[k,1:3]^*$) are used to predict the global alpha factors ($\alpha[k,1:3]^*$). The predicted alpha factors show the changed CCF risk of the modified AFW system after the construction of additional flood barriers. Parameters with the asterisk mark (*) are the CCF-related parameters for the modified system.

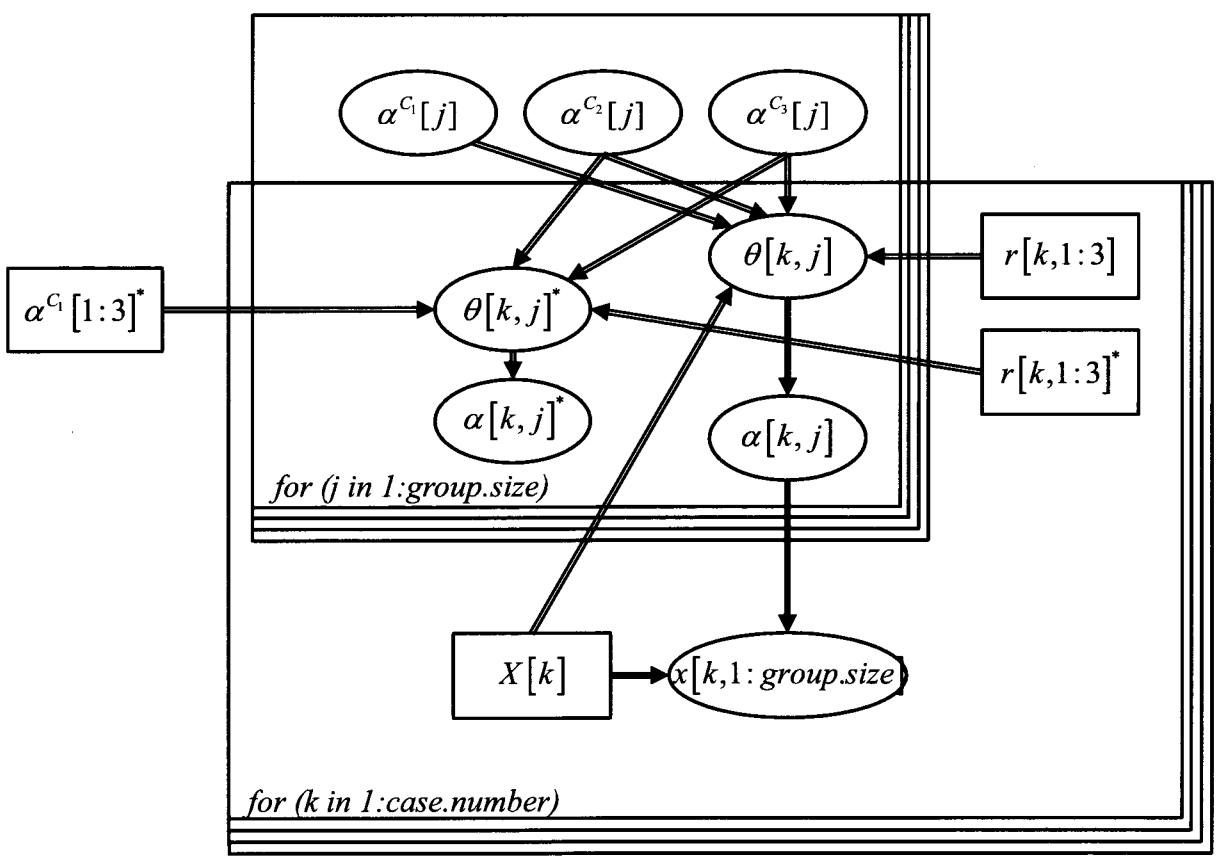

Figure 5.5 The CCF parameter estimation for modified system with flood barriers

Table 5.1 Hypothetical database for AFW pump system without flood barrier

AFW Pump System	Common causes' occurrence			Single & Common cause failure		
	Cause 1 (Flood)	Cause 2	Cause 3	Single (1/3)	Partial (2/3)	Complete (3/3)
# 1	32(25.20%)	28(22.05%)	67(52.76%)	113	11	3
# 2	17(16.04%)	78(73.58%)	11(10.38%)	98	7	1
# 3	18(20.69%)	19(21.84%)	50(57.47%)	73	9	5
# 4	29(43.94%)	6(9.09%)	31(46.97%)	53	5	8
# 5	7(14.00%)	33(66.00%)	10(20.00%)	45	4	1
# 6	15(36.60%)	9(22.00%)	17(41.40%)	33	3	5
# 7	12(35.29%)	15(44.12%)	7(20.59%)	32	2	0
# 8	2(6.45%)	22(70.97%)	7(22.58%)	29	2	0
# 9	7(31.82%)	4(18.18%)	11(50.00%)	20	2	0
# 10	10(47.62%)	8(38.10%)	3(14.29%)	20	1	0
# 11	3(15.79%)	6(31.58%)	10(52.63%)	16	2	1
# 12	7(43.75%)	3(18.75%)	6(37.50%)	14	1	1
# 13	3(20.00%)	5(33.33%)	7(46.67%)	13	1	1
# 14	5(33.33%)	3(20.00%)	7(46.67%)	12	1	2
# 15	4(36.36%)	5(45.45%)	2(18.18%)	9	1	1
# 16	1(11.11%)	6(66.67%)	2(22.22%)	7	1	1

As shown in Table 5.1, the hypothetical generic CCF database for Pump A is assumed to demonstrate the data need for the Bayesian inference. After the construction of flood barriers, the failures caused by the flood in databases will be reduced. In this example, the random failure probability of flood barriers is assumed as 0.1 and it is assumed that only random independent failure happens for the flood barriers. The common cause failure of flood

barriers will be discussed in next sections. Two sets of important CCF data are collected: one is the record of CCF events and the other is the occurrence information of common causes. Three causes and three types of failure are recorded. Usually, there is no plant-specific CCF database, so this database is useful to evaluate the causes' CCF hazard.

Table 5.2 Hypothetical database for causes' occurrence frequency

AFW Pump System	**Causes' occurrence**			**Updated causes' occurrence**		
	Cause 1 (Flood)	Cause 2	Cause 3	Cause 1 (Flood)	Cause 2	Cause 3
# 1	25.20%	22.05%	52.76%	3.26%	28.51%	68.23%
# 2	16.04%	73.58%	10.38%	1.87%	85.99%	12.13%
# 3	20.69%	21.84%	57.47%	2.54%	26.84%	70.62%
# 4	43.94%	9.09%	46.97%	7.27%	15.04%	77.70%
# 5	14.00%	66.00%	20.00%	1.60%	75.51%	22.88%
# 6	36.59%	21.95%	41.46%	5.46%	32.73%	61.82%
# 7	35.29%	44.12%	20.59%	5.17%	64.66%	30.17%
# 8	6.45%	70.97%	22.58%	0.68%	75.34%	23.97%
# 9	31.82%	18.18%	50.00%	4.46%	25.48%	70.07%
# 10	47.62%	38.10%	14.29%	8.33%	66.66%	25.00%
# 11	15.79%	31.58%	52.63%	1.84%	36.81%	61.35%
# 12	43.75%	18.75%	37.50%	7.22%	30.93%	61.86%
# 13	20.00%	33.33%	46.67%	2.44%	40.65%	56.91%
# 14	33.33%	20.00%	46.67%	4.76%	28.57%	66.67%
# 15	36.36%	45.45%	18.18%	5.41%	67.57%	27.03%
# 16	11.11%	66.67%	22.22%	1.23%	74.08%	24.69%

Table 5.2 shows the predicted common causes occurrence data. The calculation equation is given by

$$r_1^* = \frac{0.1 \bullet r_1}{0.1 \bullet r_1 + r_2 + r_3}$$
$$r_2^* = \frac{r_2}{0.1 \bullet r_1 + r_2 + r_3} \qquad \text{Equation 5.3}$$
$$r_3^* = \frac{r_3}{0.1 \bullet r_1 + r_2 + r_3}$$

Here, $r_j\,(j=1,2,3)$ refers to the original occurrence frequency of three common causes. $r_j^*\,(j=1,2,3)$ refers to the updated occurrence frequency of the three causes. 0.1 is the random failure probability of flood barriers, which is assumed before. The random failure probability of flood barriers will affect the collection of CCF events in the databases. If the flood occurs without any component failure, this failure with causal information is usually not recorded in the CCF database. Therefore, the flood barriers will defend a great number of internal flood events. Only when the barrier fails for a random cause, the respective pump will fail independently. The other extreme case is an earthquake will trigger the occurrence of flood and the failure of flood barriers, which will be discussed later. Here, the factor (0.1) means that 90% flood will be defended by the flood barrier.

Table 5.3 is the OpenBUGS script which shows the prediction process of updated global alpha factors. The same to introduction of calculation in Figure 5.5, there are mainly two parts, the first part is used to evaluate the decomposed alpha factors and the second part aims to obtain the updated CCF-related parameters by using the estimates and the result of system analysis. Therefore, based on the Bayesian inference with MCMC Gibbs Sampling, it is obtained that the posterior distributions for CCF parameters.

Table 5.3 OpenBUGS script for Example 5.1 based on two databases

```
model{
for(k in 1:case.number){                    # model's likelihood
x[k, 1:group.size] ~ dmulti(alpha[k, 1:group.size],   # Stochastic model with multinomial
X[k])                                       likelihood function
X[k] <- sum(x[k, 1:group.size])             # X is the total number of "group
                                            failure events"
alpha[k, 1:group.size] ~ ddirich(theta[k, ])  # Transition variable
for (j in 1:group.size){
theta[k, j] <- (alpha.c[1, j]*r[k, 1]       # Predicted function for the alpha
+ alpha.c[2, j]*r[k, 2] + alpha.c[3, j]*r[k, 3])*X[k]   decomposition
}
}
for (i in 1:cause.number){
alpha.c[i, 1:3] ~ ddirich (delta[i, ])
delta[i, 1] <- 1                            # A noninformative prior
delta[i, 2] <- 1                            distributions for decomposed
delta[i, 3] <- 1                            alpha-factors with each parameter
}                                           in dirichlet distributions equaling 1
for(k in 1:case.number){                    # Predict the alpha factors of the
new.alpha[k, 1:group.size] ~ ddirich(new.theta[k, ])   modified AFW system
new.X[k] <- X[k]*(r[k, 1]*ran.failure + r[k, 2]   # The updated occurrence of CCF
+ r[k, 3])                                  events
new.r[k, 1] <- r[k, 1]*ran.failure/(r[k, 1]*ran.failure   # The updated occurrence rates of
+ r[k, 2] + r[k, 3])                        common causes
new.r[k, 2] <- r[k, 2]/(r[k, 1]*ran.failure + r[k, 2]
```

```
+ r[k, 3])
new.r[k, 3] <- r[k, 3]/(r[k, 1]*ran.failure + r[k, 2]
+ r[k, 3])
for(j in 1:group.size)  {                          # The updated parameters of
new.theta[k, j] <- (new.alpha.c1[j]*new.r[k, 1]       decomposed alpha factors
+ alpha.c[2, j]*new.r[k, 2]
+ alpha.c[3, j]*new.r[k, 3])*new.X[k]
}
}
}
DATA
list(x=structure(.Data=c(...), .Dim=c(16,3)),
r=structure(.Data=c(...), .Dim=c(16,3)),
group.size=3, case.number=16, cause.number=3,
ran.failure=0.1, new.alpha.c1=c(1, 0, 0))
```

The posterior decomposed alpha factors are same to the result of Example 4.1, which is shown in Figure 4.6 ~ Figure 4.8. These estimates are not changed in this example, but the decomposed alpha factors of Cause 1 (flood) are updated according to the Equation 5.2. Because the database in the current article is for illustration only, the posterior distributions for CCF parameters of some systems do not show apparent change and some results show different changes. It results from the hypothetical random database.

The System #16 has been chosen to show the update of CCF parameters as the result shows significant change. The summary of posterior distributions for global alpha factors of AFW Pump System #16 is shown in Table 5.4 and the updated global alpha factors of other systems can be obtained similarly. Two groups of posterior distributions are shown in Table 5.4. One is the CCF parameters of AFW System #16 before flood barriers are constructed.

The other is the CCF parameters of the system after flood barriers are constructed. It is demonstrated that the building of flood barriers in System #16 will reduce the CCF risk. The mean values of Alpha-2* and Alpha-3* are smaller than that of Alpha-2 and Alpha-3. Successful flood barriers will protect pumps from CCF events by physically separating redundant pumps.

Table 5.4 Summary of posterior distributions for AFW Pump System #16

	Parameter	**Mean**	**Median**	**95% Interval**
Without Flood Barriers	Alpha-1	8.28E-01	8.40E-01	(6.26E-01, 9.59E-01)
	Alpha-2	9.84E-02	8.39E-02	(9.76E-03, 2.72E-01)
	Alpha-3	7.38E-02	5.83E-02	(4.35E-03, 2.28E-01)
With Flood Barriers	Alpha-1*	8.85E-01	9.18E-01	(6.02E-01, 9.99E-01)
	Alpha-2*	8.34E-02	4.82E-02	(8.23E-05, 3.46E-01)
	Alpha-3*	3.18E-02	4.76E-03	(3.25E-13, 2.20E-01)

Figure 5.6 demonstrates the process of updating for global alpha factors of System #16. With the construction of flood barriers in System #16, the Alpha-3 is significantly reduced. The curves of Alpha-2 and Alpha-3 move leftward, and by contrast the curve of Alpha-1 moves rightward. The CCF risk of System #16 is reduced. However, the uncertainties in the estimates are relatively increased. It shows the application of the alpha decomposition method in the evaluation of modified systems. The prediction of updated alpha factor is based on the generic operation data without flood barriers. The uncertainty has been propagated through the process of prediction. The estimates of decomposed alpha factors can provide a reliable means of prediction. The modification of system will change the PRA parameters, for instance design, diversity, layout, etc. The hierarchical Bayesian inference can complement the prediction. The occurrence of unobvious or difference changes in the estimates will be explained in the next section.

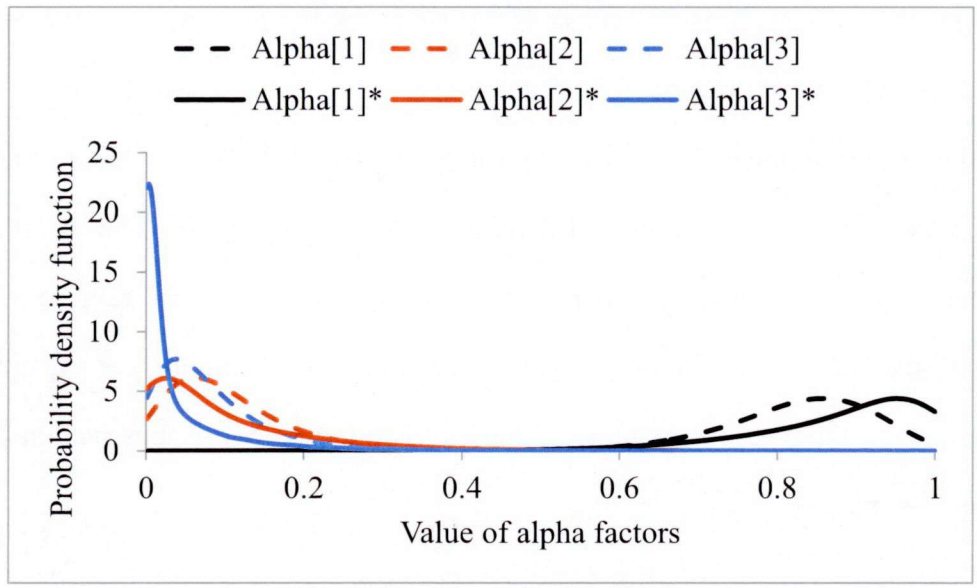

Figure 5.6 Posterior distributions for AFW Pump System #16

5.2.4. Misleading of alpha factors in the evaluation of failure risk

Besides, the global alpha factors are already proved as the integrated illustration of CCF risk, the defense against causes (for example, flood) will reduce the CCF risk and the global alpha factors will decrease. However, other issues are still needed to be discussed. For instance,

1) Defenses against causes of low CCF risk cause but high occurrence frequency will increase the value of alpha factors.
2) Multiple defense strategies are applied to improve the redundant systems.

Example 5.2 is proposed to illustrate the misleading of the alpha factor model in the evaluation of failure risk.

Example 5.2 The misleading of alpha factors from the perspective of risk representation

According to the issues provided before, the calculation with system-specific database is given to prove the misleading of alpha factors from the perspective of representing failure

risk. Defense mechanism against the cause of low CCF risk but high occurrence frequency is constructed. A hypothetical database for the explanation is assumed which contains enough cause and failure information. It is shown in Table 5.5. The data is listed before the defense strategy is introduced. The prevention of defense strategy is of a percentage of 10%, so the data for the system with defense can be obtained which is shown in Table 5.5 as well. Moreover, all the CCF risk of Cause 1 is degraded as independent failure. Let us compare the CCF parameters of the previous system and modified system after the construction of failure defense mechanism.

Table 5.5 Hypothetical system-specific database for Case 1

	Cause group	**Single failure & CCF**			**Total**
		1/3	2/3	3/3	
Without defense	Cause 1	65	2	0	67
	Cause 2	24	3	1	28
	Cause 3	24	6	2	32
	Total	113	11	3	127
With defense	Cause 1	7	0	0	7
	Cause 2	24	3	1	28
	Cause 3	24	6	2	32
	Total	55	9	3	67

The global alpha factors for the system can be obtained by the method and Openbugs script introduced in Section 4.2. The posterior distributions for global alpha factors are shown in Figure 5.7. The result shows that after the introduction of defense mechanism, the CCF risk increases. The curve of Alpha-1 moves leftward but the curves of Alpha-2 and Alpha-3 move rightward. It means that the independent failures reduce but CCF events increase. The building of defense mechanism will not certainly reduce the alpha factors involving many

components. Because Cause 1 triggers more independent failures but less dependent failure than other two causes, the alpha factors involving two and three components increase.

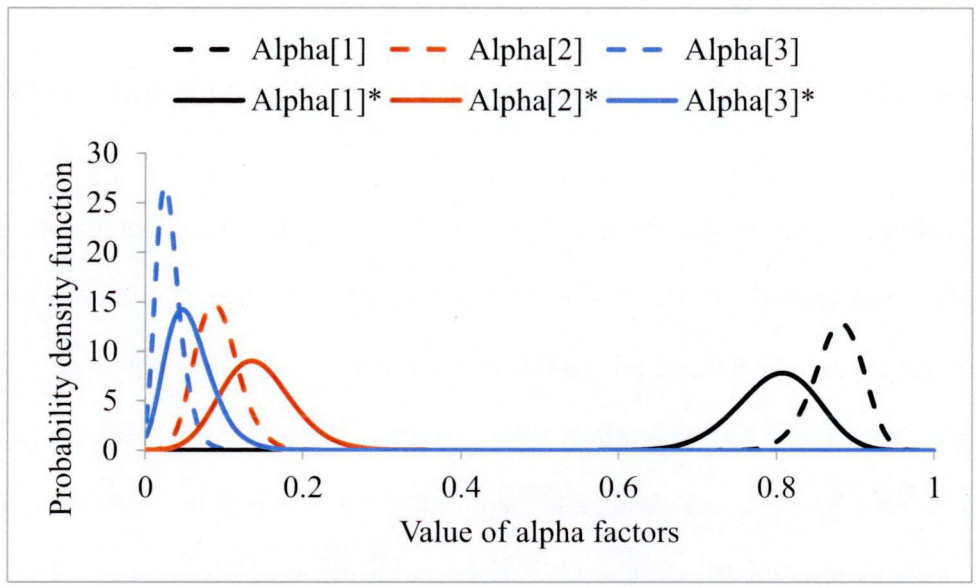

Figure 5.7 Posterior distributions for alpha factors of Case 1

Table 5.6 Summary of alpha factors for Case 1

	Parameter	Mean	Median	95% Interval
Without Flood Barriers	Alpha-1	0.8774	0.8792	(0.8145, 0.9277)
	Alpha-2	0.0920	0.0901	(0.0490, 0.1481)
	Alpha-3	0.0306	0.0283	(0.0084, 0.0651)
With Flood Barriers	Alpha-1*	0.7999	0.8027	(0.7017, 0.8831)
	Alpha-2*	0.1429	0.1398	(0.0716, 0.2332)
	Alpha-3*	0.0572	0.0532	(0.0161, 0.1223)

As a conclusion, the defense against causes of low CCF risk but high occurrence frequency will not reduce the alpha factors which represent low CCF risk (for instance, Alpha-1, etc.). In the PRA analysis, it cannot judge the CCF risk of two systems only by the value of alpha factors, which is the misleading of alpha factors. For instance, in Talbe 5.6 the

alpha factors of the system without flood barriers shows less CCF risk. However, under actual scenario, the system with flood barrier successfully prevents a great number of failures. This property is impossible to be explained by the lumped global alpha factors.

5.3. Qualitative analysis of seismic-induced flood hazard for AFW pump systems

As discussed previously, the estimates of CCF risk should reflect issues including failures, causes and system-specific design etc. Diversity or physical separation of redundant system will reduce the occurrence possibility of CCF events. Flood barriers can prevent the random flood from the safeguards alley, which is caused by the random failure of water system. However, when a severe earthquake happens, it will result in the deformation of flood barriers as well as internal flood. The CCF risk should be well analyzed for the modified AFW system. This section shows the conceptual flood hazard analysis.

Flood risk of two AFW Pump systems with different layouts is compared. The Layout #1 is a parallel placement of doors with barriers. It is simply called as barriers. All flood barriers in Layout #1 directly contact flood water. The Layout #2 is a sequential placement of doors with barriers. Only Barrier #1 directly contacts the flood water but Barrier #2 and #3 are separated from the flood from Turbine Building. When the Barrier #1 starts to leak severely, Barrier #2 will suffer the damage from flood, and finally Barrier #3.

5.3.1. Flood sources

Failures of nonsafety-related water system piping and equipment will flood the turbine building and subsequently impact safety-related components and systems in the safeguards alley. Three most credible flood sources are considered: Circulating Water (CW), Service Water (SW), and Fire Protection Water (FPW). In this section, the maximum flood water flow rate through one door is assumed as 2 m^3/min, which is larger than the drainage ability of

each AFW pump room. The drainage ability of each room is assumed as 0.5 m^3/min. The detailed occurrence probability of each flood scenario will be discussed following sections.

5.3.2. Flood propagation

The random flood water will be obstructed by the barriers and the AFW pumps can be protected. According to the seismic classification of Structures, systems and components in NPPs, the waters system in the turbine building and flood barriers are nonsafety-related but the AFW pumps are safety-related. Therefore, it is probable that water system and flood barrier fail for a severe earthquake. There are two failure mechanisms of barriers. One is the flood barrier fails because of a seismic shock. The other is that the flood barrier is flawed for the seismic shock and finally degraded to failure for the flood water. Thus, if the barrier is not flawed by the earthquake, it can prevent the ingression of flood water for a long term. To compare these two different layouts from the perspective of flood risk, three scenarios of seismic-induced flood involving the failure of barriers are considered, which is classified by the number of failed barriers. The probability for the occurrence of three scenarios is assumed in Table 5.7. This data will be integrated in the result of flood risk analysis.

1) Seismic-induced one-barrier-failure coupling with flood
2) Seismic-induced two-barrier-failure coupling with flood
3) Seismic-induced three-barrier-failure coupling with flood

Table 5.7 Probability of three seismic scenarios

Scenario	**Percentage of probability**
1) Seismic-induced one-barrier-failure	0.2
2) Seismic-induced two-barrier-failure	0.2
3) Seismic-induced three-barrier-failure	0.6

Layout #1 Parallel flood barriers

All three barriers in Layout #1 directly contact the flood water. If the severest flood happens, the seismically flawed barriers start to degrade.

1) Seismic-induced one-barrier-failure coupling with flood

The schematic diagram for the seismic-induced one-barrier-failure coupling with flood is shown in Figure 5.8. In this case, only Barrier #1 is flawed by the earthquake and at last fails for the flood. The seismically induced severest flood and barrier failure will result in the failure of Pump A. There is only an independent failure occurs. Pump B and C are protected by the successful Barriers #2 and #3.

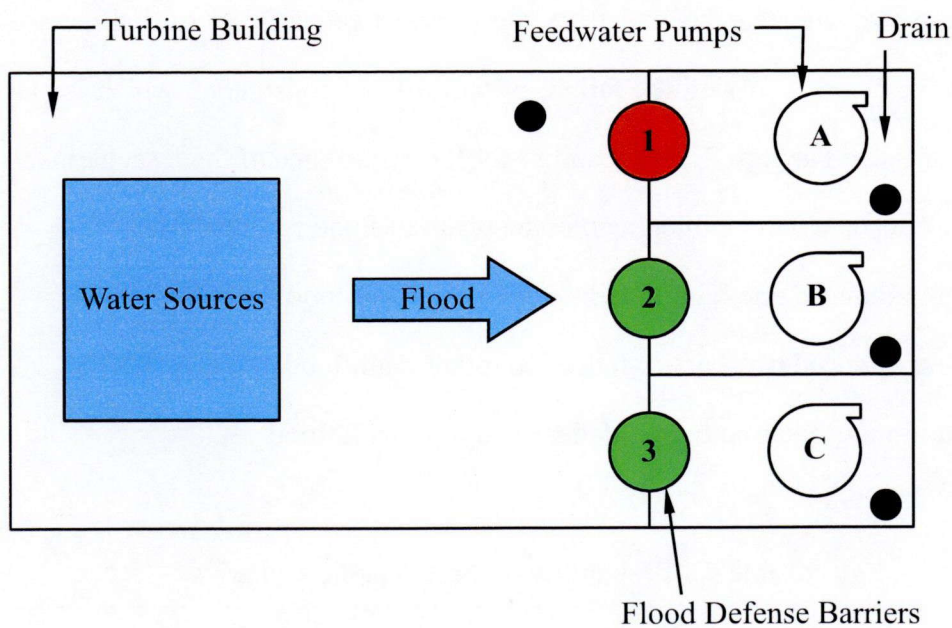

Figure 5.8 Seismic-induced one-barrier-failure coupling with flood (Layout #1)

2) Seismic-induced two-barrier-failure coupling with flood

The second scenario is the seismic-induced two-barrier-failure, which is shown in Figure 5.9. It is the same to the scenario 1 that Pump A and B fail because the function-loss of Barrier #1 and #2. A partial CCF occurs as Pump C is protected by the successful Barrier #3.

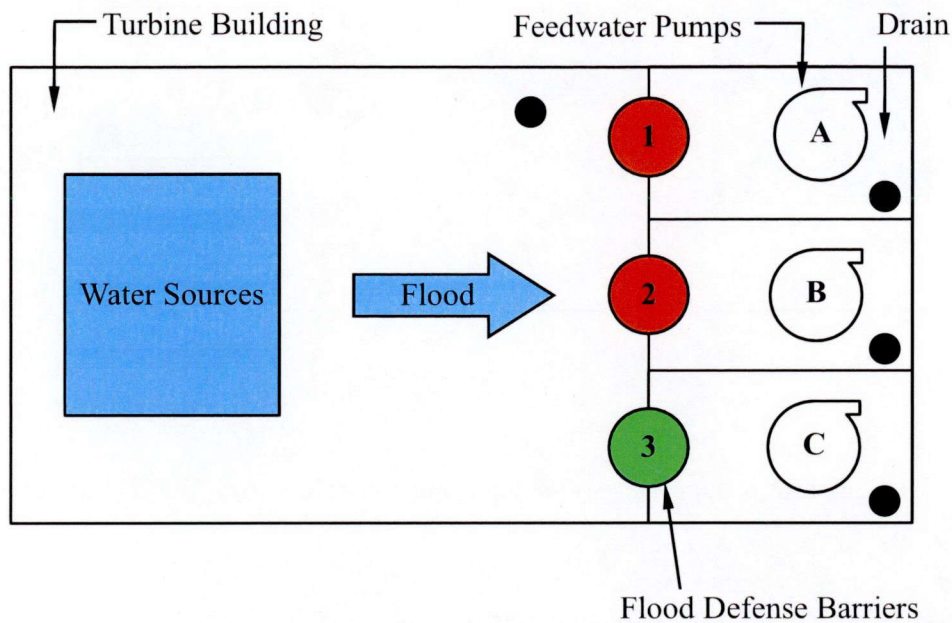

Figure 5.9 Seismic-induced two-barrier-failure coupling with flood (Layout #1)

3) Seismic-induced three-barrier-failure coupling with flood

The third scenario will be discussed in detail with the demonstration of the water flow rate through barriers. The schematic diagram for the Scenario 3 is shown in Figure 5.10. All three barriers are identical in the environment of flood. This is a shortcoming of the Layout #1 which cannot provide the defense in depth. Even though there is a possibility assigned to the Scenario #1 and #2, all the three barriers are likely to be deformed for an earthquake. The maximum flow rate through one barrier is assumed as 2 m^3/min and the drainage ability is assumed as 0.5 m^3/min. Therefore, the increasing of the leakage of the barrier will accumulate

water in the AFW Pump room until the water height reaches the Critical Water Height (CWH). If the water height reaches the CWH, the pump will be functionally covered with water.

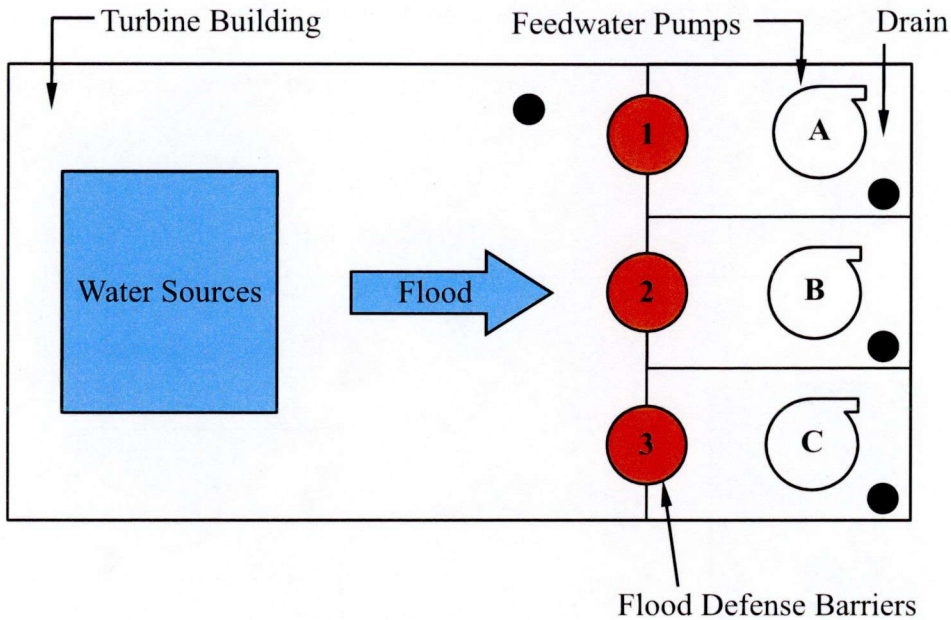

Figure 5.10 Seismic-induced three-barrier-failure coupling with flood (Layout #1)

The conceptual water flow rate and CCF events are shown in Figure 5.11. The red line refers to the drainage ability of one room and the black line refers to the water flow rate. The water flow rate will increase for the degradation of flood barriers. When it keeps increasing and exceeds the drainage ability, the water starts accumulating. After certain time duration, the accumulated water height will be more than the CWH while CCF events involving three components occur. The green line shows the time when all redundant AFW pumps fail for the flood water.

It is demonstrated that there is process of the increasing of water flow rate to one AFW pump room. The water flow rate depends on the water source and the state of the flood barrier. If the flood is of the most credible and severest volume, the state of flood barrier will determine whether and when the pump will fail.

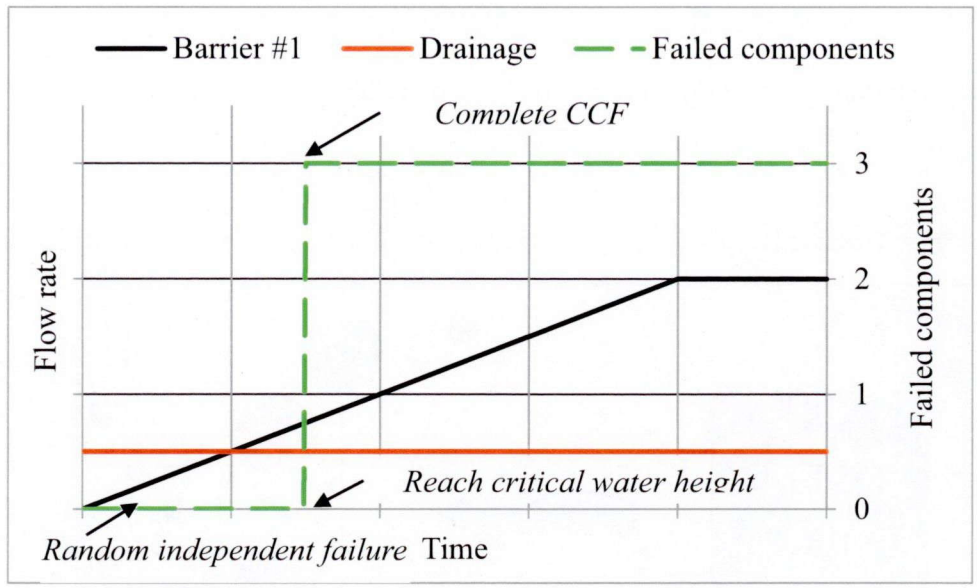

Figure 5.11 Conceptual water flow rate and flood hazard (Layout #1)

Layout #2 Sequential flood barriers

Layout #2 is of different placement of doors with barriers. The water flowing into the location of Pump B must go through Barrier #1 and #2, and the flowing into the location of Pump C must go through all three barriers. It provides a time extension even if all barrier are broken by a seismic shock. There are three scenarios the same to Layout #1 but the location of failed barriers is necessary to be discussed respectively.

1) Seismic-induced one-barrier-failure coupling with flood

There two types of locations are considered under this scenario. One is the seismically flawed barrier does not contact the flood water which is shown in Figure 5.12. The other is the seismically flawed barrier directly contact the flood water which is shown in Figure 5.12. In Figure 5.12, the flawed Barriers #2 or #3 are protected by the successful Barrier #1, so it can provide a long-term protection against flood. In Figure 5.13, the flawed Barrier #1 will

degrade under the pressure of flood. As a result, if the single failure of a barrier is uniformly distributed, the independent failure probability can be reduced to 1/3 of the Layout #1.

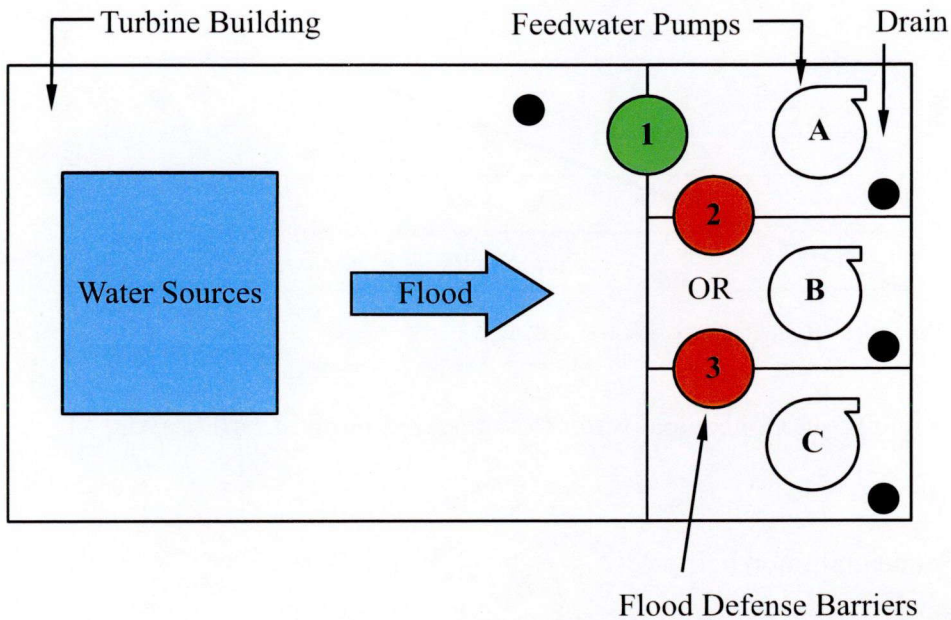

Figure 5.12 Seismic-induced failure of Barrier #2 or #3 coupling with flood (Layout #2)

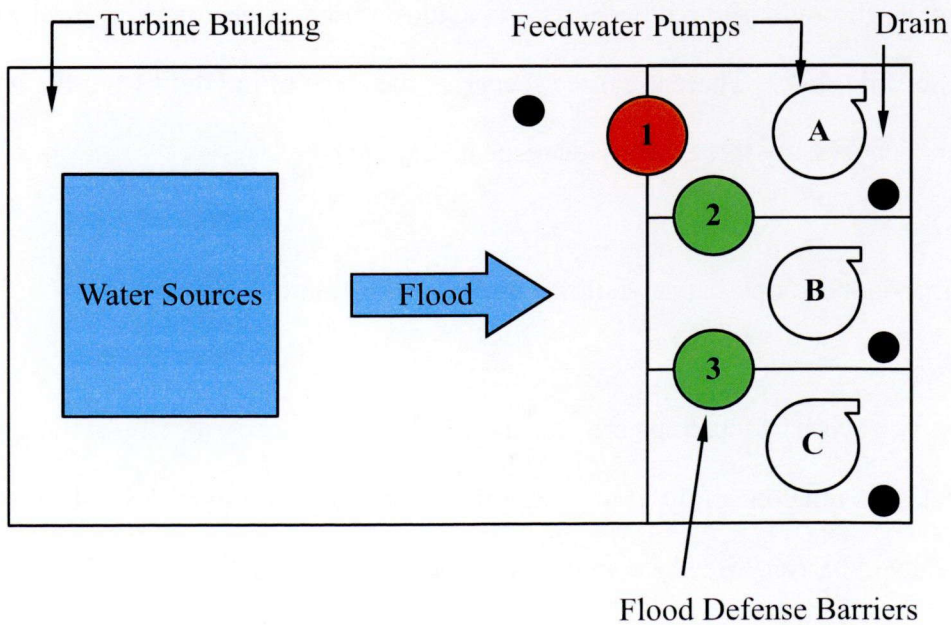

Figure 5.13 Seismic-induced failure of Barrier #1 coupling with flood (Layout #2)

2) Seismic-induced two-barrier-failure coupling with flood

There are three types of locations are considered under this scenario.

- Barrier #1 successes but #2 and #3 fail, as shown in Figure 5.14;
- Barrier #2 successes but #1 and #3 fail, as shown in Figure 5.15;
- Barrier #3 successes but #1 and #2 fail, as shown in Figure 5.16.

These three failure types will affect the availability of AFW Pump system. The flood is assumed as the severest with the maximum water flow rate through one barrier.

As shown in Figure 5.14, the successful Barrier #1 will provide a long-term protection for the AFW pump system. Even if Barriers #2 and #3 are flawed by the seismic shock, the flood risk will be screened out.

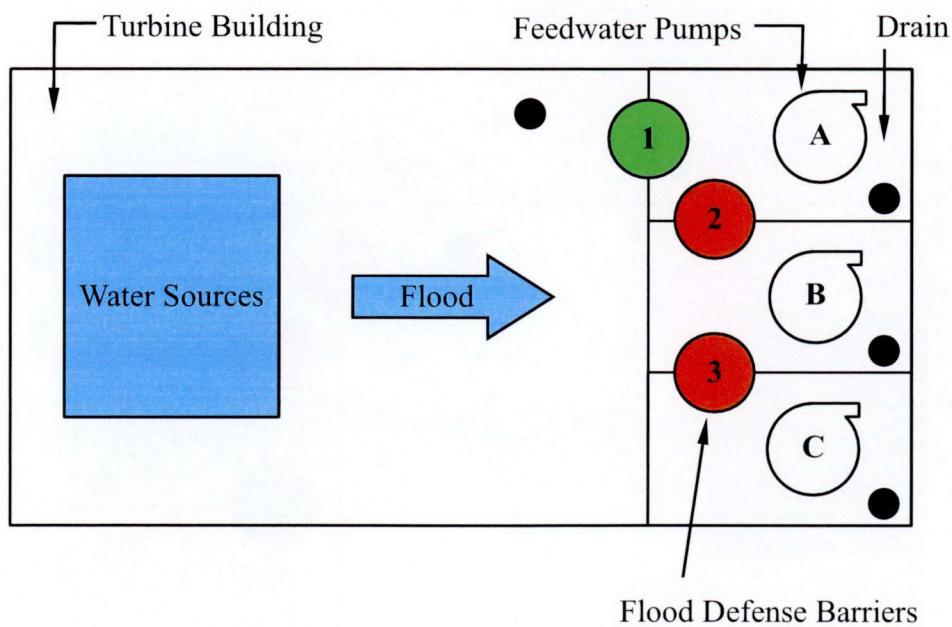

Figure 5.14 Seismic-induced failure of Barrier #2 and #3 coupling with flood (Layout #2)

As shown in Figure 5.15, Barrier #1 is flawed by the seismic shock, so Pump A is probable to fail for the flood water. However, since Barrier #2 is not flawed by the seismic shock, it can provide a long-term protection for Pumps B and C. Thus, it is an independent

failure happens under this scenario.

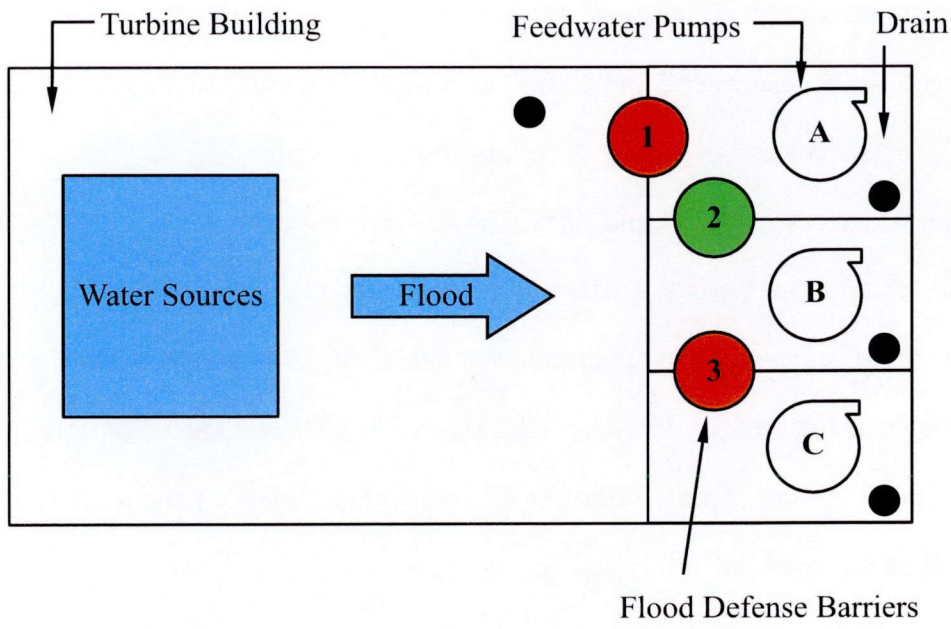

Figure 5.15 Seismic-induced failure of Barrier #1 and #3 coupling with flood (Layout #2)

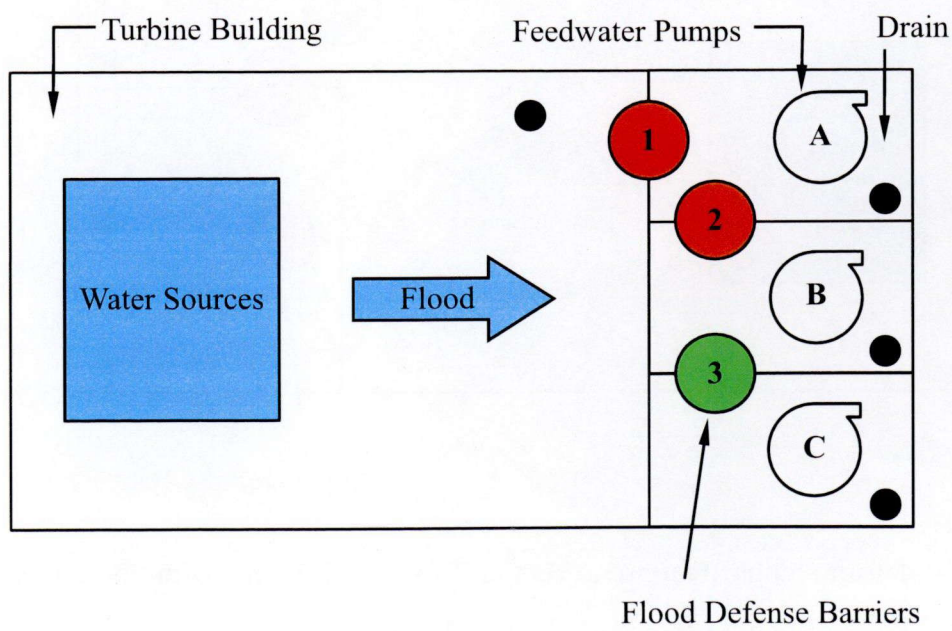

Figure 5.16 Seismic-induced failure of Barrier #1 and #2 coupling with flood (Layout #2)

As shown in Figure 5.16, Barrier #1 and #2 are flawed by the seismic shock but the

Barrier #3 is functionally successful. Under the severest situation, Pumps A and B will fail for the high water level in the room but Pump C is protected by the successful Barrier #3. Thus, the probable CCF event happens as a partial CCF event. 2/3 possibility of Layout #2 under Scenario 2 has been degraded to no failure or single failure. Only 1/3 possibility under Scenario 2 is the same to Layout #1, that partial CCF happens. It is one advantage of Layout #2 over Layout #1.

3) Seismic-induced three-barrier-failure coupling with flood

According to Table 5.7, the most probable scenario is that all three barriers fail because of the earthquake, which is demonstrated in Figure 5.17. Barriers #1, #2 and #3 fail and the severe flood water flow into the AFW Pump system. Pumps A, B, and C will fail for the water in the room. However, there is a difference for Layout #2 compared with Layout #1. The failed time for each pump is different that of respective pump in Layout #1.

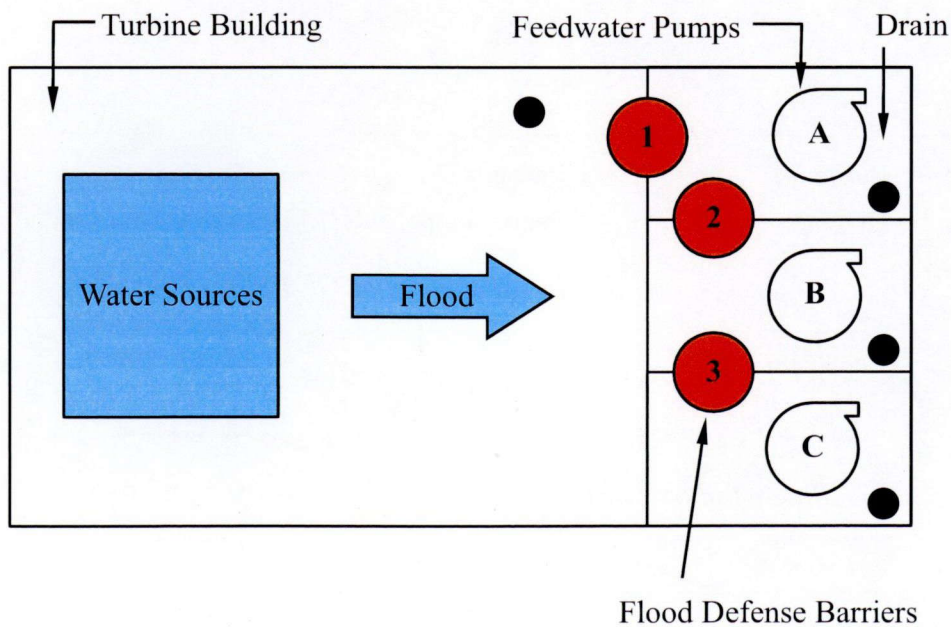

Figure 5.17 Seismic-induced failure of all barriers coupling with flood (Layout #2)

The flow rate through each barrier and the number of failed components are shown in Figure 5.18. First of all, a seismic shock occurs so that all three barriers are flawed. The internal flood water flows from the turbine building to the AFW Pump system. Secondly, the flow water contacts Barrier #1, and then the water pressure and force will damage the flawed flood barrier. The water starts to leak through the Barrier 1. With the propagation of mechanical damage, the leak rate increases until more than the drainage ability in the room of Pump A. Water starts to accumulate in the room and after certain time duration, accumulated water level will be higher that the Critical Water Height (CWH). The failure of Pump A occurs which is named as single failure (1/3) in the picture. At the same time, the accumulated water will cause Barrier #2 starting propagation of mechanical damage. When the water leak rate through Barrier #2 is higher than the drainage ability, the water starts accumulating in the room when Pump B is located and it will reach the CWH. The failure of Pump B happens which is called as partial CCF in the picture (2/3). At last, the leaked water through Barrier #3 results in the failure of Pump C when all three pumps fail as the complete CCF (3/3). Compared with Figure 5.11, the saved time for the availability of AFW system is significantly postponed.

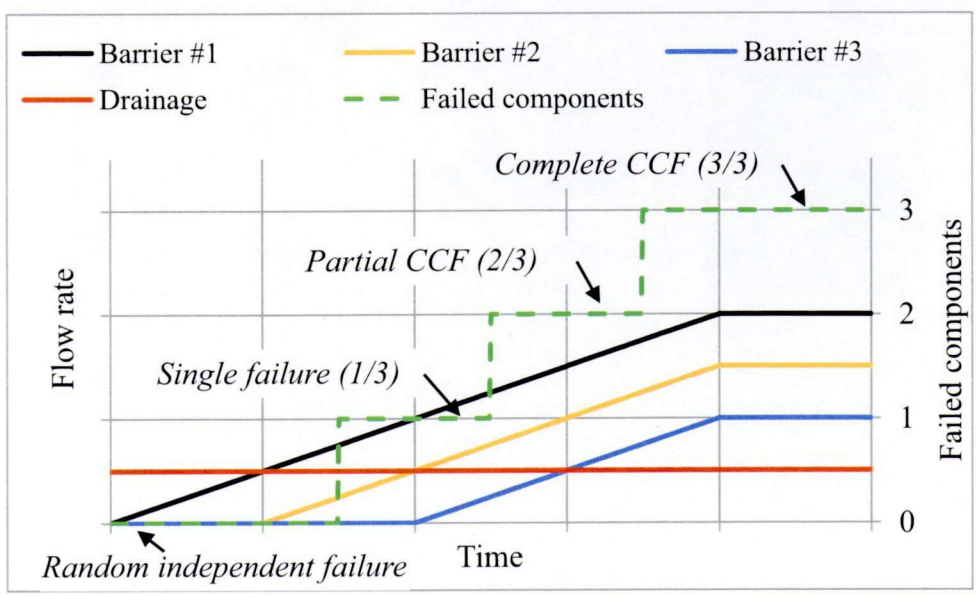

Figure 5.18 Conceptual water flow rate and flood hazard (Layout #2)

5.4. Markov Model for the Degradation of Flood Barriers

The degradation of flood barrier under the seismic shock and flood water is discussed in this section. The failure process of flood barriers is treated as a stochastic process in the current article. The current methodology aims to apply the Markov model for a quantitative degradation modeling. The Markov model is used to set up a set of linear coupled differential equations whose solution provides the time dependent probabilities of occupying states of the model. The input evidence to quantify the Markov model includes the occurrence frequency of necessary states with assumed experiments. With the repeated vibration and water experiment, the damage data for a barrier can be obtained.

This Markov modeling technique represents the failure process in a set of discrete and mutually exclusive states. The states refer to various degrees of flood barrier degradation, i.e. success, leak, deformation and failure. At the state of success, there is no water leaking through a barrier. At the state of leak, there is limited water leaking through the barrier which can be drained out by the drainage system. At the state of deformation, the water flow rate through the barrier is larger than the drainage ability, so the water will accumulate in the room. At the state of failure, it means that the water flow rate through the door is same to the situation without the flood barrier.

If there is flood water accumulated at the barrier, it can be confirmed that the state change will happen. The transition time and probability is important to be considered in the flood PRA analysis. At different time nodes, the state probability will affect the flow rate and the availability of AFW Pump system as well. Finally, the evaluation of basic events in the PRA can be adjusted according to the result of flood PRA. Let as discuss the four state Markov model for the barrier degradation.

5.4.1. Markov model for the barrier degradation

The schematic diagram of four states Markov model is described in Figure 5.19. This model is applied to simulate the degradation process of flood barriers under the situation of seismic shock as well as flood water. Transition parameters between states are assigned to model the degradation mechanism under the flood environment. As a Markov model, the transition parameters are assumed as constant. The development of physics-based barrier degradation investigation is not provided in current article, in which the transition parameters are not time-constant but physics- and scenario-dependent. There are four discrete and mutually exclusive states (S, L, D and F) in current Markov model. The definition of four states is provided in Table 5.8. Besides, four transition parameters (ϕ_{SL}, λ_{LD}, ρ_{LF} and ρ_{DF}) are assumed between states. The definition of four transition parameters is provided in Table 5.9.

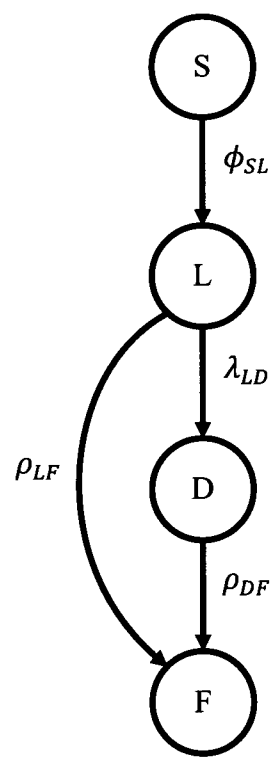

Figure 5.19 Four state Markov model for the degradation of flood barriers

Table 5.8 Description of four Markov states

State	Description
S	Success; no water leakage
L	Leak; the leakage rate is less than the drainage ability
D	Deformation; the possible water flow rate is larger than the drainage ability but not reaching maximum
F	Failure; the possible water flow rate is the same to doors without flood barrier

Table 5.9 Description of four transition parameters

Transition parameters	Description
ϕ_{SL}	Leak occurrence probability given the state of Success
λ_{LD}	Deformation occurrence probability given the state of Leak
ρ_{LF}	Failure occurrence probability given the state of Leak
ρ_{DF}	Failure occurrence probability given the state of Deformation

5.4.2. Definition of transition parameters

As introduced previously, the four transition parameters are unknown and needed to be estimated. Therefore, the Bayesian inference can be applied to estimate them. First of all, the prior distribution and likelihood functions should be given. Two failure mechanisms are described as

- Seismic-induced barrier degradation;
- Flood-induced barrier degradation.

When a seismic shock occurs, the barrier will be damaged. The state of barrier after the occurrence of shock is a stochastic result. The likelihood function of the four states is

assumed as a multinomial distribution. The noninformative conjugate prior for the multinomial distribution is the Dirichlet distribution with all parameters equaling one.

$$\begin{aligned} init.sei[1:4] &\sim dmulti(init.p[1:4]) \\ init.p[1:4] &\sim ddirich(\theta_s[1:4]), \theta_s[1:4] = [1,1,1,1] \end{aligned} \qquad \text{Equation 5.4}$$

Here, *init.sei* refers to the initial probability for the Markov model after the occurrence of an earthquake; *init.p* is the set of parameters in the mutinomial distribution; *dmulti* refers to the likelihood function of four states which means a multinomial distribution; *ddirich* refers to the noninformative conjugate prior distribution which means a Dirichlet distribution with all parameters equaling 1.

The flood-induced barrier degradation depends on the flood water volume and the water height in the room. Since the water situation is complicated and currently unpredictable, it is also assumed as stochastic process. All the transition parameters are defined with uncertainty distributions as follows.

1) Leak occurrence probability given the state of Success, ϕ_{SL}

A number of hypothetical experiments are assumed being conducted, so the occurrence of leaks is assumed to be described as independent Poisson process with the parameter $\lambda.L$. The lognormal prior for Poisson distribution is applied. The posterior distribution can be obtained by the assumptions and obtainable data.

$$\begin{aligned} n.L &\sim dpois(\lambda.L \bullet t.L) \\ \lambda.L &\sim dlnorm(\mu.L, \sigma.L) \\ \phi_{SL} &= \lambda.L \end{aligned} \qquad \text{Equation 5.5}$$

Here, $n.L$ refers the data of leaks; $\lambda.L$ is the expected occurrence frequency of leaks; $t.L$ is the experimental time; *dpois* is the likelihood function of the number of leaks which means Possion distribution; *dlnorm* is the prior distribution as lognormal.

2) Deformation occurrence probability given the state of Leak, λ_{LD}

The occurrence of deformation is assumed as a binomial distribution given the number of leak. The occurring possibility of a deformation given a leak ($p.D$) is the parameter in the binomial distribution. The likelihood function and prior distribution are given by

$$\begin{aligned} x.D &\sim dbin(p.D, n.D) \\ p.D &\sim dlnorm(\mu.D, \sigma.D) \\ \lambda_{LD} &= p.D \end{aligned} \qquad \text{Equation 5.6}$$

Here, $x.D$ is the experimental data of deformation; $p.D$ is the expected occurrence frequency of deformations given a leak; $n.D$ refers to the number of leaks that are going to degrade to deformations; *dbin* is the likelihood function of the number of deformations which is a binomial distribution.

3) Failure occurrence probability given the state of Leak, ρ_{LF}

The occurrence of failures given leaks is assumed as a binomial distribution. The occurring possibility of a failure given a leak ($p.FL$) is the parameter in the binomial distribution. The likelihood function and prior distribution are given by

$$\begin{aligned} x.FL &\sim dbin(p.FL, n.FL) \\ p.FL &\sim dlnorm(\mu.FL, \sigma.FL) \\ \rho_{LF} &= p.FL \end{aligned} \qquad \text{Equation 5.7}$$

Here, $x.FL$ is the experimental data of failures given leaks; $p.FL$ is the expected occurrence frequency of a failure given a leak; $n.FL$ is the number of leaks that are going to degrade to failures.

4) Failure occurrence probability given the state of Deformation, ρ_{DF}

The occurrence of failures given deformation is assumed as a binomial distribution. The occurring possibility of a failure ($p.FD$) given a leak is the parameter in the binomial distribution. The likelihood function and prior distribution are given by

$$\begin{aligned} x.FD &\sim dbin(p.FD, n.FD) \\ p.FD &\sim dlnorm(\mu.FD, \sigma.FD) \\ \rho_{DF} &= p.FD \end{aligned} \qquad \text{Equation 5.8}$$

Here, $x.FD$ is the experimental data of failures given deformations; $p.FD$ is the expected occurrence probability of a failure given a deformation; $n.FD$ is the number of deformations that are going to degrade to failures.

The summary of all aleatory models is provided in Table 5.10. All transition parameter can be calculated based on the experimental evidence and the assumption of aleatory models. Besides, the probability of each state is decided by the initiating states and the transition probability. The Ordinary Differential Equations (ODEs) can be used to express the relationship between parameters and states. The discussion and solution of ODEs are provided in next section.

Table 5.10 Uncertainty distribution assumption for Markov parameters

Parameter symbol	**Uncertainty Treatment**	
	Likelihood function	Prior distribution
Initiating states	Multinomial	Dirichlet
Leak	Poisson	Lognormal
Deformation	Binomial	Lognormal
Failure given Leak	Binomial	Lognormal
Failure given deformation	Binomial	Lognormal

5.4.3. Ordinary differential equations

According to the applied Markov model, the probability of states is time dependent. The Markov model can be described by a set of four coupled linear first-order Ordinary Differential Equations (ODEs). The initial condition necessary for the solution of the ODEs is decided by the seismic shock which results in the occurrence of food and barrier degradation. The initial condition can be written as Equation 5.9 and it can be calculated by Equation 5.4 based on Bayesian inference.

$$P_{t_0} = \left(P_{t_0(S)}, P_{t_0(L)}, P_{t_0(D)}, P_{t_0(F)}\right) \qquad \text{Equation 5.9}$$

The ODEs are given by

$$\frac{dP_{(S)}}{dt} = -\phi_{SL} P_{(S)} \qquad \text{Equation 5. 10}$$

$$\frac{dP_{(L)}}{dt} = \phi_{SL} P_{(S)} - \left(\lambda_{LD} + \rho_{LF}\right) P_{(L)} \qquad \text{Equation 5.11}$$

$$\frac{dP_{(D)}}{dt} = \lambda_{LD} P_{(L)} - \rho_{DF} P_{(D)} \qquad \text{Equation 5.12}$$

$$\frac{dP_{(F)}}{dt} = \lambda_{LF} P_{(L)} + \rho_{DF} P_{(D)} \qquad \text{Equation 5.13}$$

The sum of probabilities of four states remains one at any time t.

$$P_{t(S)} + P_{t(L)} + P_{t(D)} + P_{t(F)} = 1 \qquad \text{Equation 5.14}$$

There are two methods to solve the ODEs (Equations 5.10 ~ 5.13). One it the direct solution (exact solution) and the other is numerical solution (Bayesian inference with MCMC). If all the transition parameters are already known or can be exactly defined, the direct solution can be used. The Markov solution is remained unknown in current article, so the Bayesian with MCMC is used to obtain the numerical solution. Therefore, the time dependent states of flood barrier can be obtained. The flow rate is decided by sates of flood barriers, so the flow rate can be evaluated as well. The failure state of pumps can be evaluated by the flow rate and water height in the room. Finally, the time- and scenario-dependent CCF parameters can be obtained.

5.5. Quantitative CCF Modeling for the AFW Pump System Involving the Degradation of Flood Barriers

The update of CCF parameters after the construction of flood barriers in the AFW Pump system has already been discussed in Section 5.1 and 5.2. In reverse, the degradation of flood barriers will affect the CCF parameters as well. In Section 5.3, it has been demonstrated how the flood barrier qualitatively affect the occurrence of CCF events. In Section 5.4, the quantitative modeling of flood barrier after the occurring of seismic induced flood. In this

section, it is discussed how the functional state of flood barriers affects the probability distributions of CCF parameters (including global alpha factors and decomposed alpha factors).

The solution of ODEs of Markov model is computed by Bayesian inference with hypothetical databases. The probability each Markov state will decide the flow rate through barriers, which is the key point to determine whether the AFW pump will fail or not.

5.5.1. Numerical solution of Markov model

This section shows the numerical calculation of ODEs (Equation 5.10 ~ 5.13) for a single flood barrier. It is needed the data of Success, Leak, Deformation and Failure to decide the estimation of transition parameters. The hypothetical experimental data is assumed in Table 5.11. There are two parts in the experimental database. One is the state data after the occurrence of a seismic shock, and the other is the state data after a certain period of flood propagation. The seismic data is used to determine the initiating states and the flood data is used to estimate the transition parameters for the flood hazard. The transition parameters will be the average value of three equivalent experiments. The likelihood functions and prior distribution for Bayesian inference are given by Equations 5.4 ~ 5.8. The OpenBUGS script is shown in the Appendix A.

Table 5.11 Hypothetical database for the estimation of transition parameters

	Seismic shock				**Flood propagation**			
States	**S**	**L**	**D**	**F**	**S**	**L**	**D**	**F**
Experiment (1)	80	15	3	2	72	23	3	2
Experiment (2)	85	12	2	1	75	21	3	1
Experiment (3)	83	15	1	1	71	23	4	2

The summary of estimates is shown in Table 5.12. The curves of probability density functions are shown in Figure 5.20. Based on the Bayesian calculation with MCMC, the magnitude and uncertainty of all Markov transition parameters can be well evaluated. Based on current hypothetical database, the transition rate from Deformation to Failure is of the largest uncertainty, which is described by the green curve in Figure 5.20. The transition rate from Success to Leak is of the largest value but that from Leak to Failure is of the smallest value.

Table 5.12 Summary of posterior distributions for transition parameters

Transition Parameter	**Mean**	**Median**	**95% Interval**
ϕ_{SL}	1.43E-01	1.41E-01	(9.36E-02, 2.03E-01)
λ_{LD}	6.46E-02	6.19E-02	(2.69E-02, 1.19E-01)
ρ_{LF}	2.11E-02	1.84E-02	(5.20E-03, 5.21E-02)
ρ_{DF}	1.00E-01	7.83E-02	(1.76E-02, 3.02E-01)

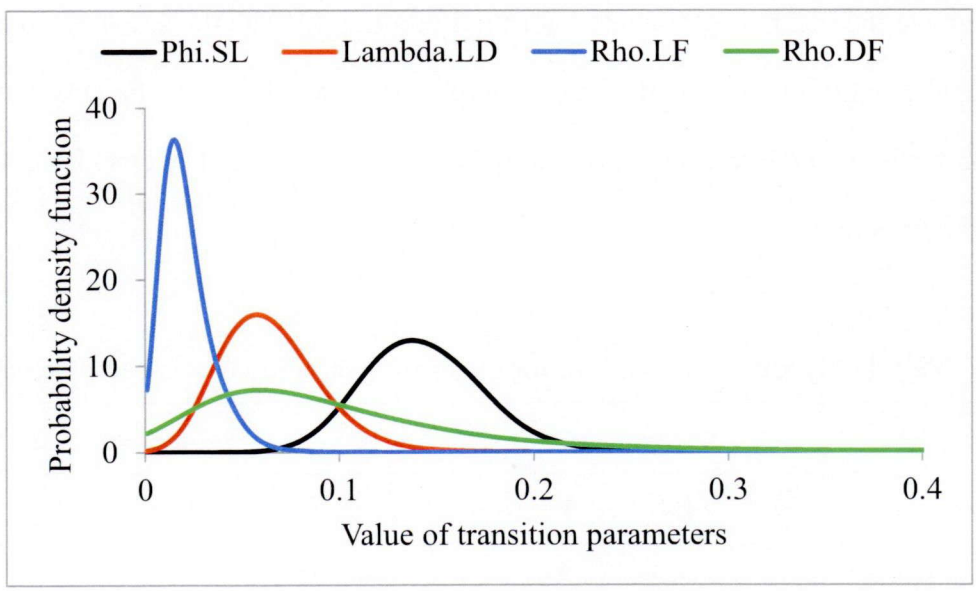

Figure 5.20 Probability density functions for four transition parameters

The solution of ODEs at each time node is shown in Figure 5.21. There are also uncertainties in the solutions. In Figure 5.21, only the mean value is used to show the trend of degradation of the flood barrier. The probability of Success will reduce because of the transition from Success to Leak under the scenario of flood. The probabilities of Leak and Deformation increase at first as a result of $\phi_{SL} > \lambda_{LD}$ and $\lambda_{LD} > \rho_{DF}$. With the reduction of Success, the probability of Leak and Deformation will decrease after certain time duration. The probability of Failure keeps increasing as it is the final state in Markov model. Finally, the degradation continues until the barrier fails.

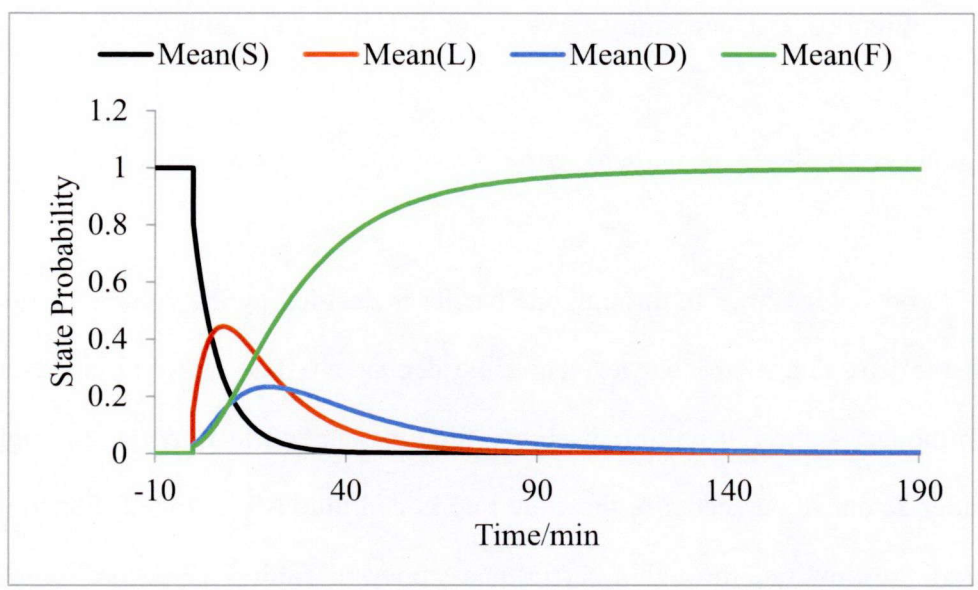

Figure 5.21 Time dependent probabilities of Markov states

In Figure 5.22, the uncertainty expression of Failure state is demonstrated. Since the numerical solutions of Markov states are obtained by MCMC method, at each time node, there are enough samples to generate a probability distribution for an interested state. The mean, median value and the interval of (2.5%, 97.5%) are shown in Figure 5.22. The uncertainty diagrams of other three states are omitted in current article.

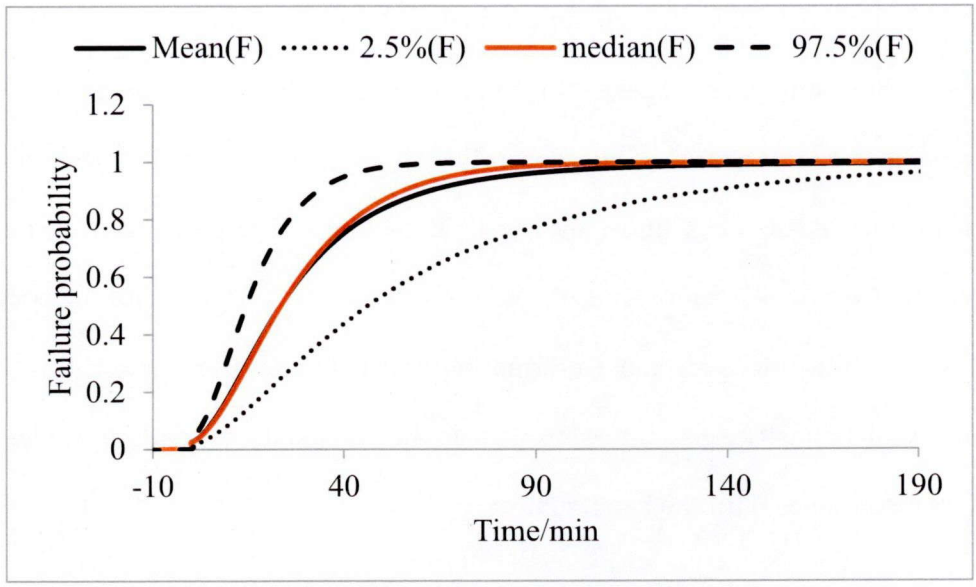

Figure 5.22 Uncertainty curves of probability of the failure state

5.5.2. *Flood water flow rate through barriers*

The flood water flow rate through one barrier is decided by the volume of flood water source and the leak rate of the barrier. The time dependent state of flood barrier has been analyzed in the last section. It will be discussed the time dependent flow rate through a flood barrier. Under actual flood scenario, the flow rate is continuously changed. For the simplest consideration, the flow rate through a barrier is assumed in Table 5.13 according to the state of the barrier in this article. If there is a severe flood with maximum water volume, the expected water flow rate through a barrier is given by

$$Flowrate = F.R_{(S)} \bullet P_{(S)} + F.R_{(L)} \bullet P_{(L)} + F.R_{(D)} \bullet P_{(D)} + F.R_{(F)} \bullet P_{(F)} \qquad \text{Equation 5.15}$$

Here, $F.R_{(state)}$ is the water flow rate through the barrier at one Markov state. To use the data listed in Table 5.13, it can be written as

$$Flowrate = 0 \bullet P_{(S)} + 0.25 \bullet P_{(L)} + 1 \bullet P_{(D)} + 2 \bullet P_{(F)} \qquad \text{Equation 5.16}$$

Therefore, the time dependent water flow rate at each time node t can be given by

$$Flowrate_t = 0 \bullet P_{t(S)} + 0.25 \bullet P_{t(L)} + 1 \bullet P_{t(D)} + 2 \bullet P_{t(F)} \qquad \text{Equation 5.17}$$

Table 5.13 Assumed water flow rate through barriers for each Markov state

States	Flow rate (m^3/min)
Success	0
Leak	0.25
Deformation	1
Failure	2

There are two layouts for the three water-proof barriers. Especially, for the Layout #2, the water flow rate through a barrier is different from other two barriers. The quantitative estimation of water flow rate is obtained with the Bayesian inference by the OpenBUGS as well. The calculation script is integrated in Appendix A.

Layout #1 Parallel flood barriers (Scenario 3)

The Scenario No.3 of seismic-induced three-barrier-failure coupling with flood is evaluated for Layout #1. The results of other two scenarios can be deduced by the result of Scenario No.3. The schematic diagram refers to Figure 5.10. Time dependent Markov states are obtained by the solution of ODEs and the water follow rate is determined by Equation 5.17.

The assumptions of calculation are listed in Table 5.14. For instance, the minimal time to reach the Critical Water Height (CWH) can be calculated as Equation 5.18. All the parameters in Equation 5.18 can be referred in Table 5.14.

$$Time_{min} = \frac{Area \times CWH}{(Flowrate_{max} - Drainage)} = \frac{80 \times 0.15}{2 - 0.5} = 8\ min \qquad \text{Equation 5.18}$$

Table 5.14 Calculation assumptions for water flow rate through a barrier

Parameters	Measurements
Single AFW pump room	80 m^2
Critical water height (CWH)	0.15 m
Drainage ability	0.5 m^3/min
Flood severity (per barrier at Turbine Building)	2 m^3/min
Minimal time to reach CWH (No flood barrier)	8 min

Figure 5.23 shows the estimation of water flow rate through a barrier in Layout #1. It takes 29 minutes for the water to be accumulated in a room until it reaches the CWH. Compared with the minimal time to reach CWH (No flood barrier) in Table 5.14, the time is postponed to 29 minutes. The reason is because the existence of flood barrier block the propagation of flood temporarily, but the barrier degrades for the seismic shock and flood. Finally, the leakage is larger than the drainage ability and then the accumulated water will fail the AFW pumps. The time dependent water flow rate and height is shown in Figure 5.23. To illustrate the uncertainty analysis of water flow rate, the mean value as well as interval (2.5%, 97.5%) is described in Table 5.15 and Figure 5.23.

Table 5.15 Time for critical water flow rate and water height (Layout #1)

Criteria	Time (min)		
	Mean	Median	95% Interval
Flow rate > Drainage	8	8	(6, 11)
Water height > CWH	29	29	(24, 38)

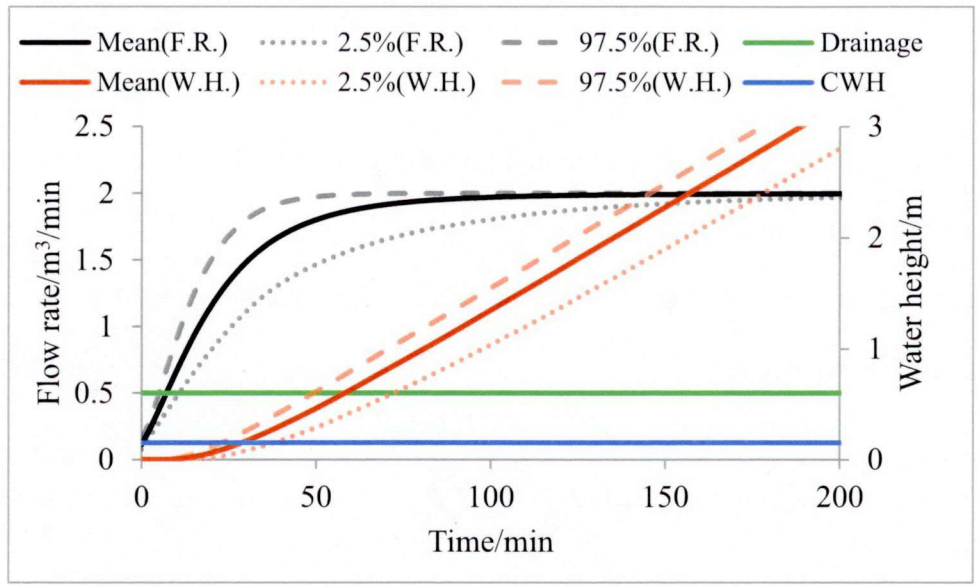

Figure 5.23 Water flow rate through barriers (Layout #1)

As a result, the number failed pumps and percentage for three scenarios (Figures 5.8 – 5.10) of Layout #1 can be concluded in Table 5.17.

Table 5.16 Failure types of each scenario of flood barriers (Layout #1)

	Percentage of probability	**Failure types**
Scenario 1	0.2	Single failure (1/3)
Scenario 2	0.2	Partial CCF (2/3)
Scenario 3	0.6	Complete CCF (3/3)

Layout #2 Sequential flood barriers (Scenario 3)

The Scenario No.3 of seismic-induced three-barrier-failure coupling with flood is evaluated for Layout #2. The results of other two scenarios can be deduced by the result of Scenario No.3. The schematic diagram refers to Figure 5.17. The calculation assumption is the same to the Layout #1 which is shown in Table 5.14.

The water flow rate through each barrier in Layout #2 is calculated in the most conservative way. Because it is difficult to distinguish whether the flood water is accumulated or flow to the next room, both of accumulated rate and flow rate (to next room) are assumed as maximum expected value.

The water flow rate via Barrier #1 in Layout #2 is the same to that of barriers in Layout #1, which is written as

$$Flowrate_{(Barrier\#1)} = 0 \bullet P_{(S)} + 0.25 \bullet P_{(L)} + 1 \bullet P_{(D)} + 2 \bullet P_{(F)} \qquad \text{Equation 5.19}$$

The degradation process is conservatively assumed as the Barrier #1. Thus, maximum water source through Barrier #2 from Room A is given by

$$a_{t(Barrier\#2)} = Max\left\{Flowrate_{t(Barrier\#1)} - Drainage, 0\right\} \qquad \text{Equation 5.20}$$

If the $a_{t_1+1(Barrier\#2)} > 0$ at time $t_1 + 1$, it means that the water starts to accumulate and the accumulated water will cause Barrier #2 starting to degrade. It is mathematically written as

$$if\ a_{t_1} = 0\ and\ a_{t_1+1} > 0,\ b_t = Flowrate_{t-t_1(Barrier\#1)} \qquad \text{Equation 5.21}$$

The water flow rate through Barrier #2 can be given by

$$Flowrate_{t(Barrier\#2)} = \begin{cases} 0 & t \le t_1 \\ Min\left\{a_t, b_t\right\} & t > t_1 \end{cases} \qquad \text{Equation 5.22}$$

Therefore, the water flow rate through Barrier #3 can be calculated similarly based on the accumulated water in Room B, which is given by

$$c_{t(Barrier\#3)} = Max\left\{Flowrate_{t(Barrier\#2)} - Drainage, 0\right\}$$
$$if\ c_{t_2} = 0\ and\ c_{t_2+1} > 0,\ d_t = Flowrate_{t-t_2(Barrier\#2)} \qquad \text{Equation 5.23}$$
$$Flowrate_{t(Barrier\#3)} = \begin{cases} 0 & t \le t_2 \\ Min\{c_t, d_t\} & t > t_2 \end{cases}$$

The critical time of that the flow rate reaches the drainage ability and the water height reaches the CWH is shown in Table 5.17. Besides, the 97.5% interval of critical time is described. It can be judged that the failure time of AFW pumps has been well postponed even based on the most conservative assumption.

Table 5.17 Time for critical water flow rate and water height (Layout #2)

	Criteria	**Time (min)**		
		Mean	Median	95% Interval
Pump A	*Flow rate > Drainage*	8	8	(6, 11)
	Water height > CWH	29	29	(24, 38)
Pump B	*Flow rate > Drainage*	17	17	(12, 17)
	Water height > CWH	44	43	(35, 62)
Pump C	*Flow rate > Drainage*	31	31	(20,53)
	Water height > CWH	73	71	(58, 120)

The water flow rate through each barrier in Layout #2 is shown in Figure 5.24. The water height in each room in Layout #2 is shown in Figure 5.25. There is a significant difference from the result for Layout #1. It is different that the time when the flow rates through barriers reach the drainage ability. Equivalently, it is also different that the time when

the water height in rooms differs from each other. The flood environment around each barrier is different from other. However, in Layout #1, all barriers directly contact the severe flood water from the turbine building. When the maximum through one barrier is less than three times of drainage ability but more than one time of drainage ability, it is impossible to occur that the complete CCF. Reversely, the complete CCF will occur in Layout #1.

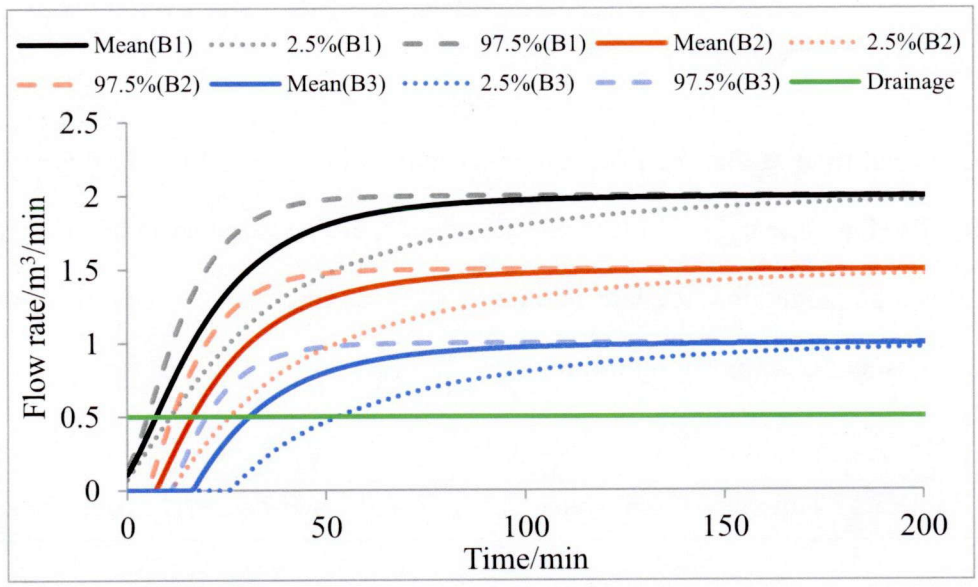

Figure 5.24 Water flow rate through each flood barrier

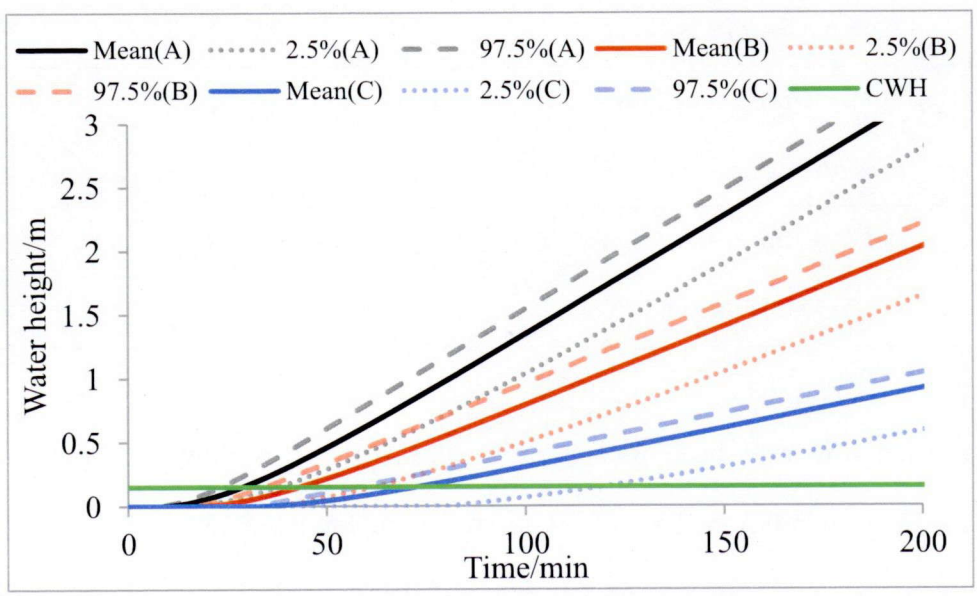

Figure 5.25 Water height in each AFW pump room

According to the possible water height in each room, the failure state of each pump can be evaluated. As a result, the failure types and related probability given the occurrence of a seismic induced flood are shown in Table 5.18. Under the situation of severest flood, the risk flood is reduced regarding to the number of failed pumps. From the perspective of Scenario (1), the half probability can be screened out since there is failure event happens. In the Layout #1 (Table 5.16), there is an absolute single failure happens under the Scenario (1). The failure risk is reduced. Equivalently, from the perspective from Scenario (2), two third of the partial CCF events is degraded to no failure or single failure. If all three barriers are flawed or failed by the seismic shock, all pumps will fail finally, but the time duration of complete CCF is longer than that of Layout #1.

Table 5.18 Failure types of each scenario of flood barriers (Layout #2)

		Percentage of probability	**Failure types**
Scenario 1	Figure 5.12	0.133	No failure (0/3)
	Figure 5.13	0.067	Single failure (1/3)
Scenario 2	Figure 5.14	0.067	No failure (0/3)
	Figure 5.15	0.067	Single failure (1/3)
	Figure 5.16	0.067	Partial CCF (2/3)
Scenario 3	Figure 5.17	0.6	Complete CCF (3/3)

5.5.3. The estimation of decomposed alpha factors of internal flood

Because the number of failed AFW pumps can be decided by the water height, it provides a means to evaluate the CCF hazard of internal flood. As introduced in previous chapter, the decomposed alpha factors represent the CCF triggering abilities of potential causes. The estimation of decomposed alpha factors aims to provide a reliable result for the

update of global alpha factors, so the updated alpha factors can reflect the specific system-related coupling factors and defense mechanisms.

The water height in the room determines whether a pump failure happens. In other words, it is the criteria to distinguish a state of success or failure, which can be described as

$$SC = \begin{cases} 0, Exp(WH) < CWH \\ 1, Exp(WH) \geq CWH \end{cases} \quad \text{Equation 5.24}$$

Here, *SC* is the acronym of state criteria; $Exp(WH)$ is the expected water height.

As shown in Table 5.13, if the state of the barrier is Deformation or Failure, the water flow rate will be larger than the drainage ability. In contrast, if the state of the barrier is Success or Leak, the water flow rate will be less than the drainage ability. Combined with the pump state criteria, the decomposed alpha factors can be calculated based on the state of barrier. Here, the Scenario (3) is taken as an example for both layouts. Other scenarios can be obtained similarly.

Layout #1 Parallel flood barriers (Scenario 3)

If all three barriers are flawed by the earthquake, the water height in three rooms is treated as identical. Therefore, when the expected water height is larger than the CWH value, the complete CCF will occur with the probability of Deformation and Failure. The decomposed alpha factor at time *t* can be written by

$$\alpha_{3\ t(Layout\#1)}^{C_1} = \left(P_{t(D)} + P_{t(F)}\right) \bullet SC \quad \text{Equation 5.25}$$

Here, $\alpha_{3\ t(Layout\#1)}^{C_1}$ refers the decomposed alpha factor at time node t of internal flood involving three components; $P_{t(D)}$ and $P_{t(F)}$ are probabilities of states Deformation and Failure at time node t; SC is the criteria whether the states AFW pump is success or failure. Because all three barriers and pumps are treated identically in Layout #1, it is differentiated for each component that the SC as well as the probability of Deformation and Failure.

The time dependent decomposed alpha factors for Layout #1 are shown in Figure 5.26. After the expected water level is higher than the CWH, the CCF risk will start to increase significantly. Moreover, it reaches the stable value of 1 in a short term. Because there is no risk of partial CCF event involving two components, the $\alpha_2^{C_1}$ is always 0.

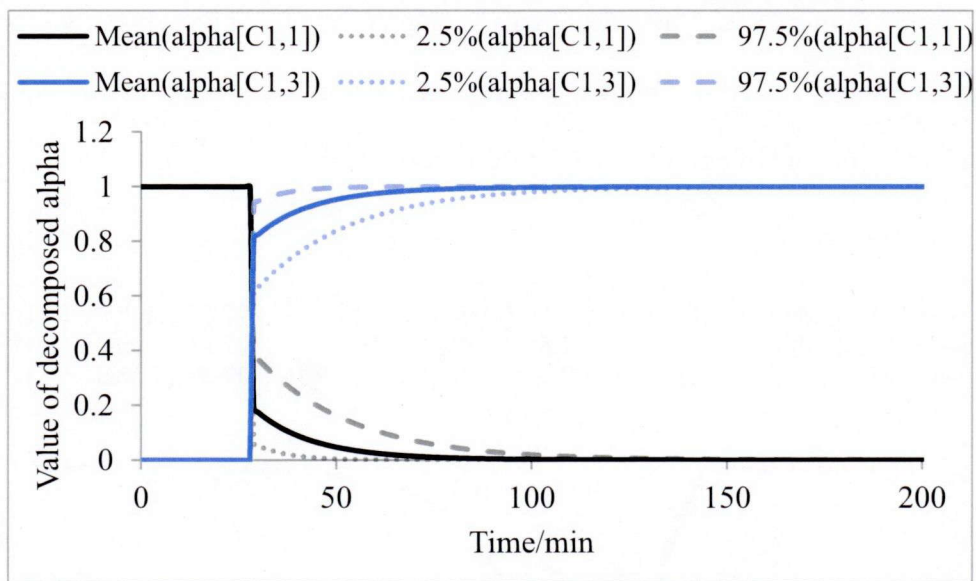

Figure 5.26 Time dependent decomposed alpha factor of internal flood (Layout #1)

Layout #2 Sequential flood barriers (Scenario 3)

All three barriers are flawed by the seismic shock, and then degrade as a result of the propagation of flood. The time of a pump failure is different from other two pumps, so there are different distributions for alpha factors depended on time. The mathematical forms of decomposed alpha factors are given by

$$\alpha_{2\ t(Layout\#2)}^{C_1} = \left(P_{t(D)1} + P_{t(F)1}\right) \bullet \left(P_{t(D)2} + P_{t(F)2}\right) \bullet SC_2 \bullet (1 - SC_3) \qquad \text{Equation 5.26}$$

$$\alpha_{3\ t(Layout\#2)}^{C_1} = \left(P_{t(D)1} + P_{t(F)1}\right) \bullet \left(P_{t(D)2} + P_{t(F)2}\right) \bullet \left(P_{t(D)3} + P_{t(F)3}\right) \bullet SC_3 \qquad \text{Equation 5.27}$$

$$\alpha_{1\ t(Layout\#2)}^{C_1} = 1 - \alpha_{2\ t(Layout\#2)}^{C_1} - \alpha_{3\ t(Layout\#2)}^{C_1} \qquad \text{Equation 5.28}$$

Here, $\alpha_{j\ t(Layout\#2)}^{C_1}$ refers the decomposed alpha factor at time node t of internal flood involving j components; $P_{t(D)i}$ and $P_{t(F)i}$ are probabilities of states Deformation and Failure for Barrier i at time node t; SC_j is the criteria for the failure involving j components.

The time dependent decomposed alpha factors for Layout #2 is shown in Figure 5.27. Compared with Figure 5.26, the decomposed alpha factors involving two and three components are significantly postponed. Because the flood is assumed as the severest, the decomposed alpha factors of complete CCF will finally reach 1.

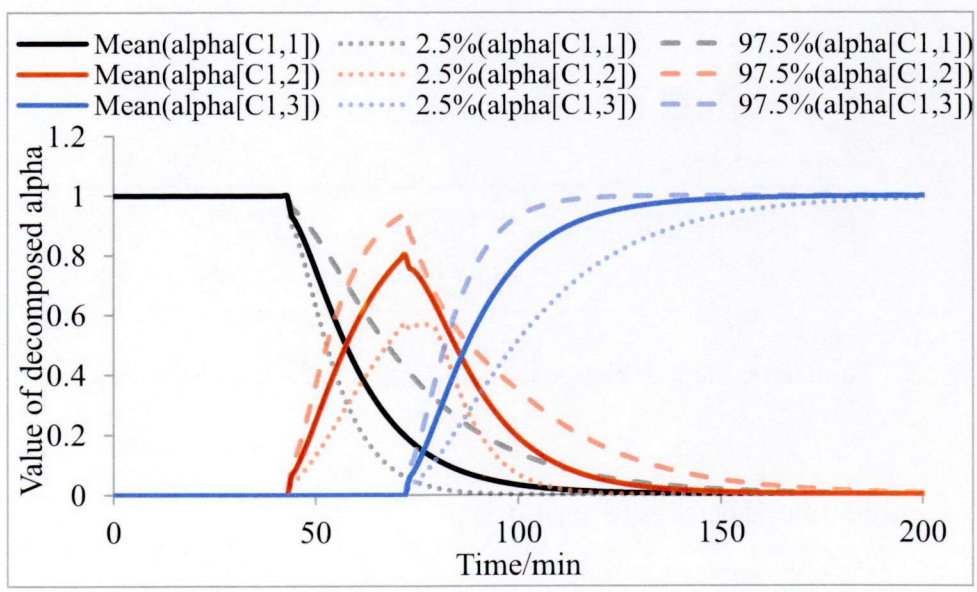

Figure 5.27 Time dependent decomposed alpha factor of internal flood (Layout #1)

5.5.4. Application of the flood risk to basic events analysis in PRA

The estimation of time dependent alpha factors is of practical meaning. The decomposed alpha factors after a long term replace the most serious situation that the internal flood will result in. There are three water sources considered in this article. They are Circulating Water (CW), Service Water (SW) and Fire Protection Water (FPW), which are shown in Figure 5.28. It is possible that all three water systems break after the occurrence of seismic shock, so the CCF of three water systems is assumed. Each water source has respective water flow rate and occurrence rate which is described in Table 5.19. This is used to estimate the flood risk which will be used to update the global alpha factors.

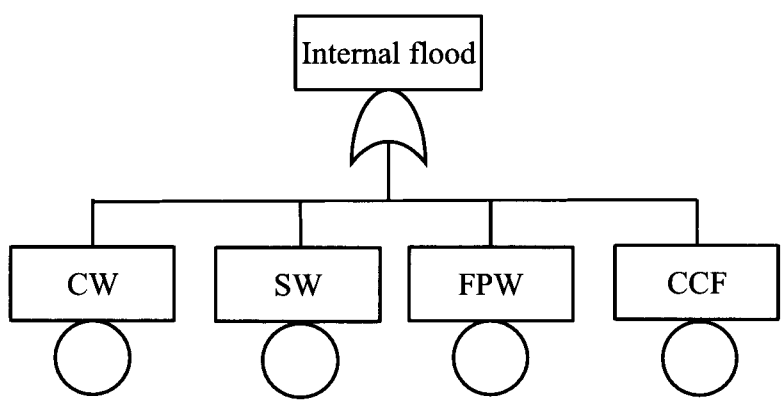

Figure 5.28 Fault tree for water sources break

Table 5.19 Hypothetical flow rate of water sources break

Water sources	**Flow rate through barrier #1 (m^3/min)**	**Probability**
Circulating Water (CW)	1.2	1.30E-04
Service Water (SW)	0.75	1.80E-05
Fire Protection Water (FPW)	0.5	5.10E-04
Three water sources (CCF)	2	1.40E-05

The flow rate through barriers determines the number of AFW pumps. Based on the previous, it can be decided the probability of failure scenario of barrier for two layouts. Take the circulating water system as an example. The flow rate (1.2 m^3/min) is larger than the drainage ability (0.5 m^3/min). In the Layout, Scenario 1 happens with the possibility percentage of 0.2 and there is a single failure. Scenario 2 happens with the possibility percentage of 0.2, there is a partial CCF. Scenario 3 happens with the possibility percentage of 0.6, there is a partial CCF.

Therefore, the summary of each flood and failed pumps is shown in Table 5.20. It can be judged that the CCF risk is significantly degraded from Layout #1 to Layout #2. For instance, when the Barrier #1 is luckily successful, there is no failure occurred. In Layout #2, only the severe flood will cause a complete failure.

Table 5.20 Probabilty of each failure type for different scenario

Failure types		**Probability**			
		CW	**SW**	**FPW**	**CCF**
Layout #1	0/3	0	0	1 (5.10E-04)	0
	1/3	0.2 (2.60E-05)	0.2 (3.60E-06)	0	0.2 (2.80E-06)
	2/3	0.2 (2.60E-05)	0.2 (3.60E-06)	0	0.2 (2.80E-06)
	3/3	0.6 (7.80E-05)	0.6 (1.08E-05)	0	0.6 (8.40E-06)
Layout #2	0/3	0.2 (2.60E-05)	0.2 (3.60E-06)	1 (5.10E-04)	0.2 (2.80E-06)
	1/3	0.133 (1.73E-05)	0.8 (1.44E-05)	0	0.133 (1.86E-06)
	2/3	0.667 (8.67E-05)	0	0	0.067 (9.38E-07)
	3/3	0	0	0	0.6 (8.40E-06)

The calculated decomposed alpha factors are shown in Table 5.21. Usually, the flood scenarios will be screened out that causes no failure, this phenomena has been discussed in the misleading of alpha factors. This information can be reflected in the collection of causes

occurrence rate but will not be reflected in the alpha factors. The estimates of decomposed alpha factors of internal flood can be used to update the global alpha factors.

Table 5.21 The estimated decomposed alpha factors for internal flood

Failure types		Probability	Percentage	Decomposed alpha factors
Layout #1	0/3	5.10E-04	Screened out	-
	1/3	3.24E-05	20.00%	$\alpha_1^{C_1} = 0.2$
	2/3	3.24E-05	20.00%	$\alpha_2^{C_1} = 0.2$
	3/3	9.72E-05	60.00%	$\alpha_3^{C_1} = 0.6$
Layout #2	0/3	5.42E-04	Screened out	-
	1/3	3.36E-05	25.89%	$\alpha_1^{C_1} = 0.2589$
	2/3	8.76E-05	67.63%	$\alpha_2^{C_1} = 0.6763$
	3/3	8.40E-06	6.48%	$\alpha_3^{C_1} = 0.0648$

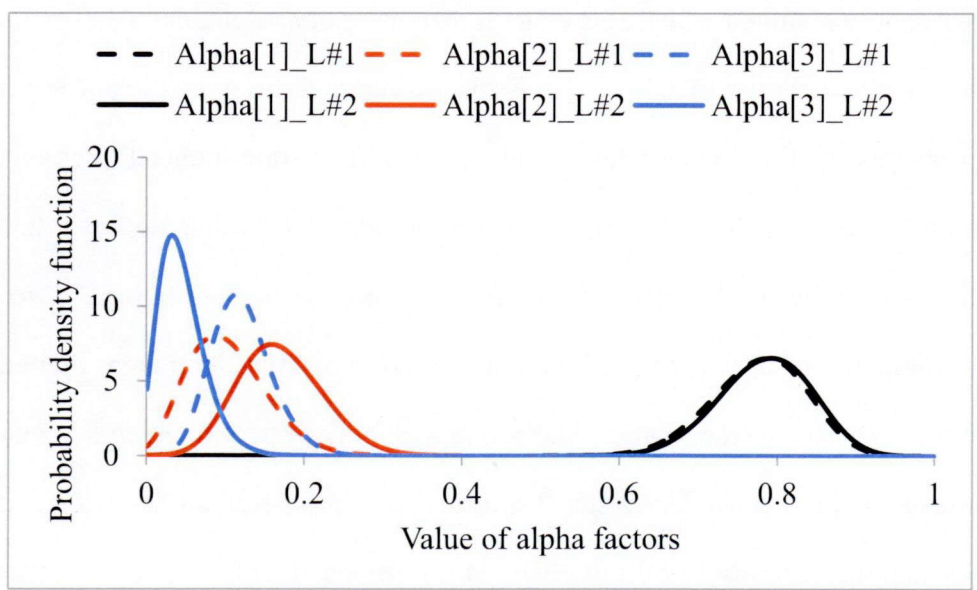

Figure 5.29 The prediction of global alpha factors

For instance, based on the estimates of decomposed alpha factors of internal flood, the prediction of global alpha factor is demonstrated on Figure 5.29. The global alpha factors of the AFW pump system of Layout #2 is of less complete CCF than the system of Layout #1. This application shows the alpha factors are affected by the CCF risk of causes. If more causal information can be used in the evaluation of CCF risk, the results will represent the system-specific design and the innate risk of common causes.

5.6. Summary and Results

Advantages of the alpha decomposition method on the prediction of CCF parameters have been specifically described. The AFW pump system has been taken as an example to illustrate how to evaluate the system- and design- specific CCF parameters. In Section 5.1, flood barrier are recommended to be built in the turbine building to protect the safety-related components from the risk of internal flood. The construction of such flood defense measures will change the distributions for CCF parameters. The decomposed alpha factors of internal flood are reasonably obtained which is used to update the global alpha factors. The misleading of alpha factors in evaluation of failure risk is discovered and discussed. From Section 5.2 to 5.4, the degradation of flood barrier under the scenario of seismic-induced internal flood has been taken into account. The state of flood barrier will affect the water flow rate to the AFW pump rooms and finally, it will affect the number of failed redundant pumps. Two different layouts are compared to prove the CCF parameters are not only component number related but also system-specific design related. Markov model and ordinary differential equations are used to evaluate the time dependent water flow rate and decomposed alpha factors. At last, the global alpha factors are updated by the obtained decomposed alpha factors of internal flood for two layouts.

The current research only considers the Markov transition parameters as time independent which can be obtained by the process of Bayesian inference. In actual flood PRA,

the transition rate between two Markov states is decided by the flood environment. It is very conservative and of large uncertainty to consider the degradation of flood barrier with constant transition parameters. The physics-based Markov model should be built in future research. The dynamic flood scenario and flow rate should be better established.

This page is intentionally left blank.

Chapter 6: CONCLUSIONS

Common causes are of different abilities to trigger independent or dependent failures. Traditional alpha factor model uses the ratio of failure types to describe the CCF risk of redundant systems. However, the estimates of CCF parameters should reflect issues including failure data, cause information, coupling factor and system-specific design etc. Based on the alpha factor model and causal inference, the alpha decomposition method is proposed to quantitatively evaluate CCF parameters. Global alpha factors are decomposed according to a function of two types of elements. Explanatory variables include occurrence frequencies and CCF triggering abilities (denoted as decomposed alpha factors). The regression model of the alpha decomposition method is established and proved by the theory of conditional probability as well as Hybrid Bayesian Network. Moreover, it is demonstrated the alpha decomposition method can be validated by the hypothetical system-specific database.

Based on the evidence of generic failure data, causal information and design information, etc., Bayesian approaches are applied to numerically compute the posterior distributions for CCF parameters. Databases are recommended to be built, which combine the CCF events recording and causes occurrence information. Hierarchical Bayesian models are used to solve the regression model (the alpha decomposition method). Numerical examples show the calculation process of two-stage Bayesian inference with the MCMC method. Decomposed alpha factors are risk characteristics of potential causes. This research can assist analysts to rank CCF risk significance of causes. The uncertainty analysis in the estimation of alpha factors is able to be conducted by decomposed alpha factors as well. The uncertainty in the estimates of CCF parameter can be reduced.

The quantitative estimation of CCF parameters involving specific defense barriers has been discussed. The AFW pump system has been analyzed to illustrate how the specific design and defense strategy affect CCF parameters. First of all, flood barrier are recommended to be built in the turbine building to protect safety-related components from the

risk of internal flood. Usually, there is no operation database for AFW pump system with the recommended flood barrier. However, the construction or degradation of flood defense measures will change the distributions for CCF parameters. The decomposed alpha factors of internal flood are reasonably obtained which is used to update the global alpha factors. The misleading characteristic of alpha factors regarding risk evaluation is discovered and discussed. It is found that the defense against causes of high occurrence rate but low CCF risk will increase the alpha factors which represent partial or complete CCF.

On the other side of the coin, the degradation of flood barrier will increase the CCF risk of the AFW pump system. Under the scenario of seismic-induced internal flood, the CCF risk has been investigated. The state of flood barrier will affect the water flow rate to the AFW pump rooms and finally, it will affect the number of failed redundant pumps. Two different layouts are compared to prove the CCF parameters are not only component number related but also system-specific design related. Markov model and ordinary differential equations are used to evaluate the time dependent water flow rate and decomposed alpha factors. The application of this research explains that even if not enough plant-specific operation databases are available, the well-established estimates of common causes' risk can be used to predict the CCF parameters.

As a shortcoming of current research, the transition parameters in the Markov model are treated as time-constant. In future research, it should be included that the physic-based investigation of flood barrier degradation. More accurate calculation of dynamic flow rate and degradation rate should be established as the internal PRA analysis is an important contributor to the external events initiated severe accident.

APPENDIX A

OpenBUGS script for the degradation of flood barrier and decomposed alpha factors

```
model{
for(k in 1:case.number){                          # model's likelihood
x[k, 1:group.size] ~ dmulti(alpha[k, 1:group.size],   # Stochastic model with multinomial
X[k])                                             likelihood function
X[k] <- sum(x[k, 1:group.size])                   # X is the total number of "group
                                                  failure events"
alpha[k, 1:group.size] ~ ddirich(theta[k, ])      # Transition variable
for (j in 1:group.size){
theta[k, j] <- (alpha.c[1, j]*r[k, 1] + alpha.c[2, j]*r[k,   # Predicted function for the alpha
2] + alpha.c[3, j]*r[k, 3])*X[k]                  decomposition
}
}
for (i in 1:cause.number){                        # A noninformative prior
alpha.c[i, 1:3] ~ ddirich (delta[i, ])            distributions for decomposed
delta[i, 1] <- 1                                  alpha-factors
delta[i, 2] <- 1                                  # Each parameter in dirichlet
delta[i, 3] <- 1                                  distributions is 1
}
for(i in 1:exp.round)                             # The harzard of seismic shock
{
sei.F[i, 1:state.number] ~ dmulti(p.state[i,
1:state.number], N[i])
N[i] <- sum(sei.F[i, 1:state.number])
```

```
p.state[i, 1:state.number] ~ ddirich(eta[i, ])
for (j in 1:state.number){
eta[i, j] <- 1
}
}
for(i in 1:state.number){                    # Calculate the initiating states
init[i] <- sum(p.state[, i])/exp.round
}
for(i in 1:exp.round)  {                     # Stochastic models for of Leaks
n.L[i] ~ dpois(mean.L[i])                    # Number of Leaks
mean.L[i] <- lambda[i]*time.L[i]
lambda[i] ~ dlnorm(mu.L[i], tau.L[i])        # Distribution for leak rate
mu.L[i] <- log(prior.mean.L[i]) - pow(sigma.L[i],
2)/2
sigma.L[i] <- log(RF.L[i])/1.645
tau.L[i] <- pow(sigma.L[i], -2)
n.L[i] <- sei.F[i, 1] -flood.F[i, 1]
}
for(i in 1:exp.round){                       # Stochastic model for the numbers
x.D[i] ~ dbin(p.D[i], n.D[i])                   of Deformation
p.D[i] ~ dlnorm(mu.D[i], tau.D[i])
mu.D[i] <- log(prior.mean.D[i]) - pow(sigma.D[i],
2)/2
sigma.D[i] <- log(RF.D[i])/1.645
tau.D[i] <- pow(sigma.D[i], -2)
n.D[i] <- sei.F[i, 2] + sei.F[i, 1] - flood.F[i, 1]
```

```
x.D[i] <- flood.F[i, 3] - sei.F[i, 3] + x.F2[i]
}
for(h in 1:exp.round)  {                    # Stochastic models for the numbers
                                              of Failures given Leaks
x.F1[h] ~ dbin(p.F1[h], n.F1[h])            # Number of Failures
p.F1[h] ~ dlnorm(mu.F1[h], tau.F1[h])       # Conditional probability of failure
mu.F1[h] <- log(prior.mean.F1[h]) -           given leak
Pow(sigma.F1[h], 2)/2
sigma.F1[h] <- log(RF.F1[h])/1.645
tau.F1[h] <- pow(sigma.F1[h], -2)
n.F1[h] <- sei.F[h, 2] + sei.F[h, 1] - flood.F[h, 1]
}
for(h in 1:exp.round){                      # Stochastic models for the numbers
x.F2[h] ~ dbin(p.F2[h], n.F2[h])              of Failures given Deformations
p.F2[h] ~ dlnorm(mu.F2[h], tau.F2[h])       # Conditional probability of failure
mu.F2[h] <- log(prior.mean.F2[h]) -           given leak
pow(sigma.F2[h], 2)/2
sigma.F2[h] <- log(RF.F2[h])/1.645
tau.F2[h] <- pow(sigma.F2[h], -2)
n.F2[h] <- x.D[h]
x.F2[h] <- flood.F[h, 4] - sei.F[h, 4] - x.F1[h]
}
phi.SL<-sum(lambda[])/exp.round             # Transition parameters
lambda.LD <- sum(p.D[])/exp.round
rho.LF <- sum(p.F1[])/exp.round
rho.DF <- sum(p.F2[])/exp.round
```

```
solution[1:n.grid, 1:dim] <- ode(init[1:dim],          # Markov ordinary differential
times[1:n.grid], D(P[1:dim], t), origin, tol)            equations
D(P[1], t) <- -phi.SL*P[1]
D(P[2], t) <- phi.SL*P[1] - lambda.LD*P[2] -
rho.LF*P[2]
D(P[3], t) <- lambda.LD*P[2] - rho.DF*P[3]
D(P[4], t) <- rho.LF*P[2] + rho.DF*P[3]
for(j in 1:n.grid) {                                   # Flow rate for flood barrier
flowrate.1[j] <- 0*solution[j,1] + 0.25*solution[j,2] +   degradation
1*solution[j,3] + 2*solution[j,4]
flowrate.2[j] <- flowrate.1[j] - 0.5
accum.rate1[j] <- flowrate.1[j] - 0.5
flowrate.3[j] <- flowrate.2[j] - 0.5
accum.rate2[j] <- flowrate.2[j] - 0.5
accum.rate3[j] <- flowrate.3[j] - 0.5
}
init.flowrate <- 0*init[1] + 0.25 *init[2] + 1*init[3] +
2*init[4]
#for(j in 8:n.grid){
#waterheight.1[j] <- sum(accum.rate1[8:j])/area
#}
#for(j in 17:n.grid){
#waterheight.2[j] <- sum(accum.rate2[17:j])/area
#}
#for(j in 31:n.grid){
#waterheight.3[j] <- sum(accum.rate3[31:j])/area
```

```
#}
#for (j in 1:43){
#new.alpha.c1[j,1] <-1
#}
#for (j in 44:72){
#new.alpha.c1[j,2] <- (solution[j,3] +
solution[j,4])*(solution[j-43,3] + solution[j-43,4])
#new.alpha.c1[j,1] <- 1- (solution[j,3] +
solution[j,4])*(solution[j-43,3] + solution[j-43,4])
}
#for (j in 73:n.grid){
#new.alpha.c1[j,3] <- (solution[j,3] +
solution[j,4])*(solution[j-43,3] +
solution[j-43,4])*(solution[j-72,3] + solution[j-72,4])
#new.alpha.c1[j,2] <- 1 - new.alpha.c1[j,1] -
new.alpha.c1[j,3]
#new.alpha.c1[j,1] <- 1- (solution[j,3] +
solution[j,4])*(solution[j-43,3] + solution[j-43,4])
#}
}
DATA
list(x=structure(.Data=c(...), .Dim=c(16,3)),
r=structure(.Data=c(...), .Dim=c(16,3)),
group.size=3, case.number=16, cause.number=3,
sei.F=structure(.Data=c(...), .Dim=c(3, 4)),
flood.F=structure(.Data=c(...), .Dim=c(3, 4)),
```

```
state.number = 4, exp.round=3, n.grid = 300, dim = 4,
origin = 0, tol = 1.0E-8, prior.mean.L =
c(0.0001,0.0001,0.0001), RF.L = c(100,100,100),
time.L = c(60,60,60), prior.mean.F1 = c(0.1,0.1,0.1),
RF.F1 = c(10,10,10), prior.mean.F2 = c(0.1,0.1,0.1),
RF.F2 = c(10,10,10), prior.mean.D = c(0.1,0.1,0.1),
RF.D = c(10,10,10), x.F1 = c(0, 0, 0), times = c(...))
```

REFERENCES

[1] A. Mosleh, K. Fleming, G. Parry, H. Paula, D. Worledge and D. Rasmuson, *Procedures for treating common cause failures in safety and reliability studies*, NUREG/CR-4780, U.S. Nuclear Regulatory Commission, (1988).

[2] A. Mosleh, D. Rasmuson and F. Marshall, *Guidelines on modeling common-cause failures in probabilistic risk assessment*, NUREG/CR-5485, U.S. Nuclear Regulatory Commission, (1998).

[3] A. Mosleh, G. Parry and A. Zikria, An approach to the analysis of common cause failure data for plant-specific application, *Nuclear Engineering and Design* 150 (1994), pp. 25-47.

[4] D. Kelly, H. Song, G. DeMoss, K. Coyne and D. Marksberry, Common-cause failure treatment in event assessment: basis for a proposed new model, *Proceedings of the international conference on probabilistic safety assessment and management (PSAM 10)*, June 7-11, 2010, Seattle, USA, (2010). [CD-ROM]

[5] T. Wierman D. Rasmuson and A. Mosleh, *Common-cause failure database and analysis system: event data collection, classification, and coding*, NUREG/CR-6268, Rev.1, U.S. Nuclear Regulatory Commission, (2007).

[6] U.S. Nuclear Regulatory Commission, *CCF parameter estimations (2010 Update)*, U.S. Nuclear Regulatory Commission, (2012).

[7] X. Zheng, A. Yamaguchi and T. Takata, α-decomposition method: a new approach to the analysis of common cause failure, *Proceedings of the international conference on PSAM11 & ESREL 2012*, June 25-29, 2012, Helsinki, Finland, (2012). [CD-ROM]

[8] X. Zheng, A. Yamaguchi and T. Takata, Probabilistic common cause failure modeling after the introduction of defense mechanisms, *Proceedings of the international conference on nuclear thermal-hydraulics operation and safety (NUTHOS-9)*, Sept. 9-13, 2012, Kaohsiung, Taiwan, (2012). [CD-ROM]

[9] Dominion Resources Inc., *Safety significance evaluation of Kewaunee power station turbine building internal floods, Volume 1 & 2, Revision 1*, Dominion Resources Inc., (2005).

[10] D. Kelly and S. Curtis, *Bayesian inference for probabilistic risk assessment: a practitioner's guidebook*, Springer, New York, (2011).

[11] X. Zheng, A. Yamaguchi and T. Takata, Quantitative risk assessment of common cause failure involving the degradation of defense barrier against seismic induced internal flood, *Proceedings of Japan-Korea symposium on nuclear thermal hydraulics and safety (NTHAS8)*, Dec. 9-12, Beppu, Japan, (2012). [CD-ROM]

[12] D. Rasmuson and D. Kelly, Common-cause failure analysis in event assessment, *Journal of Risk and Reliability*, Vol.222 (2008), pp. 521-532.

[13] D. Kelly and S. Curtis, Bayesian inference in probabilistic risk assessment – the current state of the art, *Reliability Engineering and System Safety* 94 (2009), pp. 628-643.

[14] A. Yamaguchi, Seismic fragility analysis of the heat transport system of LMFBR considering partial correlation of multiple failure modes, *Proceedings of the international conference on structural mechanics in reactor technology (SMiRT 11)*, Aug. 18-23, 1991, Tokyo, Japan, (1991). [CD-ROM]

[15] A. Yamaguchi, M. Kato and T. Takata, Epistemic uncertainty reduction in the PSA of nuclear power plant using Bayesian approach and information entropy, *Proceedings of the international conference on probabilistic safety assessment and management (PSAM 10)*, June 7-11, 2010, Seattle, USA, (2010). [CD-ROM]

[16] I. Ntzoufras, *Bayesian modeling using WinBUGS*, Wiley, New Jersey, (2009).

[17] T. Wierman, D.Rasumuson, N.Stockton, *Common-Cause Failure Event Insights*, NUREG/CR-6819, Vol.1~4, U.S. Nuclear Regulatory Commission, (2003).

[18] D. Koller and N. Friedman, *Probabilistic Graphical Models*, Cambridge, Massachusetts: The MIT Press, London, (2009).

[19] J. Pearl, *Causality: models, reasoning, and inference, second edition*, Cambridge University Press, New York, (2009).

[20] P. Congdon, *Bayesian Statistical modeling*, John Wiley & Sons, Ltd, West Sussex, (2006).

[21] D. Gamerman and H. F.Lopes, *Markov Chain Monte Carlo: stochastic simulation for Bayesian inference, second edition*, Chapman & Hall/CRC, Florida, (2006).

[22] J. Kruschke, *Doing Bayesian data analysis: a tutorial with R and BUGS*, Academic Press, Elsevier Inc., (2011).

[23] J. Albert, *Bayesian Computation with R*, second edition. Springer, New York, (2009).

[24] K. Fleming, Markov models for evaluating risk-informed in-service inspection strategies for nuclear power plant piping systems, *Reliability Engineering & System Safety 83* (2004), pp.27-45.

[25] K. Fleming, S. Unwin, D. Kelly et al., *Treatment of Passive Component Reliability in Risk-Informed Safety Margin Characterization*, FY 2010 Report, INL/EXT-10-20013, Idaho National Laboratory, USA, (2010).

[26] H. Dezfuli, D. Kelly, C. Smith, K. Vedros and W. Galyean, *Bayesian inference for NASA probabilistic risk and reliability analysis*, NASA, Washington DC, USA, (2009).

[27] K. Fleming, A reliability model for common mode failure in redundant safety systems, *Proceedings of the sixth annual Pittsburgh conference on modeling and simulation*, April 23-25, (1975).

[28] A. Mosleh, N. Siu, A multi-parameter, event-based common-cause failure model, *In proceedings of the ninth international conference on structural mechanics in reactor technology*, Lausanne, Switzerland, August, (1987).

[29] F. Marshall, D. Rasmuson and A. Mosleh, Common-cause failure parameter estimations, NUREG/CR-5497, U.S. Nuclear Regulatory Commission, (1998).

[30] R. Neapolitan, *Learning Bayesian networks,* Pearson Prentice Hall, Upper Saddle

River, New Jersey, (2004).

[31] A. Yamaguchi, Y. Kirimoto and K. Ebisawa, Tsunami PRA standard development by Atomic Energy Society Japan (AESJ) (4) unsolved issues and future works, *Proceedings of the international conference on PSAM & ESREL 2012*, June 25-29, 2012, Helsinki, Finland, (2012). [CD-ROM]

ACKNOWLEDGEMENTS

I owe a great debt of gratitude to too many people who have helped make this dissertation possible.

First and foremost, I would like express my sincere appreciation to advisor, Professor Akira Yamaguchi for his guidance and continuous support of my Ph.D study and research. I also extend this gratitude to Associate professor Takashi Takata for his contribution to this research. It is fortunate that professors show a genuine interest in this topic and provided enlightened comments through consistent discussion. I acknowledge Professor Takao Nakamura and Associate Professor Eiji Hoashi for precious comments on the current dissertation.

Thank you to Professor Xuewu Cao at Shanghai Jiao Tong University for the precious recommendation to Yamaguchi Laboratory. I would like to thank Dr.Yuki Ohnishi for kind help and sharing experience during last three years. Thank you to Mrs.Azuma, Mrs.Yamamoto and other Ms./Mrs. Secretaries for patient support and help.

I would also like to acknowledge all of my research colleagues at Yamaguchi Laboratory, Osaka University. Most of members are younger than me, but thank you for taking the time to help me and teaching me Japanese. It has been a great opportunity to study with them. I sincerely thank past members of Yamaguchi Laboratory: Dr.Makoto Shibahara, Dr.Toshinori Matsumoto, Mr.Satoshi Shinzaki and Mr.Shuhei Matsunaka. Thanks for sharing their wisdom and friendship with me.

Finally, I owe a great debt to my family for so much love and support through all my life.

It is impossible to thank everyone who has helped me and given me valuable feedback, but it was impossible to finish this dissertation without their support.

LIST OF PUBLICATIONS

Journals

[1] Xiaoyu Zheng, Akira Yamaguchi, Takashi Takata, Quantitative common cause failure modeling for auxiliary feedwater system involving of the seismic-induced degradation of flood barriers, *Journal of Nuclear Science and Technology*, Submitted (2013).

[2] Xiaoyu Zheng, Akira Yamaguchi, Takashi Takata, Probabilistic common cause failure modeling for auxiliary feedwater system after the introduction of flood barriers, *Journal of Nuclear Science and Technology*, Submitted (2012).

[3] Xiaoyu Zheng, Akira Yamaguchi, Takashi Takata, α-Decomposition for Estimating Parameters in Common Cause Failure Modeling Based on Causal Inference, *Reliability Engineering & System Safety*, Submitted (2012).

International conferences

[1] Xiaoyu Zheng, Akira Yamaguchi and Takashi Takata, Quantitative risk assessment of common cause failure involving the degradation of defense barrier against seismic induced internal flood, *Proceedings of Japan-Korea symposium on nuclear thermal hydraulics and safety (NTHAS8)*, Dec. 9-12, Beppu, Japan, (2012).

[2] Xiaoyu Zheng, Akira Yamaguchi, Takashi Takata, Probabilistic common cause failure modeling after the introduction of defense mechanisms, *Proceedings of the international conference on nuclear thermal-hydraulics operation and safety (NUTHOS-9)*, Sept. 9-13, 2012, Kaohsiung, Taiwan, (2012).

[3] Xiaoyu Zheng, Akira Yamaguchi, Takashi Takata, α-decomposition method: a new approach to the analysis of common cause failure, *Proceedings of the international conference on PSAM11 & ESREL 2012*, June 25-29, 2012, Helsinki, Finland, (2012).